University of New Hampshire

University of New Hampshire Scholars' Repository

Doctoral Dissertations

Student Scholarship

Fall 2020

DYNAMIC PERFORMANCE OF PARTIALLY SATURATED AND UNSATURATED SOILS

Sayedmasoud Mousavi
University of New Hampshire, Durham

Follow this and additional works at: https://scholars.unh.edu/dissertation

DYNAMIC PERFORMANCE OF PARTIALLY SATURATED AND UNSATURATED

SOILS

By

SAYEDMASOUD MOUSAVI

B.Sc., Isfahan University of Technology, 2013

M.Sc., Sharif University of Technology, 2016

DISSERTATION

Submitted to the University of New Hampshire

in Partial Fulfilment of

the Requirements of the Degree of

Doctor of Philosophy

in

Civil and Environmental Engineering

September 2020

This dissertation was examined and approved in partial fulfillment of the requirements for the degree of Doctor of Philosophy in Civil and Environmental Engineering by:

Dissertation Director, Dr. Majid Ghayoomi, Associate Professor of Civil and Environmental Engineering at the University of New Hampshire.

Dr. Jean Benoit, Professor of Civil and Environmental Engineering at the University of New Hampshire.

Dr. Stephen Jones, Research associate professor of Natural Resources and the Environment at the University of New Hampshire.

Dr. John S. McCartney, Professor and Department Chair of Department of Structural Engineering at the University of California San Diego.

Dr. Mohammad Khosravi, Assistant Professor of Civil Engineering Department at Montana State University.

On Monday, June 29, 2020

Approval signatures are on file with the University of New Hampshire Graduate School.

DEDICATION

This dissertation is dedicated to my parents, my sister, my brother, and my wife for their endless love, support, and encouragement.

ACKNOWLEDGMENT

TABLE OF CONTENTS

LIST OF TABLES

LIST OF FIGURES

xv

xvi

xviii

ABSTRACT

DYNAMIC PERFORMANCE OF PARTIALLY SATURATED AND UNSATURATED SOILS

By

Sayedmasoud Mousavi

University of New Hampshire

The vast majority of surface structures are located on or surrounded by unsaturated and partially saturated soil deposits. Previous studies revealed that degree of saturation in soils can significantly impact the seismic performance of geotechnical systems. Yet, the fundamental understanding of the mechanisms by which the degree of saturation impacts their performance during seismic loading is not mature. This Ph.D. dissertation aimed to evaluate and characterize the dynamic response of soils including excess pore pressure generation, induced volumetric deformation, shear modulus, and material damping at different states of saturation and a wide range of degrees of saturation. Three different desaturation methods, including Microbial Induced Partial Saturation (MIPS), wet-compaction, and tensiometric suction control techniques were used to evaluate the impact of state of saturation, saturation level, and the path to reach that level on the dynamic properties and performance of sands containing variable non-plastic fines. Results from this study indicated that MIPS treatment of soil specimens, even with a small reduction in degree of saturation, can result in a significant reduction in the excess pore pressure generation. Experimental data suggested a meaningful impact of the state of saturation and desaturation technique on dynamic response of tested specimens. On the basis of experimental data and theoretical considerations, semi-empirical models were developed to estimate the excess pore pressure generation and volumetric deformation in sand and silty sands under unsaturated and partially saturated states. The comparison of experimental measurements as well as available data in literature showed the suitability of the developed models to capture the trends in dynamic soil response with the degree of saturation.

CHAPTER 1

INTRODUCTION

1.1. RESEARCH MOTIVATION

Unsaturated soils are widely available in shallow ground above the ground water table (GWT), where their strength and stiffness are controlled and impacted by inter-particle suction forces (Lu and Likos 2006; Ghayoomi et al. 2011; Khosravi and McCartney 2012; Hoyos et al. 2015). Air bubbles can also be entrapped below the ground water table as a result of gas exsolution (e.g., pore fluid pressure drop, bio respiration) or immiscible displacement (e.g., drainage and imbibition) where these bubbles, even in minute amounts, can significantly affect undrained, dynamic soil response (Chaney et al. 1979; Yoshimi et al. 1989; Okamura and Soga 2006; Okamura et al. 2011; Eseller-Bayat et al. 2013). Taking advantage of this effect, Induced Partial Saturation (IPS) techniques such as the use of biogenic gas induction have been explored as an effective means to mitigate liquefaction (Okamura and Soga 2006; Yegian et al. 2007; He et al. 2013). However, depending on the soil type, stress state, and degree of saturation, the occluded bubbles in these partially saturated soils may not introduce suction (Finno et al. 2017). Thus, depending on the soil's state of saturation (i.e., partially saturated soil below GWT with occluded gas bubbles, or

unsaturated soil above GWT), the existence of air-water-solid interfaces in soils may impact their response to mechanical and dynamic loading through different mechanisms. This research mechanistically characterizes, differentiates, and formulates the service condition dynamic response of unsaturated and partially saturated sands and silty sands under different initial conditions and loading scenarios. Figure 1-1 depicts a generic profile of unsaturated and partially saturated soils above and below GWT.
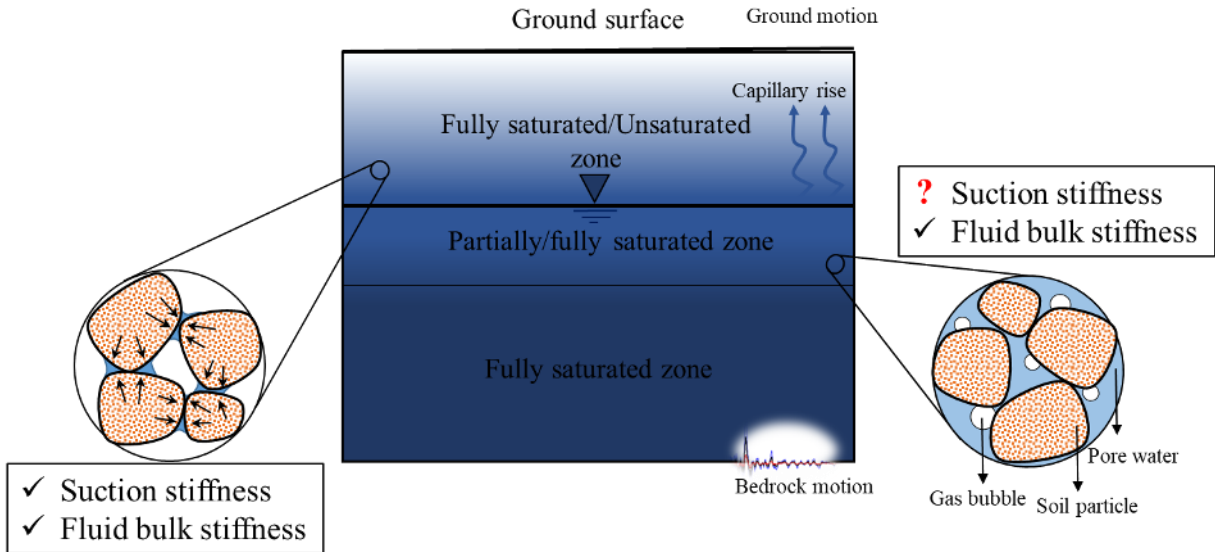
Figure 1-1. A generic soil profile with unsaturated and partially saturated soil layers.

Past research mainly focused on strength and stiffness evaluation, failure mechanisms, and liquefaction assessment of saturated, unsaturated, and partially saturated soils in limit state. There is a lack of fundamental understanding and mechanical framework to evaluate the service condition dynamic response of soils that are not fully saturated. Such framework must capture a wide range of degrees of saturation from high suction state unsaturated soils to gassy soils and should take into account the desaturation path. Estimating pre-failure dynamic response helps to address the growing demand for performance-based seismic design and analysis. Such analysis

2

requires a reliable understanding of dynamic shear modulus, damping, seismic compression, and pore-pressure generation in a three-phase media with different states of saturation.

Many geotechnical infrastructure rests on or are surrounded by unsaturated soils above GWT or are made of compacted, unsaturated soils, which could be subjected to dynamic loads. As a result of surface tension in air-water-solid three phase interface and consequently capillary rise of water, soil layers above GWT may have a negative pore water pressure, leading to development of interparticle capillary suction and elevated soil stiffness. Although unsaturated soils, in comparison with fully saturated soils, are likely to exhibit less deformation and lower excess pore pressure due to their higher shear strength and lower damping, they are likely to increase seismic motion amplification (Mirshekari and Ghayoomi 2017). While the impact of degree of saturation is indirectly reflected in shear wave velocity measurement of unsaturated soil layers, the seasonal and spatial fluctuation of GWT and water infiltration may lead to unknown saturation profiles and uncertainty in site specific response and dynamic performance assessment at the time and location of a specific seismic event. While intense earthquakes with intermediate to large shear strain levels are expected to have the most devastating consequences, past studies mostly focused on evaluation of dynamic properties of unsaturated soils in small strain conditions. Further, excess pore pressure generation in partially saturated soil, even if does not lead to full liquefaction, and seismically induced compression in unsaturated soil may still result in excessive settlement.

On the other hand, the soil immediately below the groundwater level may also exhibit a primary wave velocity of one-third to two-thirds of that in fully saturated soils, implying that this soil layer is partially saturated (Tsukamoto 2019). Further, desaturation of soil below GWT such as Microbial Induced Partial Saturation (MIPS) for liquefaction mitigation is an advancing front in geotechnical earthquake engineering. Although investigations signified the approach's

3

effectiveness in controlling ultimate failure conditions (e.g., liquefaction), they did not characterize the performance of these artificially made partially saturated soils in service condition where liquefaction is not expected. Other desaturation techniques like air injection (Okamura et al. 2011) or chemical methods (Eseller-Bayat et al. 2013) will also require such scrutiny. Discrete gas bubbles, depending on their source, distribution, and concentration may or may not contribute to inter-particle forces (Pham et al. 2016; Finno et al. 2017). Thus, a comprehensive study on soil dynamic properties should encompass the full range of saturation, covering states from gassy soils to unsaturated soils with different response mechanisms, to avoid faulty or overly conservative performance assessment.

Although current investigations on desaturation for liquefaction mitigation have focused on clean sands, past experience from liquefaction failure case histories (Yamamuro and Lade 1998) indicated that silty sands are also prone to flow liquefaction with limited improvement options due to their low permeability. MIPS can offer a promising and sustainable method to improve liquefaction resistance of sands containing cohesionless fines. Specifically, the presence of fines may increase retainability of gas bubbles and inter-particle suction forces. However, excessive gas generation may lead to formation of fractures in soils and disturbance of their structure (Pham et al. 2017), which in turn adversely affects the dynamic performance of the treated system. Therefore, concurrent consideration of liquefaction resistance, physics of generated bubbles, and dynamic performance of treated systems in service condition is necessary to develop a viable method for liquefaction mitigation in silty sands.

1.2.   RESEARCH OBJECTIVES AND SCOPE

This Ph.D. dissertation desires to experimentally evaluate and characterize the response of soils including excess pore pressure generation, induced volumetric deformation, shear modulus, and damping to dynamic loading at different states of saturation and a wide range of degrees of saturation. Three different techniques, including MIPS, wet-compaction, and tensiometric suction control technique are employed to evaluate the impact of state of saturation, saturation level, and the path to reach that level on dynamic properties and performance of sand and silty sands. Specifically, the primary objectives of this research are listed below:

(1) The first objective is to characterize compositional, mechanical, and environmental factors affecting the efficiency of MIPS treatment for desaturation of soil. The efficiency is defined as the ratio of volume of gas bubbles maintained in soil to total expected volume of gas predicted from bioenergetic calculations. Results of this step are used to calibrate the MIPS treatment process based on soil type and fines content, overburden stress, density, temperature, and pH.

(2) The next objective is to investigate the performance and effectiveness of MIPS process for mitigation of seismically induced excess pore pressure generation in sands with variable non-plastic fines content. This includes a series of undrained, strain-controlled cyclic Direct Simple Shear (DSS) tests on MIPS treated and untreated (i.e., fully saturated) clean sand and silty sand specimens subjected to different dynamic loadings. To fulfill this objective, the impact of degree of saturation on the magnitude of excess pore pressure generation in partially saturated soils under dynamic excitation was characterized and formulated.

5

(3) The third objective is to evaluate the impact of the state of saturation and the degree of saturation on seismically-induced volumetric deformation of soils. This includes two sets of DSS tests on unsaturated and partially saturated soil specimens prepared with (a) tensiometric control of suction and (b) wet-compaction technique at variable degrees of saturation. Results of these tests along with MIPS treated tests are utilized to characterize and formulate the seismically induced volumetric deformation in sands and silty sands.

(4) Finally, the fourth objective is to compile experimental data from the three sets of experiments (i.e., MIPS, suction control, and wet-compaction) and interpret the trends in dynamic shear modulus and damping. This includes characterizing the impact of fines content, state of saturation, degree of saturation, and desaturation method on strain-dependent dynamic properties of soils.

1.3.   DISSERTATION STRUCTURE

The results and findings in this research are described in 9 chapters. In addition to this chapter, **Chapter 2** is intended to provide a basic scientific background required for understanding of primary objectives and findings in this research. It includes a review of unsaturated soil mechanics, description of different state of saturations, review of different bio-mediated processes, and a literature review on the impact of saturation level on liquefaction potential, seismically induced volumetric deformation, and dynamic properties of soils.

Chapter 3 provides information about the experimental program. It describes the DSS setup utilized in the study. Then, it provides properties of the soils used in the research and the methods implemented for the preparation of the soils are explained. Then, the methods used to control the degree of saturation are discussed.

Chapter 4 investigates the geotechnical and environmental factors affecting the performance and efficiency of MIPS process for desaturation of different artificial and natural soils. This chapter responds to "Objective 1" and the results presented herein were published in Environmental Geotechnics Journal (Mousavi et al. 2019).

Chapter 5 investigates the performance and the effectiveness of MIPS process for mitigation of seismically induced excess pore pressure in sands with variable non-plastic fines content. This chapter responds to "Objective 2" and the results presented herein are published in ASCE Journal of Geotechnical and Geoenvironmental Engineering, ASCE Geo-congress 2019, and 4th European conference on unsaturated soils (Mousavi and Ghayoomi 2019, 2020a; b)

Chapter 6 explores the impact of state of saturation and degree of saturation on seismically-induced volumetric deformation of soils while formulating seismic compression. This chapter responds to "Objective 3" and the results presented herein are submitted for publication in ASCE Journal of Geotechnical and Geoenvironmental Engineering (Mousavi and Ghayoomi 2020c; Mousavi et al. 2020).

Chapter 7 characterizes the impact of fines content, state of saturation, degree of saturation, and method to achieve the target degree of saturation on strain-dependent dynamic properties of soils. This chapter responds to "Objective 4" and the results presented herein will be modified and submitted to Journal of Soil Dynamics and Earthquake Engineering.

Chapter 8 summarizes and concludes the outcomes of this research and provides recommendations for future research.

Chapter 9 compiles the list of references cited in the dissertation manuscript.

CHAPTER 2

SCIENTIFIC BACKGROUND

2.1. ABSTRACT

This chapter provides basic scientific background to support discussions made in this dissertation. It includes a review of bio-mediated processes, bio-denitrification process for MIPS, fundamental of unsaturated soil mechanics, states of saturation and their potential impacts on mechanical and dynamic soil response, physical and mechanical behavior of silty sands, induced partial saturation methods for liquefaction mitigation in soils, dynamic properties of unsaturated soils, and seismically induced volumetric deformation in unsaturated soils. The chapter concludes with a summary of the key related topics.

2.2. BIO-MEDIATED PROCESSES IN GEOTECHNICAL ENGINEERING

Although ignored for centuries with respect to mechanical behavior, considering soil as a living ecosystem have provided innovative and exciting opportunities for utilizing natural biological processes to modify the engineering properties of the subsurface soils (e.g. strength, stiffness, permeability). A gram of soil typically hosts 40 million bacterial cells (Whitman et al. 1998). In

addition, microorganisms are ubiquitously present in a variety of geo-environments, including shallow to deep and granular to fine sediments owing to their great diversity, adaptability, small cellular size, and their fast reproduction rate (Rebata-Landa and Santamarina 2006). Bio-mediated processes including mineral precipitation, bio-desaturation, and biofilm and biopolymer formation utilize geochemical reactions regulated by biological processes to enhance physical (e.g., grain size distribution, void ratio/density), hydraulic (e.g., permeability, fluid bulk modulus, water content and soil-water-retention), mechanical (e.g., cohesion, friction angle, stiffness), and dynamic (e.g., shear modulus and damping) properties of soils. Through the better understanding of biological processes and their effects on hydro-mechanical and dynamic soil properties in recent years, this new field has shown the potential to meet society's ever-expanding needs for innovative and sustainable treatment processes that can improve soils that support new and existing infrastructure. The application of biological processes for soil improvement in geotechnical engineering has been recognized as one of the priority research areas in the new millennium by the United States National Research Council (NCR, 2006).

To date, two bio-mediated processes including Microbial Induced Calcite Precipitation (MICP) and Microbial Induced Partial Saturation (MIPS) are identified and investigated as potential means to improve dynamic performance of soils, specifically their liquefaction resistance (Dejong et al. 2013). MICP is a soil improvement process that is catalyzed by a broad range of microbial metabolic activities, resulting in precipitation of calcite. The precipitated calcite bonds with soil particles, changing the physical, mechanical, and hydraulic properties of the soil (Dejong et al. 2013). Calcite precipitation can be achieved by various bio-mediated processes including urea hydrolysis, denitrification, and sulphate reduction among others (DeJong et al. 2010). The process can be catalyzed by indigenous soil biota (bio-stimulation) or by providing necessary

bacteria or enzymes to accelerate the process (bio-augmentation). The feasibility of MICP as a sustainable improvement technique has been explored for various geotechnical applications including reduction of wind and water-induced erosion (Bang et al. 2010), improving resistance against static and cyclic induced liquefaction (Montoya et al. 2013; Zamani and Montoya 2019), slope and soil cut stabilization (van Paassen 2011), and reducing swelling potential in clayey subgrade (Islam et al. 2020). Research has shown that MICP treatment can lead to comparable improvement levels to conventional methods (e.g., cement treatment). For example, Burbank et al. (2013) compared the ratio of cyclic stress ratio required for liquefaction of MICP treated soil to that of untreated soils with those obtained from cement treatment and revealed that 2.2-2.6% calcite precipitation results in similar improvement in liquefaction resistance to 2% Portland cement treatment. Microbial induced partial saturation (MIPS) using anerobic biological reactions is another process that is utilized to mitigate excess pore pressure generation in soils (Rebata-Landa and Santamarina 2011). The following section provides a theoretical background on this method.

2.3.   MICROBIAL INDUCED PARTIAL SATURATION (MIPS)

Induced partial saturation (IPS) has become popular in geotechnical and geo-environmental engineering to enhance undrained shear strength and liquefaction resistance of soils (Okamura and Soga 2006; Yegian et al. 2007; Okamura et al. 2011; Rebata-Landa and Santamarina 2011; Eseller-Bayat et al. 2013; He et al. 2015; Mele et al. 2019), decrease primary consolidation settlement (Puzrin et al. 2011), control the hydraulic conductivity of soils (Dror et al. 2004), and/or promote in situ bioremediation (Fry et al. 1997). Specifically, IPS may be an attractive, non-disruptive and cost-effective alternative option to other conventional earthquake-induced liquefaction mitigation methods such as densification and cementation. Previous research has shown that even a small

reduction in soils' degree of water saturation can significantly reduce the rise of pore water pressure and consequently reduce soils' susceptibility to liquefaction (Chaney et al. 1979; Yoshimi et al. 1989; Yegian et al. 2007).

Historically, several techniques have been implemented to reduce the liquefaction potential through induced partial saturation. More recently, a technique to implement anaerobic microbial respiration to induce partial saturation for liquefaction mitigation was proposed by Rebata-Landa and Santamarina (2011). They reviewed CO_2, H_2, CH_4, and N_2 as the most common biogenic gases found near the surface. Nitrogen gas (N_2) produced by denitrification, a microbial-mediated anaerobic dissimilatory reduction of nitrate, presents a highly suitable biogenic gas since it is neither explosive nor greenhouse; it is chemically inert and has very low solubility in water. Microbial Induced Partial Saturation (MIPS) using denitrification offers the following advantages: (1) it introduces a non-disruptive, cost-effective method, which could potentially be used under or around existing infrastructure; (2) it forms comparatively uniform distribution of bubbles in saturated soil if nutrient liquid is injected in relatively homogeneous soil with consistent bacterial cell distribution; and (3) interestingly, biological denitrification can also induce calcium carbonate ($CaCO_3$) precipitation and enhance soils' hydro-mechanical properties through cementation (O'Donnell et al. 2017b; a; Pham et al. 2017, 2018).

Biological denitrification is the microbial-mediated dissimilatory reduction of one or both ionic nitrogen oxides to dinitrogen and nitrous oxide gas. An alternative dissimilatory reduction pathway for nitrate and nitrite, called Dissimilatory Nitrate Reduction to Ammonium (DNRA), may occur with major ammonia production (Kraft et al. 2011). The ratio of carbon-to-nitrate would control the relative contribution of denitrification versus DNRA (Kraft et al. 2011). DNRA does not produce gas(es) and can potentially compete with denitrification, albeit at a lower overall rate.

11

Typically, denitrifiers constitute 0.1-5% of the total soil population and up to 20% of total microbial biomass. Based on the type of electron donor, they can be categorized as heterotrophic or autotrophic. Heterotrophic denitrification uses an organic carbon electron donor such as methanol, ethanol, or acetic acid and is mediated by a wide spectrum of bacteria such as *Pseudomonas, Paracoccus, Flavobacterium, Alcaligenes*, and *Bacillus* spp. (Park and Yoo 2009). On the other hand, the autotrophic denitrification process utilizes inorganic compounds (e.g., CO_2) as the carbon source and inorganic elements including hydrogen gas and sulfur compounds as the electron donor (Sierra-Alvarez et al. 2007; Karanasios et al. 2010). The stoichiometric relationships describing these processes are presented in Table 2-1.

Table 2-1. Denitrification stoichiometric relationships.

Mode	Substrate	Reaction
Heterotrophic	Ethanol	$5C_2H_5OH + 12NO_3^- \rightarrow 6N_2 + 10CO_2 + 9H_2O + 12OH^-$
Heterotrophic	Methanol	$5CH_3OH + 6NO_3^- \rightarrow 3N_2 + 5CO_2 + 7H_2O + 6OH^-$
Heterotrophic	Acetic acid	$5CH_3OO^- + 8NO_3^- \rightarrow 4N_2 + 10CO_2 + H_2O + 13OH^-$
Autotrophic	Hydrogen gas	$2NO_3^- + 5H_2 \rightarrow N_2 + 4H_2O + 2OH^-$
Autotrophic	Sulphur	$6S + 6NO_3^- + 2H_2O \rightarrow 3N_2 + 5SO_4^{2-} + 2H^+$

Microbial-mediated denitrification is catalyzed through a battery of reactions by the action of four independent and intracellular enzymes (Kraft et al. 2011) (Figure 2-1). Depending on the presence of genes that encode the required enzymes for catalyzing reduction steps, denitrification may not always lead to N_2 production. NO or N_2O may come as the final product instead, which is often considered to be "incomplete" (Saggar et al. 2013). Several environmental factors have been reported to impact denitrification including enzyme activity, denitrification rate, and relative

proportions of NO, N₂O, and N₂. The most influential parameters in complete denitrification are C (organic electron donor) availability and C/N ratio (Akunna et al. 1992; Yang et al. 2012), soil moisture and dissolved oxygen (DO) (Smith and Tiedje 1979; Yang et al. 2012), temperature (Saggar et al. 2013), and soil pH (Weier and Gilliam 1986; Saggar et al. 2013) among other factors (e.g., the nutrient concentration, the metabolic state of the organism, and the co-existence of this organism with other native soil microorganisms). It is generally considered that higher organic carbon concentration increases the reduction of N_2O to N_2. However, denitrification reactions at anaerobic digesters with rich electron donor mainly occur via DNRA, resulting in higher ammonium production (Smith and Tiedje 1979; Akunna et al. 1992; Yang et al. 2012). Denitrification rate increases with increasing soil moisture and N_2 becomes the dominant end-product in saturated soils with low concentrations of dissolved oxygen (Smith and Tiedje 1979; Yang et al. 2012). Previous work has demonstrated lower N_2 to N_2O ratio and denitrification rate in the temperature range of 2 to 25°C (Maag and Vinther 1996; Saggar et al. 2013). It is generally accepted that denitrification rate and N_2 to N_2O ratio are higher in neutral and slightly alkaline soils (Šimek and Cooper 2002). Among environmental factors, pH and temperature are more difficult to manage and thus more crucial in the process of desaturation.
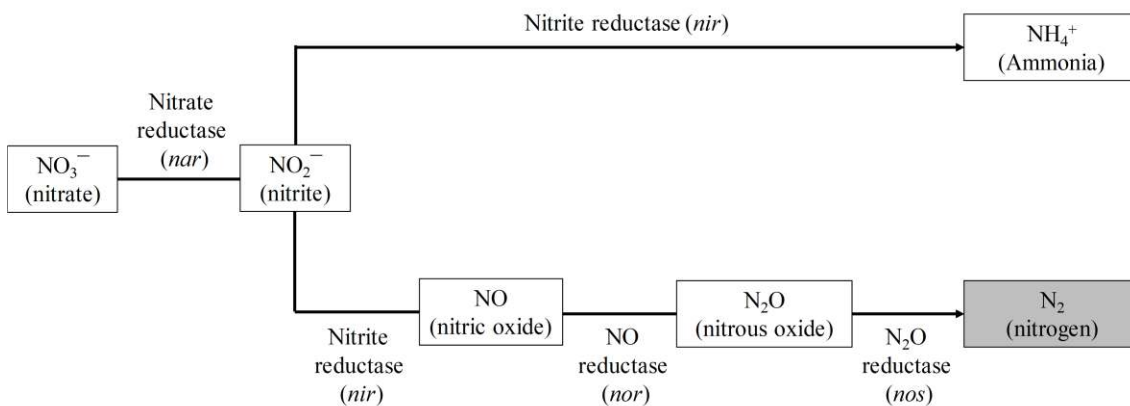
Figure 2-1. Dissimilatory reduction of nitrate, enzymes and products (Kraft et al. 2011).

2.4.   PHYSICS OF GAS BUBBLES IN POROUS MEDIA

The entrapment of gas in porous media has been studied in many fields such as soil science, petroleum engineering, and hazardous waste (Fry et al. 1997; Guarnaccia et al. 1997; Rouf et al. 2016). Two mechanisms of gas entrapment are reported in the literature: 1) gas entrapment due to immiscible displacement; 2) entrapment due to exsolution of gas. The first mechanism, reported in soil science, was investigated to understand the effect of entrapped gas due to water table fluctuation (drainage and imbibition) on the hydrology of soil systems (Li et al. 2013). The gas entrapment in the imbibition process is due to existence of pores with high entry capillary pressures (i.e. small pore throats), which restricts water saturation. Capillary forces due to surface tension, viscous forces due to pressure gradient, and buoyancy forces due to density differences between gas and water affect the residual saturation of soil. Gas remains trapped in pores when the capillary forces are higher than viscous and buoyancy forces applied on the bubble (Fry et al. 1997).

In gas exsolution process, gas bubble growth can occur in random nucleation sites and the generated gas bubble can be trapped in random pores, regardless of their size, where the volume of trapped gas depends on number of nucleation sites (Fry et al. 1997). The nucleation of gas bubbles in porous media is thought to start from geo-metrical imperfections (e.g. cavities) in soil particles (Wilt 1986). The nucleated gas bubble can migrate upward due to buoyancy or viscous forces as long as the bubble size is smaller than the surrounding pore throat. Gas bubbles may also get stuck in the pores while merge during migration and form bigger gas bubbles than the surrounding pore throat. The gas entrapment also depends on the gas bubbles growth rate where the gas migration is more likely to happen in slower gas bubble growth (Mahabadi et al. 2018). Once trapped in a pore, the gas remains trapped if the capillary forces are more than the viscous or buoyancy forces (Fry et al. 1997). At this stage, the gas bubble can only grow larger into the

surrounding pores when bubble gas pressure (P_g) surpasses pore water pressure (P_w) plus the threshold pressure required for gas transport beyond the pore scale (e.g. capillary pressure of a surrounding throat). Many mechanisms for gas bubble expansion beyond the pore scale are proposed (Wheeler 1988; Jain and Juanes 2009; Boudreau 2012). However, only two mechanisms are found to provide reasonable, quantitative predictions of bubble internal pressure and its rise through the medium (Boudreau 2012):

(1) Capillary invasion: A bubble can expand by pushing the pore water through pore throats; thus, invading the pore throat without matrix deformation (Figure 2-2a).

(2) Fracture opening: Bubble expansion occurs by overcoming tensile and compressive stresses between particles and fracturing the medium or dilating pre-existing fractures (Figure 2-2b).
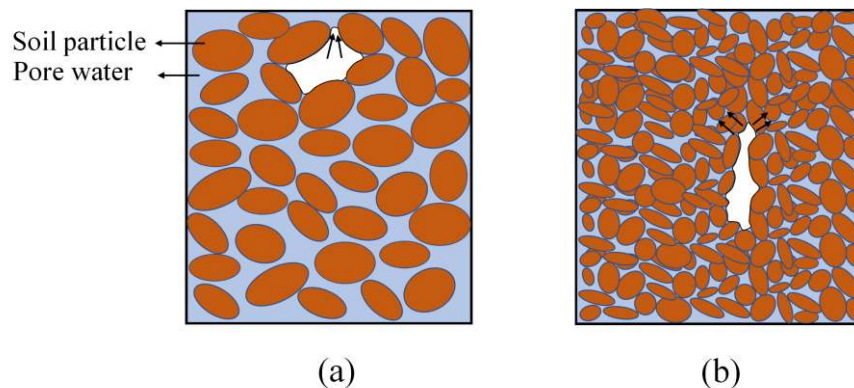
Figure 2-2. Gas transport mechanisms: (a) capillary invasion; (b) fracture opening (after Boudreau 2012).

Capillary invasion occurs if the gas bubble's internal pressure exceeds the capillary pressure as a result of surface tension between gas bubble and soil grains, plus the pore water pressure. Using the Young-Laplace equation for a cylindrical pore and assuming a zero-contact

angle between gas and water, the capillary invasion pressure can be approximated by (Boudreau 2012):

$$P_g - P_w \geq \frac{2T_s}{r_{th}}$$

(2-1)

where r_{th} is the throat radius and T_s is the surface tension between the gas and water (~0.072 N/m for water at 20°C). Jain and Juanes (2009) derived an equation for capillary invasion for a regular 2-D sediment where the gas pressure to invade a throat is inversely proportional to the radius of the grains (r_g), as follows:

$$P_g - P_w \geq \frac{2}{\sqrt{1+(1+\frac{d}{2r_g})^2}-1} \frac{T_s}{r_g}$$

(2-2)

where d is defined as the gap between soil grains. Assuming soil grains are in contact and for 3D condition Equation (2-2) can be written as:

$$P_g - P_w \geq 10\frac{T_s}{r_g}$$

(2-3)

Fracture opening will occur if P_g in a bubble exceeds the sum of the total horizontal stress, σ_h, and the tensile strength, $T_{tensile}$. Assuming Linear Elastic Fracture Mechanics (LEFM) concepts, Jain and Juanes (2009) developed an equation to predict required P_g to fracture a sediment, as follows:

$$P_g - P_w \geq \sigma'_h + T_{tensile}$$

(2-4)

where σ'_h is the effective horizontal stress. The tensile strength resulted from cohesion between particles, capillary forces against fracturing, and length of fracture due to stress concentration at the fracture tip can be defined as (Jain and Juanes 2009):

$$T_{tensile} = C_{LEFM} \frac{T_s (r_g)^{-0.5}}{\sqrt{\pi a}}$$

<div align="right">(2-5)</div>

where a is the half-length of the fracture and C_{LEFM} is a factor that depends on the geometry of fracture (for a disk-shaped fracture $C_{LEFM} = \pi/2$ (Boudreau 2012)).

These equations do not always apply to natural conditions because they do not consider the exact geometry of grains and pre-existing fractures in sediments (Boudreau 2012; Jain and Juanes 2009). However, they provide instructive results by formulating the parameters involved in capillary invasion versus fracture opening. Based on Equations (2-3) and (2-4), both invasion pressures are inversely related to grain size. However, fracture opening pressure is proportional to the square-root of r_g while capillary invasion is proportional to r_g. Therefore, at the same stress level, the fracture-opening transport mode is favored over capillary invasion for finer grained soils. Based on Equation (2-4), fracturing also depends on the soil stress level and could be the dominant gas transport mode at shallow depths (low stresses).

2.5. INTRODUCTION TO UNSATURATED SOIL MECHANICS

Unsaturated soils are typically referred to soils above the water table where soil degree of saturation fluctuates between full saturation and dry condition due to capillary water rise, water infiltration, seasonal fluctuation of ground water, and/or evaporation (Figure 2-3). Existence of air-water-solid interfaces in unsaturated soil can significantly impact the hydraulic (e.g., permeability, pore fluid modulus), mechanical (e.g., shear strength and stiffness), and dynamic (e.g., shear modulus and damping) response of soils (Lu and Likos 2004, 2006; Ghayoomi et al. 2011; Khosravi and McCartney 2012; Dong et al. 2016; Mousavi and Ghayoomi 2018, 2020a; Borghei et al. 2020). The change in soil mechanical properties in unsaturated soils can be attributed to suction development as a result of capillary rise and adsorption. Capillary water is caused by

curved air-water interfaces in pore space because of water surface tension and is the primary mechanism for soil-water-retention (SWR) in intermediate to high saturation levels (i.e., low suction ranges) (Lu and Likos 2004). Adsorption is caused by chemical cementation, van der Waals attraction, and double-layer repulsion and is the primary mechanism for SWR in intermediate to low saturation levels (i.e., high suction ranges) (Zhang and Lu 2020). The capillary suction is the primary mechanism affecting the interparticle stress and stiffness in granular and non-plastic soils while capillary and adsorption both play significant role in stiffness of low to high plastic fines. The matric suction, ψ_m, is commonly quantified as the difference between the air and water pressures:

$$\psi = u_a - u_w \tag{2-6}$$

where u_a= air pressure and u_w= water pressure.
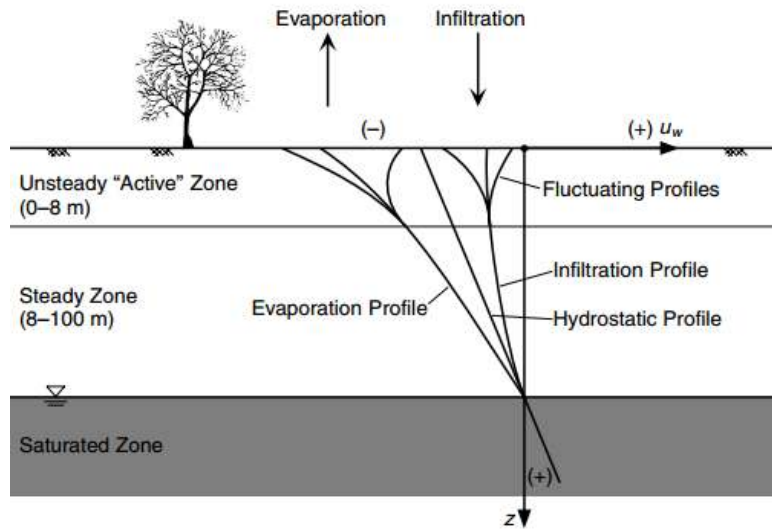
Figure 2-3. A typical soil profile (after Lu and Likos 2004).

18

2.5.1. Soil water retention

The magnitude of matric suction in a soil is a function of the soil type and characteristics and the degree of saturation. The relationship between matric suction and degree of saturation is recognized as a constitutive function and is referred to as Soil Water Retention Curve (SWRC). SWRC is primarily a function of soil grain size distribution and density. Several models are proposed to capture the constitutive relationship between matric suction known as SWRC models (e.g., van Genuchten 1980; Fredlund and Anqing Xing 1994; Lu 2016). For example, van Genuchten (1986) proposed the following equation for estimation of SWRC:

$$S_e = \frac{S - S_r}{1 - S_r} = (\frac{1}{1 + (\alpha\psi)^n})^m \tag{2-7}$$

where S_e= effective degree of saturation, S= soil degree of saturation, S_r= residual degree of saturation, and α, n, and m are empirical fitting parameters. Parameter α represents the inverse of air entry suction, parameter n is related to the distribution of soil pore size, and parameter m controls the shape of SWRC and usually is assumed to be 1-1/n. The air entry suction is defined as the suction level above which an increase in suction level results in dramatic desaturation of soils started from the largest pore (with the lowest capillary suction). Figure 2-4 conceptually shows the location of air entry suction in a typical unsaturated soil zone. Further, Figure 2-5 depicts the location of air entry suction in a generic SWRC (point b) and a conceptual soil element schematic at this location (element b). The SWRC in Figure 2-5 is shown in terms volumetric water content, θ, versus matric suction. The location of the residual degree of saturation inside SWRC and its soil elemental shape are illustrated in Figure 2-5 (point d). Depending on the saturation level between the air entry suction and the residual saturation state, unsaturated soil

zones can be categorized into different regimes with specific characteristics. The distinctions between these regimes are explained in the following section.
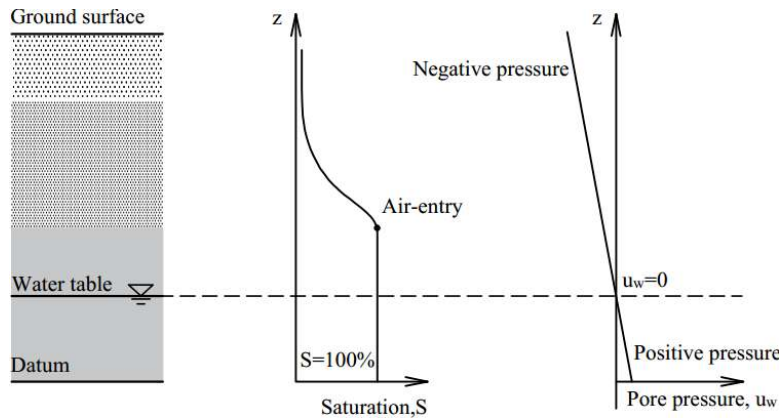
Figure 2-4. A typical unsaturated soil profile along with illustrations of water and pressure profiles (after Lu and Likos 2004).
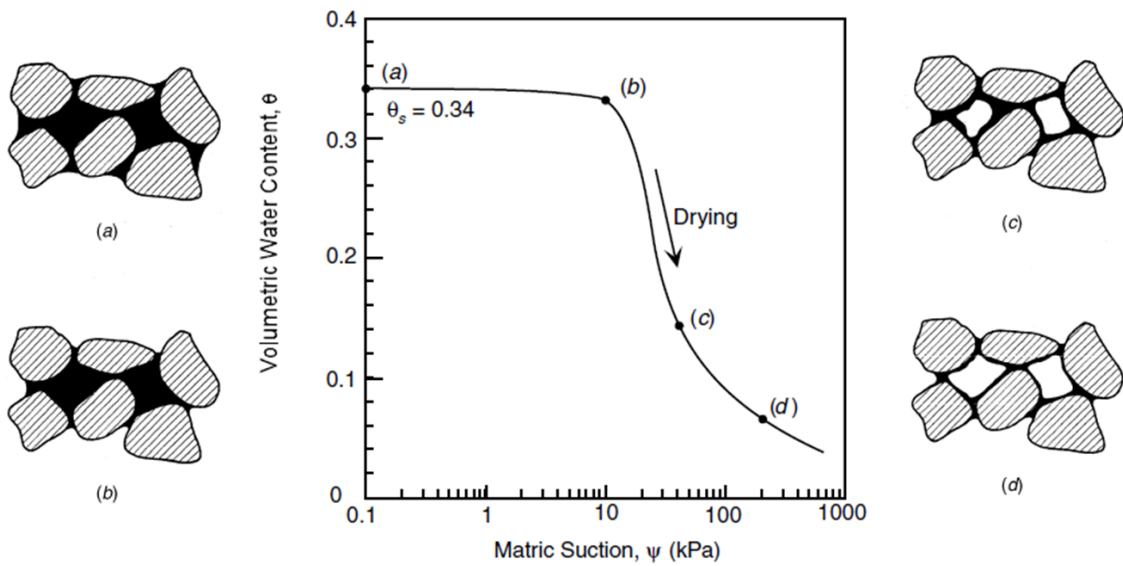
Figure 2-5. A generic SWRC along with conceptual soil elements at different unsaturated soil regimes (after Lu and Likos 2004).

2.5.2. Unsaturated soil regimes

An unsaturated zone encompasses three different regimes: (1) a *capillary fringe* regime located right above the GWT, (2) a *funicular regime* characterized by a continuous water phase, and (3) a *residual* or *pendular regime* characterized by continuous air phase and discontinuous water phase existing in the form of adsorbed water layers around the particles. Figure 2-6 illustrates conceptual soil elements located at in different depths with different unsaturated soil regimes. The first regime is characterized by continuous and nearly water saturated pores with negative pore water pressure. While the negative pore pressure in this zone can significantly impact interparticle forces, the bulk fluid modulus and hydraulic conductivity of soil could be assumed to be the same as fully saturated soil. The height of *capillary fringe* mainly depends on the effective diameter of soil particles (D_{10}), void ratio (e), and soil type and can be estimated by following equation:

$$h_c = \frac{C}{e * D_{10}}$$
(2-8)

where, h_c= height of the capillary zone and C= an empirical coefficient which depends on the angularity and shape of the individual soil grains.
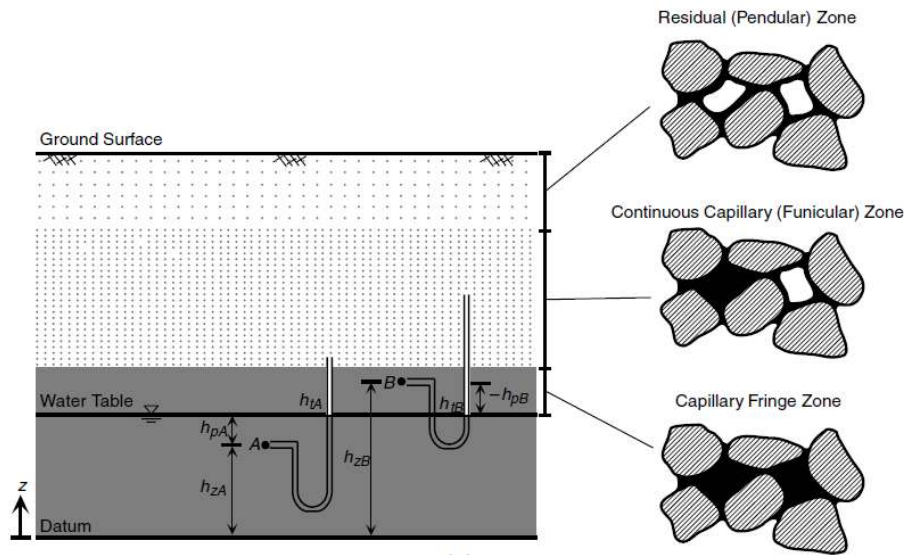
Figure 2-6. A Conceptual unsaturated soil profile along with conceptual soil elements illustrating different unsaturated soil regimes (after Lu and Likos 2004).

In the *funicular regime* the soil dramatically desaturates once the matric suction becomes larger than the air entry value. In this regime, hydro-mechanical soil properties are affected by existence of air-water-solid interfaces. In the *residual regime* the adsorption suction is the main mechanism of controlling soil's dynamic and mechanical response. The impact of adsorption suction is more pronounced in low to high plastic soils compared to non-plastic and granular material.

2.5.3. State of stress in unsaturated soils

Terzaghi (1943) separated the soil particles contact stresses from pore water pressure and introduced the concept of the effective stress in two phase medium (i.e., dry or fully saturated soils), expressed in Equation (2-9):

$$\sigma' = \sigma - u_w \tag{2-9}$$

where σ' is the effective stress and σ is total stress. Equation (2-9) has been found to be considerably accurate for interpretation of mechanical behavior of dry or fully saturated soils and is still being used in current geotechnical practice; however, it may fail to describe the state of stress in a three phase medium. The consideration of three phase interaction forces into mechanical response of soils and definition of state of stress in unsaturated soils has been an area of research for several years. The work was initiated by Bishop (1959) who incorporated the effect of negative pore water pressure in unsaturated soils into the Terzaghi's effective stress principal by introducing a scaling effective stress parameter χ:

$$\sigma' = \sigma - u_a + \chi(u_a - u_w) \tag{2-10}$$

Where the parameter χ is a function of degree of saturation ($0 \leq \chi \leq 1$) and reflects the contribution of matric suction to soil interparticle stresses. Several empirical relationships have been proposed to define the parameter χ. Lu et al. (2010) extended the Bishop's equation by introducing the concept of suction stress and establishing a new effective stress equation as a function of net normal stress, σ_{net} and suction stress, σ_S:

$$\sigma' = \sigma_{net} + \sigma_S \tag{2-11}$$

where $\sigma_{net} = \sigma - u_a$ and $\sigma_S = S_e(u_a - u_w)$. Although Equation (2-11) may provide a basis to interpret the impact of interparticle suction in unsaturated soils with negative pore water pressure, the definition of state of stress for partially saturated soils (i.e., soils containing occluded air bubbles with positive pore pressure) has been under debate. The following section describes different states of saturation and their possible impact on suction stress and effective stress.

2.5.4. States of saturation in soils

Water saturation has significant impact on soils' state of stress and response to static and dynamic loads (Lu et al. 2010; Okamura and Noguchi 2009; Finno et al. 2017). The degree of saturation can affect soils' dynamic response through two potential mechanisms: 1) Existence of gas, even in minute amounts, in pore fluid decreases the bulk modulus of fluid, reduces the excess pore pressure during undrained dynamic loading, and increases liquefaction resistance (e.g., Chaney 1978; ; Yoshimi et al. 1989; Okamura et al. 2009; Yegian et al. 2007); 2) Degree of saturation influences the inter-particle contact forces in three-phase air-water-solid system, changing the effective stress and dynamic properties of soils (e.g., Hoyos et al. 2015). The extent of these effects varies depending on the state of saturation and the soil-water-retention path taken to reach that state.

The distinctions between different states of saturation and their possible effects on dynamic response are highlighted using a generic Soil-Water Retention Curve (SWRC), shown in Figure 2-7. A fully saturated soil at point (a) can follow two different desaturation paths. In a drying path, the soil is allowed to drain under increasing suction from (a) to (b) and (c), continued to a residual water content at point (d). The desaturation can also follow path (a) to (f) where discrete air bubbles are introduced with zero suction and can eventually grow and move towards point (g), although the shape of this path is not known. In the wetting path, water can be introduced to the soil starting from any point on the drying path (e.g., point d), and lead to point (e) with occluded air bubbles. Conceptual schematics of the three-phase soil element at each point are also shown in Figure 2-7.
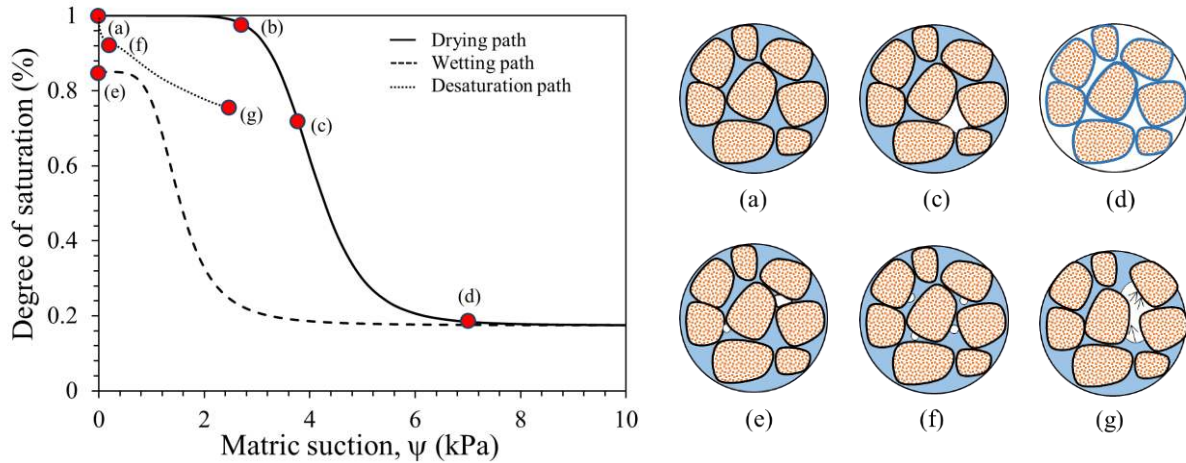
Figure 2-7. A generic soil-water-retention curve along with conceptual three-phase soil element schematics.

The effect of the degree of saturation on the dynamic response of soils should be discussed through consideration of either or both matric suction and pore fluid stiffness. Suction is related to the degree of saturation through SWRC while pore fluid stiffness, K_f, depends on the degree of saturation, the bulk modulus of water, and the bulk modulus of air (Rebata-Landa and Santamarina 2012). The fluid bulk modulus is very sensitive to the presence of gas due to very low volumetric stiffness of gases, where a small volume of gas significantly decreases the fluid bulk modulus and consequently excess pore water generation. The fluid bulk modulus, K_f, can be estimated using the following equation (Eseller-Bayat et al. 2013):

$$K_f = \frac{1}{\dfrac{S}{K_w} + \dfrac{1-S}{K_a}} \tag{2-12}$$

where K_a and K_w are the bulk modulus of gas bubble and water, respectively. The relationship between K_f and the degree of saturation is plotted in Figure 2-8. Six zones of state of saturation are identified and described in Figure 2-7. These zones differ in the state of saturation and the path taken to reach that state. The state of saturation is classified as "fully saturated", "partially

saturated", and "Unsaturated". "Gassy soils" with discrete gas bubbles at high degrees of saturation (Finno et al. 2017) would fall under the partially saturated soil category.
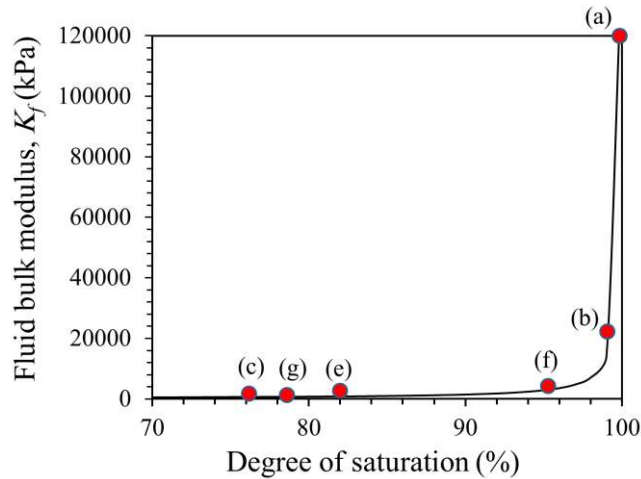
Figure 2-8. Variations of fluid bulk modulus with degree of saturation.

Zone a-b: This zone includes saturated soil matrix below or above the Ground Water Level (GWL), where Terzaghi's effective stress principle is applied and fluid bulk modulus is at its maximum value.

Zone b-d: Point (b) represents the air-entry pressure, where further increase in matric suction (or depth above GWL) from point (b) results in reduction of the degree of saturation. Negative pore water pressure in this zone reflects in inter-particle contact forces, effective stress, and stiffness. The degree of saturation also changes the pore fluid stiffness where only 20% reduction in S_r results in a significant reduction in K_f (Figure 2-8). At point (d), near the residual water content, the pore water exists primarily in the form of disconnected menisci among the soil grains.

Zone d-e: This zone represents the imbibition/wetting process in unsaturated soils at which a decrease in matric suction (or rise in GWL) causes a hysteresis behavior in SWRC of soil. At this zone, for the same matric suction, soil has lower water retention than on the drying path. In addition, even at zero suction, entrapped air is present in soil pores, which can only be dissolved through diffusion of air in water (Fredlund and Rahardjo 1993).

Table 2-2. State of saturation zones and their identifiers.

Zone	a-b	b-d	d-e	e-a	a-f	f-g
S_r (%)	~100	<100	<100	~80-100	~85-100	~85-50
Suction	Zero	Positive	Positive	Zero	Zero	Positive
State of saturation	Fully Saturated	Unsaturated	Unsaturated	Partially saturated	Partially saturated/ gassy soil	Unsaturated
Path	Drying	Drying	Wetting	Wetting	Desaturation	Desaturation
Example Application / type of saturation	Below or above GWL	Above capillary height/ drying	Above capillary height / drying or wet tamped	Below GWL/ suction-controlled or wet tamped	Bellow GWL / IPS	Bellow GWL / IPS by gas exsolution

Zone e-a: At this zone, the soil is fully submerged in water below GWL with approximately zero matric suction (point "a"). The saturation state is classified as partially saturated where the degree of saturation is less than 100% (point "e"). The gas entrapment could be a result of drainage and imbibition process. The volume of the entrapped gas and the degree of saturation at this stage are expected to depend on the soil type and density. Although the presence of gas at this state has a lesser effect on inter-particle forces, it is expected to affect the fluid bulk modulus and undrained dynamic response.

Zone a-f: This zone represents the desaturation process by exsolution of gas (e.g. microbial induced partial saturation) at high degrees of saturation (above ~85%). In this process, tiny gas bubbles are located within soil pores. Theoretical and experimental investigations (Finno et al. 2017) showed that discrete gas bubbles at this state do not contribute to inter-particle suction and changes in effective stress; called partially saturated gassy soils. However, these bubbles significantly impact the pore fluid bulk modulus and pressure response in undrained loading.

Zone f-g: Pore space can be filled with gas by further gas generation or discrete gas bubbles coalescence. At this stage, gas generation inside the pores increases gas pressure and induces capillary suction on soil particles. This results in a transition in saturation state from partially saturated to unsaturated soil (point "f"). The degree of saturation at point (f) in Figure 2-7 depends on the soil grain size and distribution, soil density, and uniformity of bubbles. If gas generation continues beyond this point, the gas pressure rises until: (1) the internal bubble gas pressure surpasses the capillary threshold pressure of a surrounding throat (capillary invasion), or (2) the internal bubble gas pressure overcomes the minimum of soil horizontal or vertical stress in a cohesionless soil (fracture opening). Based on the theoretical framework proposed by Jain and Juanes (2009), the invasion pressure is inversely proportional to grain size. Inspecting this framework reveals that fracture opening mode is more favorable than capillary invasion for finer grained soils. While both mechanisms result in gas loss and lowering the desaturation efficiency, the latter mechanism would lead to the formation of fractures in soil and disturbance of its structure (point "g").

2.6.   EFFECTS OF FINES ON SAND STRUCTURE

The addition of fines into sand can significantly alter the soil's structure. Figure 2-9 illustrates the possible effects of fines on a soil mixture structure for coarse grained, fine grained, and layered soil mixtures. At fines content lower than a threshold fines content (FC_{th}), fines either fill the void space between larger soil particles or are partially in contact with coarse grains. At this state, coarse particles are the dominant means of load transfer and control the mechanical behavior of soil. However, further addition of fines exceeding the FC_{th} transitions the mechanical behavior of soil from a coarse dominant to fines dominant. In this case, the coarse grains mainly exist in floating form surrounded by fines particle (Thevanayagam et al. 2002). The threshold fines content is defined as the fines content at which the structure of soil mixture transitions from coarse dominant to fines dominant and its value is commonly reported to be 20 to 30% for silty sands (Thevanayagam and Mohan 2000).

Recognizing the effects of fines on the structure of soils and its load transfer mechanism, Thevanayagam et al. (2002) proposed an equivalent void ratio, e^*, to interpret the behavior of sands containing fines. Thevanayagam et al. (2002) defined the equivalent void ratio as the void ratio of soil particles that actively participate in load transfer. For FC< FC_{th}, e^* is estimated by the following equation (Thevanayagam et al. 2002):

$$e^* = \frac{e + (1 - b)FC}{1 - (1 - b)FC}$$

(2-13)

where (1-*b*) is the nonactive fraction of fines in the soil mixture and varies between 0 to 1. Parameter *b* can be estimated using the following sem-empirical relationship (Rahman et al. 2008):

$$b = [1 - \exp{(-\frac{0.3\left(\frac{FC}{FC_{th}}\right)}{k}}] \times [r\left(\frac{FC}{FC_{th}}\right)]$$

<div align="right">(2-14)</div>

where $r=$ $d_{50,fines}/D_{10,sand}$ and $k=$ 1-$r^{0.25}$. $d_{50,fines}$ is the median grain size of fines and $D_{10,sand}$ is the lower 10% fractile of the host sand. For fines content higher than FC_{th}, the equivalent void ratio is defined as the void ratio of soil assuming that coarse particles are not present (Thevanayagam et al. 2002):

$$e_f = \frac{e}{FC}$$

<div align="right">(2-15)</div>

Where e_f is the void ratio of the fines' matrix.
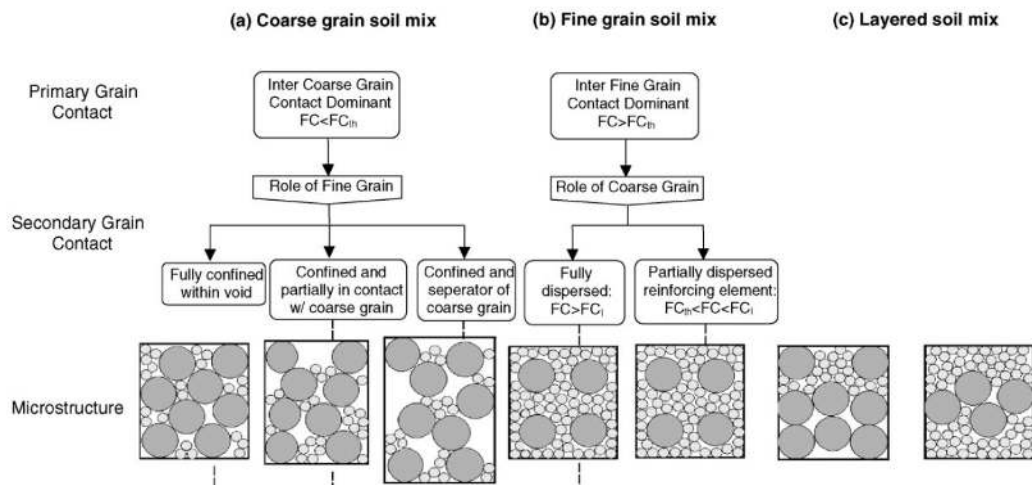
Figure 2-9. Impacts of fines on soil structure (after Thevanayagam et al. 2002).

Fines content also impacts the maximum and minimum void ratio of soil (e_{min} and e_{max}). e_{min} and e_{max} quantify the range of void ratio that a soil can experience. Previous studies have shown that the e_{min} and e_{max} tend to decrease initially with adding fines up to the threshold fines content (Yamamuro and Lade 1998; Thevanayagam et al. 2002). Further addition of fines above

the threshold fines content results in increase in e_{min} and e_{max}. Figure 2-10 illustrates the effect of fines content on minimum void ratio.
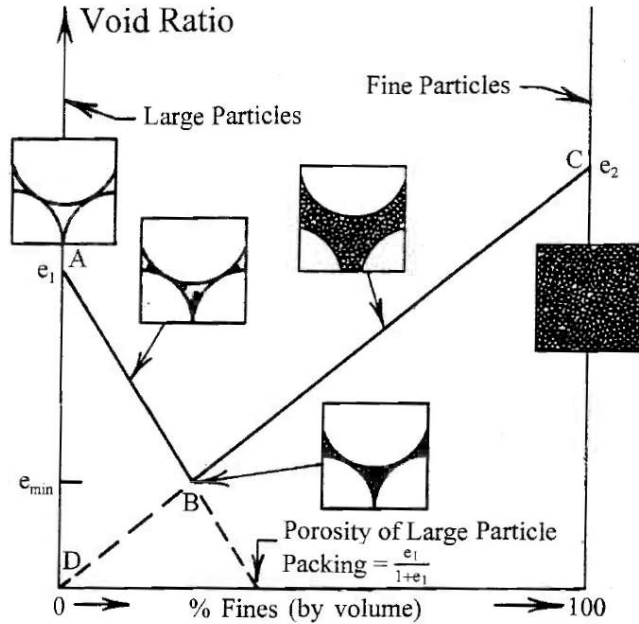
Figure 2-10. Impacts of fines on soil structure (after Lade et al. 1998).

2.7. EXCESS PORE PRESSURE GENERATION AND LIQUEFACTION RESISTANCE OF SOILS

2.7.1. Earthquake induced liquefaction in soils

Soil liquefaction has been a major cause of damage during past earthquakes. Earthquake-induced liquefaction can lead to bearing failure, slope failure, floating of underground structures, settlement, and extreme lateral deformations. Earthquake-induced liquefaction mostly occurs in loose of critical, saturated cohesionnless soils where the soil loses its shear strength during dynamic loading as a result of excessive pore water pressure. The excess pore pressure normalized

31

by initial vertical effective stress is commonly reported as a measure of liquefaction initiation. This ratio is referred to as the excess pore pressure ratio, r_u:

$$r_u = \frac{\Delta u}{\sigma'_v} \tag{2-16}$$

where Δu = the excess pore pressure and σ'_{v0} = the vertical effective stress. Liquefaction initiation is often defined as the condition when the r_u reaches close to 1 (i.e., soil vertical effective stress is close to zero, $\sigma'_v \approx 0$). Several factors such as the number of loading cycles, relative density, confining stress, depositional method, fabric, prior stress-strain history, age, cementation, and other environmental factors impact the resistance of soils (Kramer 1996; Idriss and Boulanger 2006). The liquefaction susceptibility of soils is commonly evaluated by comparing the applied uniform cyclic stress ratio (CSR) and the required CSR to trigger liquefaction (i.e., $r_u \approx 1$ or cyclic shear strain amplitude, $\gamma = 0.3\%$), often referred to as cyclic resistance ratio (CRR). The CSR in a simple shear testing condition is defined as the cyclic shear stress applying on the soil divided by the initial vertical effective stress:

$$CSR = \frac{\tau_{cyc}}{\sigma'_{v0}} \tag{2-17}$$

The CRR for a soil with given initial condition is assessed by conducting tests at different CSR and number of cycles and forming a series of CSR versus number of cycles to cause initial liquefaction plots, as shown for example in Figure 2-11.
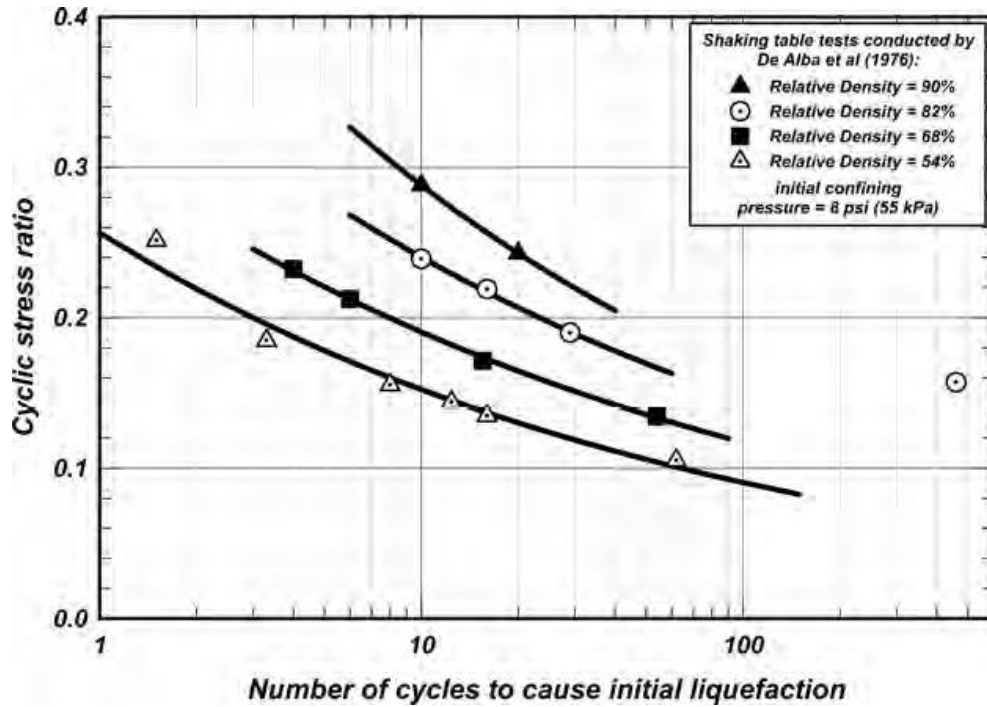
Figure 2-11. Required cyclic stress ratio versus number of cycles to cause initial liquefaction from shaking table tests (De Alba et al. 1976).

2.7.2. Mechanisms of pore pressure generation in soils

High tendency of loose saturated soils to compressive response, the momentary prevention of water drainage, and very high bulk modulus of pore fluid would result in a build-up of pore pressure in response to shaking. The excess pore pressure in soils is related to the volumetric strains $(\Delta\varepsilon_{vd})$ induced by seismic loading (Martin et al. 1975) and can be presented as a function of the volumetric stain increment as well as soil and pore fluid stiffness parameters for one cycle of loading as follows (Martin et al. 1975; Finn et al. 1976):

$$\Delta u = \frac{\Delta\varepsilon_{vd}}{\dfrac{1}{E_r} + \dfrac{n_p}{K_f}} \qquad (2\text{-}18)$$

33

where E_r is the rebound modulus of soil skeleton, n_p is the porosity of soil. The excess pore pressure generation in partially saturated soils can be derived by substituting Equation (2-12) to Equation (2-18):

$$\Delta u = \frac{\Delta\varepsilon_{vd}}{\frac{1}{E_r} + n(\frac{S}{K_w} + \frac{1-S}{K_a})} \tag{2-19}$$

Equation (2-19) indicates the degree of saturation can impact the excess pore pressure generation through two mechanisms; directly through a change in pore fluid bulk modulus and indirectly through a change in induced volumetric deformation. According to Equation (2-19), the excess pore pressure generation in soils decreases as the degree of saturation decreases. Further, the excess pore pressure generation can impact the induced shear strain and volumetric deformations in soils where higher excess pore pressure generation in a seismic event can result in strain softening and higher volumetric deformation in soils. Therefore, partial saturation can also impact the excess pore pressure generation through limiting volumetric deformations in the soil deposits. This is discussed further in section 2.8. In addition to the mechanisms discussed above for partially saturated soils, the excess pore pressure generation in unsaturated soil above the GWT is expected to be impacted by increased suction stiffness which can potentially impact the volumetric deformations in soils (Ghayoomi et al. 2011; Yee et al. 2014).

2.7.3. Impact of the degree of saturation on liquefaction resistance of soils

Several studies investigated the impact of degree of saturation on liquefaction resistance of partially saturated and unsaturated soils. Okamura and Soga (2006) performed stress-controlled cyclic triaxial tests on partially saturated sands and revealed that the increase in liquefaction resistance of partially saturated soils containing occluded gas bubbles (i.e., zero suction condition) can be uniquely related to the elevated potential of volumetric strain due to compression of pore

fluid under undrained dynamic loading. The potential volumetric deformation of soils during undrained loading is mainly controlled by bulk fluid modulus and increases as the bulk fluid modulus decreases (or the degree of saturated decreases). The compression of pore fluid in a partially saturated soil can be obtained by using Boyle-Charles law:

$$u_{a0}V_{a0} = (u_{a0} + \Delta u)(V_{a0} + \Delta V_a) \tag{2-20}$$

where u_{a0} and V_{a0} are the absolute initial pressure and initial volume of pore air, respectively, and Δu_a and ΔV_a are the air pore and volume change due to compression of pore air. If it is assumed that occluded air bubbles have nearly equal pore air and water pressures, the potential volumetric strain during undrained loading, ε_v^*, in a partially saturated soil can be obtained from Equation (2-20) by substituting the absolute water pressure, p_0, for absolute air pressure:

$$\varepsilon_v^* = \frac{\sigma'_{v0}}{p_0 + \sigma'_{v0}}(1 - S)\frac{e}{1 + e} \tag{2-21}$$

Okamura and Soga (2006) proposed the following relationship between ε_v^* and liquefaction resistance of partially saturated sands:

$$LRR = \log(6500\varepsilon_v^* + 10) \tag{2-22}$$

where LRR is defined as the ratio of CSR required to liquefy a partially saturated soil to the CSR required to liquefy the same soil in fully saturated condition.
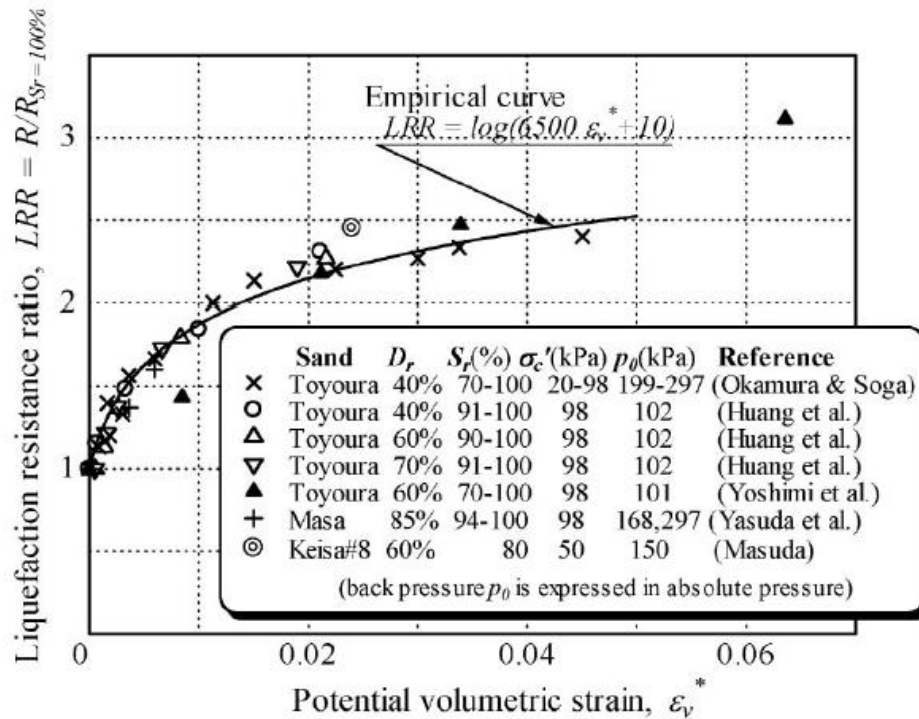
Figure 2-12. Relationship between LRR and potential volumetric strain (Okamura and Noguchi 2009).

Okamura and Noguchi (2009) performed two series of stress-controlled undrained triaxial tests on virtually partially saturated silt with zero suction and unsaturated silt at different suction levels. Based on their experimental results, they demonstrated that, in addition to potential volumetric strain, suction in unsaturated soil has a significant impact on liquefaction resistance of silt, revealing that the liquefaction resistant of unsaturated soils is affected by two mechanisms of bulk fluid modulus reduction and suction development, shown in Figure 2-13.
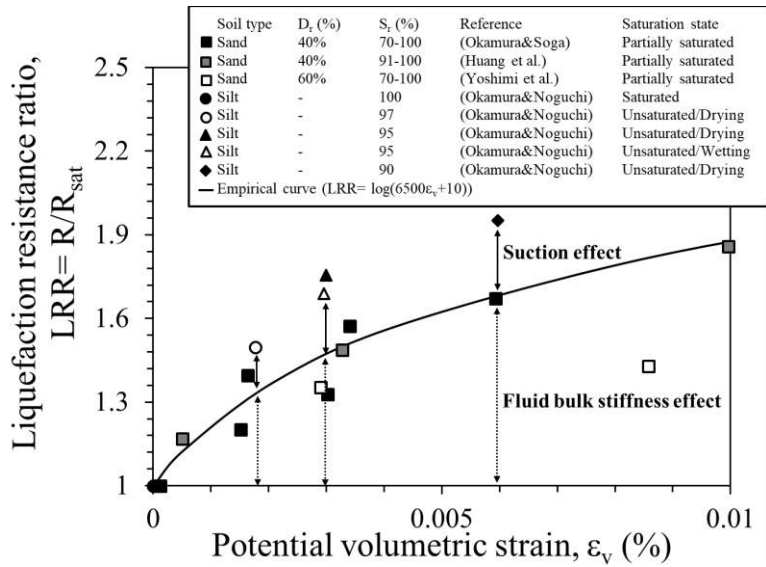
Figure 2-13. Liquefaction resistance ratio vs. potential volumetric strain of unsaturated soils (Okamura and Noguchi 2009).

2.7.4. Induced partial saturation for liquefaction mitigation

Several methods have been developed to induce partial saturation in soils. Such methods either use immiscible displacement of gas, which leaves a residual volume of gas behind (e.g., gas injection, drainage and recharge) (Yegian et al. 2007; Okamura et al. 2011) or are based on exsolution of gas from liquid due to supersaturation (e.g., by chemical reaction, pressure drop, and microbial activity) (Fry et al. 1997; Eseller-Bayat et al. 2013; Mousavi and Ghayoomi 2019). Although the methods in the first category can successfully reduce the degree of saturation, they may not offer effective and non-disruptive measures for sands containing fines. For example, soil drainage and recharge method induces deformation due to the changes of stress while gas injection may cause non-uniform distribution due to the percolation of air bubbles along preferential paths (Rebata-Landa and Santamarina 2011). Further, gas injection may not be applicable for sands containing fines since high gas pressure, required to overcome pores' entry capillary pressure, may

37

exceed the inter-particles contact stresses, which would disrupt the soil matrix by fracturing the soil (Okamura et al. 2011). Gas exsolution techniques are more suitable in terms of application as they are less-disruptive and can be implemented in a wide range of soils as the soil is desaturated by the expansion of bubbles inside the pore space.

Eseller-Bayat et al. (2013) evaluated IPS mitigation of liquefaction by conducting strain-controlled shake table tests on sand specimens mixed with sodium perborate. Their experimental results showed that this technique could achieve a degree of saturation of 40–90%. No initial liquefaction was reported in IPS samples, even at degrees of saturation as high as 90% (Eseller-Bayat et al. 2013) (Figure 2-14). He et al. (2013) performed shake table tests on MIPS treated samples with variable degrees of saturation. Results showed more than 50% reduction in the generated excess pore pressure within desaturated clean sands when the degree of saturation was lowered to 95-80% (He et al. 2013).
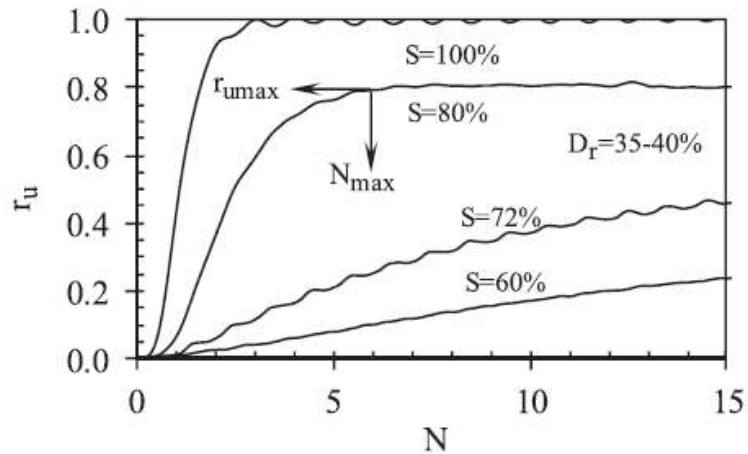
Figure 2-14. Excess pore pressure ratio versus number of cycles (N) (Eseller-Bayat et al. 2013).

2.8. SEISMICALLY-INDUCED SETTLEMENT

Seismic settlement in unsaturated and partially saturated soils may occur under two mechanisms: (1) seismic compression of air voids during shaking, and (2) post-shaking induced settlement due to the dissipation of excess pore pressure (Ghayoomi et al. 2013; Zeybek and Madabhushi 2019). Similar to dry soils, the tendency of soil particles to densify during shaking and the existence of highly compressible air in pores of unsaturated soils allow rearrangement of particles to a denser state which is referred to as seismic compression (Duku et al. 2008). However, low compressibility of pore water may also result in an increase of pore pressure in unsaturated soils at higher degree of saturation under undrained conditions (Unno et al. 2008; Eseller-Bayat et al. 2013; Mele et al. 2019; Mousavi and Ghayoomi 2020a). The increased pore pressure could lead to softening of the soil and consequently significant increase in the induced shear strain levels (Ishihara and Yoshimine 1992). Similar to fully saturated soils, the dissipation of this excess pore pressure after seismic loading results in a volumetric contraction; referred to as reconsolidation settlement (Tokimatsu and Seed 1987; Ishihara and Yoshimine 1992; Ghayoomi et al. 2011). Therefore, seismic settlement in unsaturated soils has the features of both dry soils and fully saturated soils, where matric suction is expected to be the dominant factor in soils with low to intermediate degrees of saturation and excess pore pressure generation and dissipation to be the governing factor in soils with high levels of saturation but similar loading and initial conditions. Ghayoomi et al. (2013) proposed that the seismically induced settlement in soils with variable saturation levels can be approximated through the summation of seismic compression and reconsolidation as follows:

$$\varepsilon_v = \varepsilon_{v-compression} + \varepsilon_{v-reconsolidation} \qquad (2\text{-}23)$$

where ε_v is the total induced volumetric strain, and $\varepsilon_{v\text{-}compression}$ and $\varepsilon_{v\text{-}reconsolidation}$ are the induced volumetric strains due to the seismic compression and reconsolidation, respectively. The following

sections are intended to briefly review the previous research on the reconsolidation settlement and seismic compression of unsaturated and saturated soils.

2.8.1. Reconsolidation settlement of unsaturated soils

Based on laboratory tests and historical post-earthquake reconsolidation settlement data, several semi-empirical predictive methods have been developed and calibrated (Tokimatsu and Seed 1987; Ishihara and Yoshimine 1992; Cetin et al. 2009). Lee and Albaisa (1974) investigated post-seismic settlement of saturated sands and indicated that the volumetric straining is strongly correlated with the excess pore pressure ratio in soils for r_u< 1. Ghayoomi et al. (2013) and Zeybek and Madabhushi (2019) synthesized the relation between pore fluid pressure ratio and post-shaking reconsolidation volumetric strains reported by Lee and Albaisa (1974) and proposed that the post-consolidation strains in unsaturated soils can be estimated based on the strains induced in the same soil in saturated condition and the magnitude of excess pore pressure generation in unsaturated condition; i.e., Equation (2-24):

$$\varepsilon_{v-reconsolidation(unsat)} = f(\varepsilon_{v-reconsolidation(sat)}, r_u) \tag{2-24}$$

However, this equation may only hold valid for seismic demands lower than what is required to fully liquefy the soil in fully saturated condition (Lee and Albaisa 1974; Ishihara and Yoshimine 1992). According to the experimental results by Lee and Albaisa (1974), continued loading following initial liquefaction progressively increases the induced axial strains and can consequently result in substantially higher reconsolidation volumetric strains while r_u remains unchanged (i.e., r_u= 1). In addition, Ishihara and Yoshimine (1992) performed a large number of stress-controlled simple shear tests on fully saturated sands and confirmed this observation. Their results revealed that when the seismic demand is higher than the one required to initially liquefy the soil sample; post liquefaction loading can result in substantial increase (i.e., up to almost 4

times) in reconsolidation settlement of soils (Figure 2-15). Ishihara and Yoshimine (1992) suggested that the amplitude of maximum induced shear strain is the most appropriate parameter correlating the seismic demand to the induced seismic settlement.
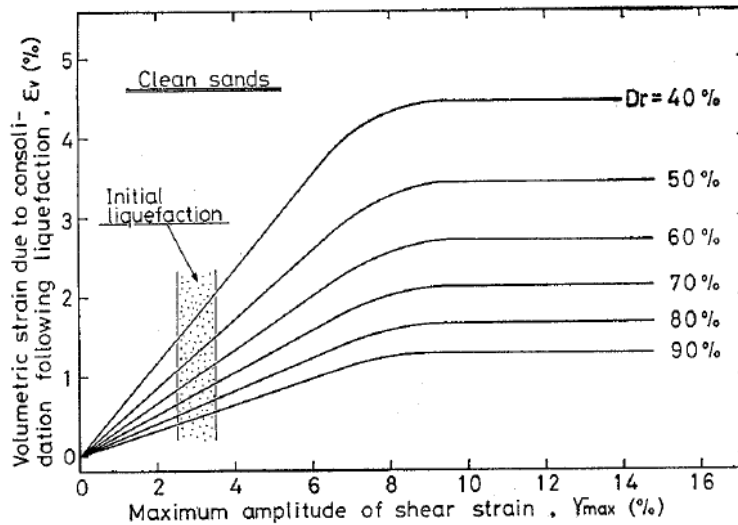
Figure 2-15. Reconsolidation volumetric strains in fully saturated sand versus maximum amplitude of shear strain (Ishihara and Yoshimine 1992).

2.8.2. Seismic compression of unsaturated soils

Previous studies revealed that seismic compression in sands and silty sands is mainly governed by the seismic demand (i.e., effective induced shear strains and equivalent number of cycles) and volumetric deformation characteristics of material (e.g., relative density, fines content, effective stress, and degree of saturation) (Tokimatsu and Seed 1987; Duku et al. 2008; Yee et al. 2014). Several models have been developed to relate volumetric compression to seismic demand and material characteristics (Tokimatsu and Seed 1987; Pradel 1998; Ghayoomi et al. 2013; Yee et al. 2014). These models are simplified since they use an equivalent linear framework to estimate the peak shear strain of each soil layer from its compatible strain-dependent shear modulus and an

41

equivalent cyclic shear stress without consideration of mechanisms of wave propagation in soil deposits. Tokimatsu and Seed (1987) developed a chart solution to correlate SPT blow counts, seismic demand, and seismic compression in dry soils. Pradel (1988) utilized Tokimatsu and Seed's (1987) results and proposed a predictive equation to estimate $\varepsilon_{v\text{-compression}}$ in dry sands. Ghayoomi et al. (2013) adopted this model and proposed that $\varepsilon_{v\text{-compression}}$ in unsaturated sands may be linearly related to the degree of saturation; i.e., Equation (2-25).

$$\varepsilon_{v-compression} = \gamma_e \left[\frac{\left(\frac{D_r}{0.15}\right)^2}{20} \right]^{-1.2} \left(\frac{N}{15}\right)^{0.45} (1-S) \tag{2-25}$$

where D_r= relative density, N= number of cycles, S= degree of saturation, and γ_e= effective shear strain. Further, Yee et al. (2014) investigated seismic compression of unsaturated sand by conducting a series of strained-controlled CSS tests on three natural soils with variable FC, relative density, overburden stress, and seismic demand. They utilized results of the CSS tests plus previous CSS tests on sixteen different sands and a non-plastic silty sands reported by Duku et al. (2008) and Whang et al. (2004) to develop a volumetric strain material model (VSMM) for estimation of seismic compression of sands containing low plasticity fines; i.e., Equation (2-26):

$$\varepsilon_{v-compression} = a \left[\gamma_e - \gamma_{tv}\right]^b (K_{FC})(K_{\sigma,\varepsilon})(C_N)(K_S) \tag{2-26}$$

where γ_{tv} is volumetric threshold shear strain below which cyclic loading does not result in permanent volumetric deformation (Hsu and Vucetic 2004), a and b are fitting parameters, and K_{FC}, $K_{\sigma,\varepsilon}$, C_N, and K_S are reduction factors for fines content, overburden stress, number of cycles, and degree of saturation, respectively. Yee et al. (2014) reported no significant impact of degree of saturation on the compression for sands with FC< 10% and incorporated a step function for the impact of water saturation in the model; i.e., Equation (2-27):

42

$$K_S = \begin{cases} -0.017S + 1 & (S < 30\%) \\ 0.5 & (30\% \leq S < 50\%) \\ 0.05S - 2 & (50\% \leq S < 60\%) \\ 1 & (S > 60\%) \end{cases} \qquad (2\text{-}27)$$

where, K_s is the ratio of volumetric strain in unsaturated soil with a given degree of saturation, S, to that of the dry soil (i.e., $\varepsilon_{v,unsat}/\varepsilon_{v,dry}$). It is noteworthy that (2-27) did not capture the trends of seismic compression with the degree of saturation in one of the three soils tested by Yee et al. (2014) and provided a very approximate estimate for the other two.

Figure 2-16 presents the typical seismic compression values of unsaturated soils using the predictive models proposed by Ghayoomi et al. (2013) and Yee et al. (2014). The data in Figure 2-16 displays the normalized values of estimated volumetric strains in unsaturated soils to their corresponding ε_v in dry condition (i.e., $\varepsilon_{v,unsat}/\varepsilon_{v,dry}$). The amplitude of the induced cyclic shear strain is the key factor affecting the seismic compression where an increase in γ_e results in a substantial increase in volumetric strains (Figure 2-16a). Therefore, the estimation of an equivalent shear strain level representing the irregular earthquake motions in unsaturated soils is of critical importance. Effective shear strain in a soil layer can be calculated using the updated effective stress by iteratively solving the relationship between stress and strain in an equivalent linear system ($\gamma_e = \tau_e/G$) and a shear modulus reduction function. It is well established that the degree of saturation can significantly alter the shear modulus and consequently the induced shear strains in unsaturated soils. Therefore, the degree of saturation may impact both seismic demand and volumetric strain material characteristics during undrained loading. Equations (2-25) and (2-26) consider the impact of suction stiffness on seismic compression both indirectly through updated shear strain and directly through a VSMM (i.e., K_s in Equation (2-26) and (1-S) in Equation (2-25)). The effect of the degree of saturation on the volumetric potential of soils using Equations (2-25) and (2-26) is shown in Figure 2-16b.
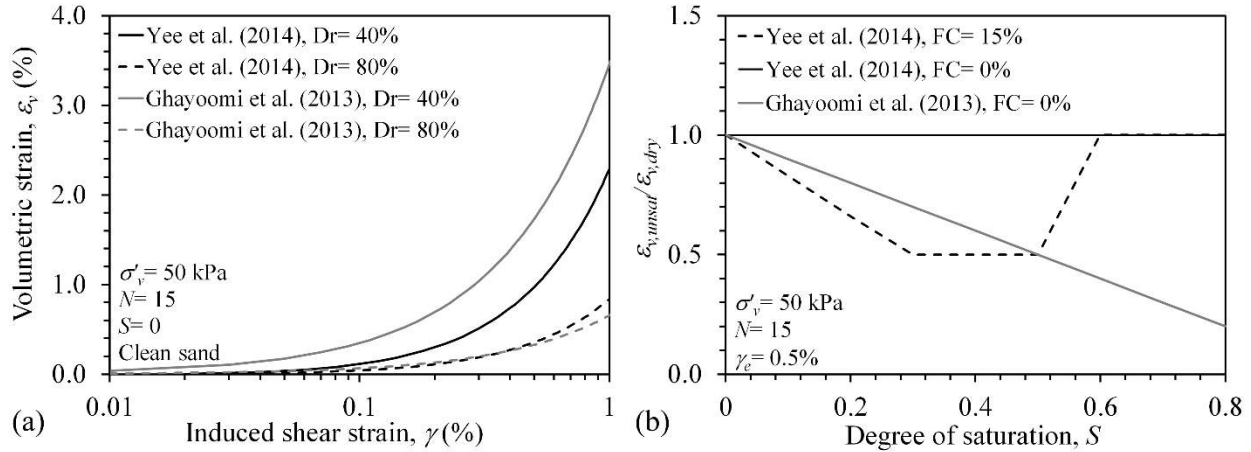
Figure 2-16. Comparisons of Equations (2-25) and (2-26) for estimation of seismic compression in in (a) dry and (b) unsaturated soils.

2.9. DYNAMIC PROPERTIES OF SOILS

The dynamic properties of soils are commonly expressed in terms of dynamic shear modulus and damping ratio. The dynamic shear modulus represents the stiffness of soils in shear while damping ratio represents the amount of energy dissipation during dynamic loading. Several factors including soil type, void ratio, effective mean confining stress, stress history, and degree of saturation can affect dynamic shear modulus and damping ratio of soils (Seed and Idriss 1970; Oztoprak and Bolton 2013; Oh and Vanapalli 2014; Hoyos et al. 2015; Ghayoomi et al. 2017; Le and Ghayoomi 2017; Khosravi et al. 2018). In addition, previous studies indicated that shear modulus and damping ratio are highly controlled by the amplitude of induced shear strain, γ. The strain dependent dynamic soil properties are usually presented in semi-logarithmic plots, as shown in Figure 2-17 and Figure 2-18. In general, shear modulus follows a nonlinear decreasing trend as γ increases while damping ratio follows a reverse trend (Hardin and Drnevich 1972). Depending on shear strain amplitude, shear modulus and damping ratio of soils fall into three major ranges: (1) linear elastic, (2) nonlinear elastic, and (3) nonlinear range. The transition from linear to nonlinear elastic ranges is often marked by the elastic threshold strain, γ_t^e, and the shear strain

44

level that separated the nonlinear elastic to nonlinear range is referred to as the cyclic threshold strain, γ_t^c or volumetric threshold shear strain, γ_{vt}. The γ_{vt} is the shear strain below which shear straining of soil does not result in volumetric deformation and is commonly reported to be around 0.01% to 0.03% for most of sands (Hsu and Vucetic 2004). The maximum shear modulus, G_{max}, and minimum damping ratio, D_{min}, occur at small shear strains in linear elastic range, typically $\gamma <$ 10^{-4}% (Kramer 1996). G_{max} and D_{min} are also referred to as small strain dynamic properties of soil. While dynamic soil properties under shear stains in the elastic ranges are irrespective of the number of cycles imposed on soil element, continuous shear straining of soil at $\gamma > \gamma_{vt}$ results in elevation of shear modulus and reduction in damping ratio, shown for different N values (Figure 2-17 and Figure 2-18).
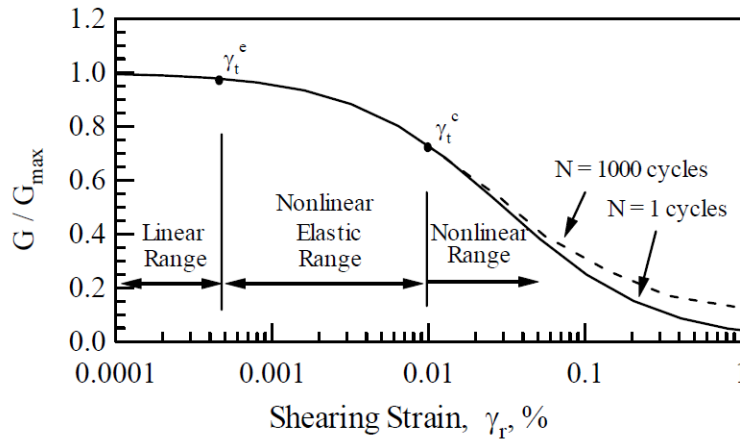
Figure 2-17. Typical normalized shear modulus reduction (Menq 2003).
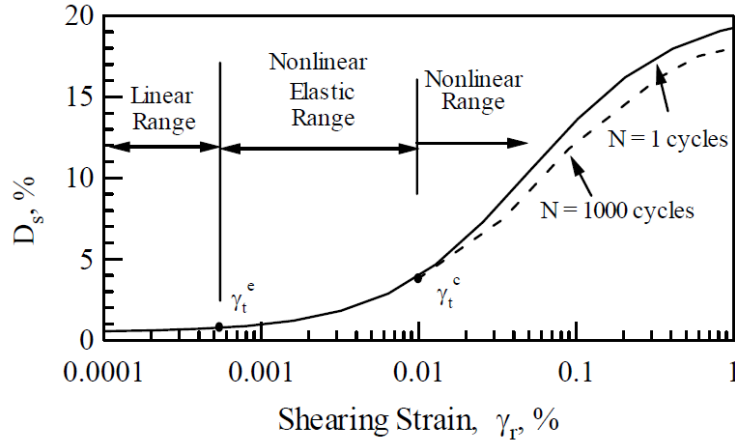
Figure 2-18. Typical damping ratio increase curve (Menq 2003).

2.9.1. Strain-dependent shear modulus

The strain dependent shear moduli are commonly estimated as a function of maximum shear modulus of soils at small strain and the shear stain amplitude. The small strain shear modulus can be obtained directly from geophysical in-situ methods, element scale laboratory tests (e.g., bender element or resonant column tests), or be estimated from empirical methods (Hardin and Drnevich 1972; Seed et al. 1986). For example, Hardin and Black (1966) proposed following equation for prediction of G_{max} in dry or fully saturated conditions:

$$G_{max} = A \times F(e)P_a^{1-n}P'^n \tag{2-28}$$

where A and n= material dependent fitting parameters; p'= mean effective stress, P_a= atmospheric pressure, and $F(e)$= function of void ratio. Table 2-3 presents typical values of A and n for different sandy soils.

Table 2-3. Typical values for parameters *A* and *n*.

Soil type	*A*	*n*	*c*	Reference
Round grain Ottawa sand	7000	0.5	2.17	Hardin and Richart
Angular grained crushed quartz	3300	0.5	2.97	(1963)
Three kinds of clean sand	7000	0.5	2.17	Yu and Richart (1984)
Toyoura sand	8400	0.5	2.17	(Kokusho 1980)

F(e) is commonly expressed as in Equation (2-29):

$$F(e) = \frac{(c-e)^2}{1+e} \tag{2-29}$$

where *c* and is a fitting parameter. Typical values of parameter *c* are presented in Table 2-3. Although Equation (2-28) can estimate G_{max} by considering each soil as a separate material with different fitting parameters, researchers have attempted to correlate the G_{max} of sands containing fines to that of the base clean sand. Several correlations have been proposed by (1) using the equivalent granular void ratio, e^*, instead of *e*, (Thevanayagam and Mohan 2000; Rahman et al. 2008) (2) relating the fitting parameters (e.g., A, n, or c) to soils' fine content (Iwasaki and Tatsuoka 1977; Salgado et al. 2000), or (3) estimating G_{max} using a critical state approach (Hsiao et al. 2015; Yang and Liu 2016; Goudarzy et al. 2018).

The strain dependent shear modulus for nonlinear shear strain amplitudes (i.e., $\gamma > 10^{-4}\%$) are commonly presented using nonlinear hyperbolic reduction functions (Darendeli 2001; Menq 2003; Oztoprak and Bolton 2013). The general form of a hyperbolic modulus reduction model is expressed in Equation (2-30):

$$\frac{G}{G_{max}} = \frac{1}{1 + \frac{\gamma}{\gamma_r}} \qquad (2\text{-}30)$$

where γ_r= reference shear strain corresponding to $\frac{G}{G_{max}} = 0.5$. Menq (2003) conducted a set of torsional shear and resonant column tests on sandy and gravelly soils and modified Equation (2-30) to capture the impact of soil gradation and effective stress on modulus reduction model:

$$\frac{G}{G_{max}} = \frac{1}{1 + (\frac{\gamma}{\gamma_r})^a} \qquad (2\text{-}31)$$

where:

$$\gamma_r = 0.12 \times C_u^{-0.6}(\frac{P\prime}{P_a})^{0.5C_u^{-0.15}} \qquad (2\text{-}32)$$

$$a = 0.86 + 0.1 \times \log(\frac{P\prime}{P_a}) \qquad (2\text{-}33)$$

where C_u= coefficient of uniformity.

2.9.2. Impact of degree of saturation on shear modulus of soils

The proposed equations for estimation of both G_{max} and G suggest that the shear moduli of soils may significantly be influenced by interparticle forces. Most studies on the impact of degree of saturation on soil shear modulus have focused on small-strain shear modulus of unsaturated soils and reported that matric suction generally increases the shear modulus (e.g., Qian et al. 1991, Picornell and Nazarian 1998, Mancuso et al. 2002, Ghayoomi and McCartney 2011; Hoyos et al. 2015). For example, bender element tests by Ghayoomi and McCartney (2011) showed that G_{max} values in unsaturated soil can be approximately 5 to 10% higher than those in dry condition (Figure 2-19). Hoyos et al (2015) conducted resonant column and bender element tests on suction controlled unsaturated silty sands to measure the variations of G_{max} with matric suction level.

Results indicated that an increase in matric suction from 50 kPa to 400 kPa can increase G_{max} of

silty sands up to approximately twofold (Figure 2-20).
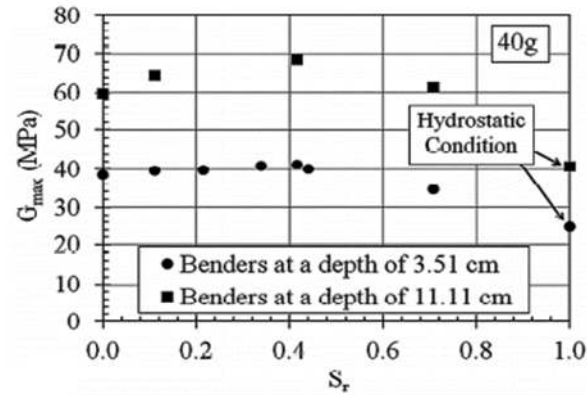
Figure 2-19. Effect of Saturation on G_{max} values of Ottawa sand (after Ghayoomi and McCartney 2011).
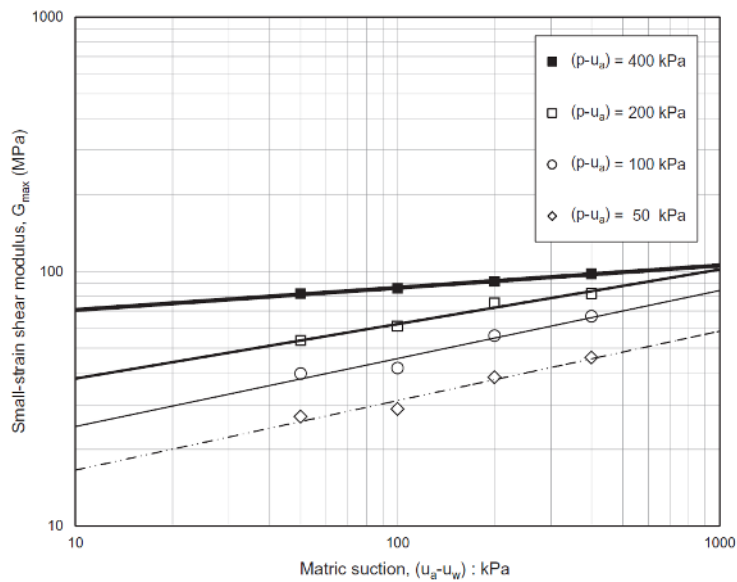
Figure 2-20. Effect of matric suction on G_{max} values of a silty sand (after Hoyos et al 2015).

Although most of these studies reported an increase in shear modulus of soils by decreasing the degree of saturation, little attention has been paid to the effect of the state of saturation on the shear modulus. As discussed, dynamic response is expected to depend on the state of saturation (partially or unsaturated) and the path to that state (drainage and imbibition or desaturation). For example, experimental observations by Kim et al. (2003) on subgrade soils revealed that G_{max} values at a given water content for specimens prepared by controlling water content through wet compaction were significantly smaller than those that were prepared through suction-induced drying path (Figure 2-21). This is likely due to different saturation states in the soil, as wet compaction may lead to entrapment of air in pores at high S. Khosravi and McCartney (2012) discussed how water hysteresis can influence the dynamic shear modulus, shown in Figure 2-22. Their experimental results indicated, at the same suction level, soil specimen tested in wetting path exhibited higher modulus values than those tested in drying path.
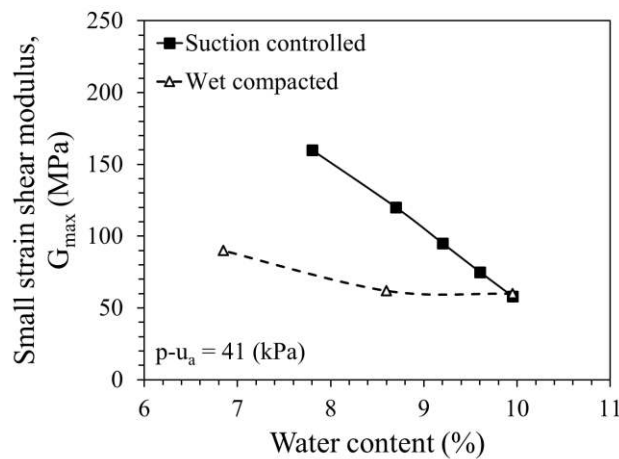
Figure 2-21. Effect of saturation control method on G_{max} (after Kim et al. 2003).
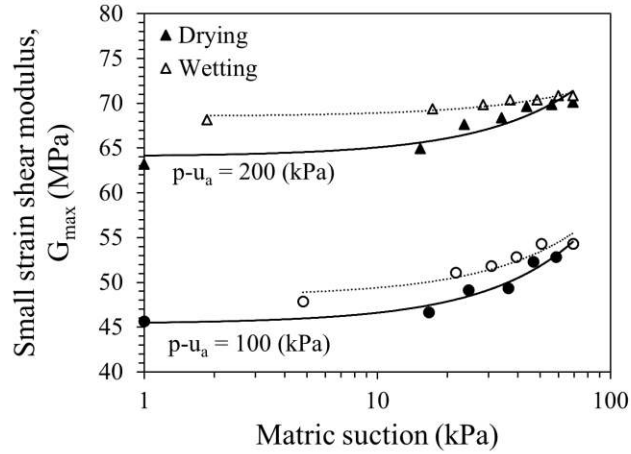
Figure 2-22. G$_{max}$ variation with suction in drying and wetting cycles (after Khosravi and McCartney 2012).

2.9.3. Empirical models for estimation of shear modulus of unsaturated soils

Past studies mostly focused to extend available G_{max} formula by considering the impact of degree of saturation, net normal stress, or matric suction (Mancuso et al. 2002; Sawangsuriya et al. 2009; Khosravi and McCartney 2012; Heitor et al. 2013; Oh and Vanapalli 2014). For example, Sawangsuriya et al. (2009) extended Equation (2-28) for unsaturated soils by considering the net stress, degree of saturation, and matric suction in the following form:

$$G_{max} = A \times F(e)[(\sigma - u_a) + S^\kappa(\psi)]^{\gamma_2} \tag{2-34}$$

where κ and γ_2 are empirical parameters. Oh and Vanapali (2014) suggested that the maximum shear modulus in unsaturated soils can be related to that of saturated soils:

$$G_{max}^{unsat} = G_{max}^{sat}[1 + \zeta\psi S^\xi] \tag{2-35}$$

where ζ and ξ are fitting parameters and G_{max}^{unsat} and G_{max}^{sat} reperesent the small-strain shear modulus of unsaturated and saturated soils, respectively. More recently, Dong et al. (2016)

compiled available literature data and conducted a series of bender element tests and proposed following equation for estimation of G_{max}^{unsat}:

$$G_{max}^{unsat} = G_0^{sat} \left(\frac{1}{S_e}\right)^\beta \left(\frac{\sigma'}{P_a} + 1\right)^{\gamma_0} \qquad (2\text{-}36)$$

where G_0^{sat} is the shear modulus of saturated soil at zero external effective stress condition, and β and γ_0 are fitting parameters. Experimental data by Dong et al. (2016) indicated an average γ_0 of 0.5 and following correlation between β and van Genuchten SWRC fitting parameter n:

$$\beta = 9.6n^{-6} \qquad (2\text{-}37)$$

Although extensive research has been conducted on small strain modulus of unsaturated soils, fewer studies have been performed on the impact of degree of saturation on the strain dependent shear modulus (Hoyos et al. 2015; Ghayoomi et al. 2017; Le and Ghayoomi 2017). Dong et al. (2016) compared results of small strain tests to finite strain tests ($\gamma = 1\%$) and indicated that depending on the strain level, the shear modulus of soils is affected by different mechanisms; while small strain shear modulus is affected by both effective stress and suction stiffness, the shear modulus of unsaturated soils at finite strain is only affected by suction stiffness (Dong et al. 2016).

2.9.4. Damping ratio

Several equations have been developed to estimate strain dependent damping ratio of soils. For example, Menq (2003) proposed an empirical relationship to estimate minimum damping ratio in granular soils:

$$D_{min} = 0.55 * C_u^{0.1} * D_{50}^{-0.3} * \left(\frac{P'}{P_a}\right)^{-0.08} \qquad (2\text{-}38)$$

Alternatively, Seed and Idriss (1970) proposed an empirical equation to estimate maximum damping ratio, D_{max}, exhibited by soils subjected to large strains.

$$D_{max}(\%) = x - 1.5(log_{10} N) \tag{2-39}$$

where, x is a constant value set to be 28 and 33 for clean saturated and clean dry sands, respectively and N is the number of cycles.

The strain dependent damping ratio between the maximum and minimum values are commonly related to modulus ratio (G/G_{max}). For example, Hardin and Drnevch (1972) proposed the following equation for the estimation of strain dependence damping ratio:

$$D = D_{max}\left(1 - \frac{G}{G_{max}}\right) \tag{2-40}$$

Further, Menq (2003) proposed the following expression for the estimation of strain dependent damping ratio:

$$D = b\left(\frac{G}{G_{max}}\right)^{0.1} * D_{masing} + D_{min} \tag{2-41}$$

where D_{masing} is the damping ratio based on Masing behaviour (Masing 1926) and b is a scaling coefficient which depends on the number of the cycle of loading. Despite shear modulus, limited studies were conducted on the effect of degree of saturation on damping ratio of soils (Hoyos et al. 2015; Ghayoomi and Le 2017). In general, previous studies suggested that, as opposed to shear modulus, an increase in matric suction results in reduction in damping ratio (Hoyos et al. 2015; Ghayoomi and Le 2017) (e.g., Figure 2-23). However, based on comparisons of Figure 2-23 and Figure 2-22, one would conclude that the impact of matric suction is more pronounced on shear modulus than damping ratio.
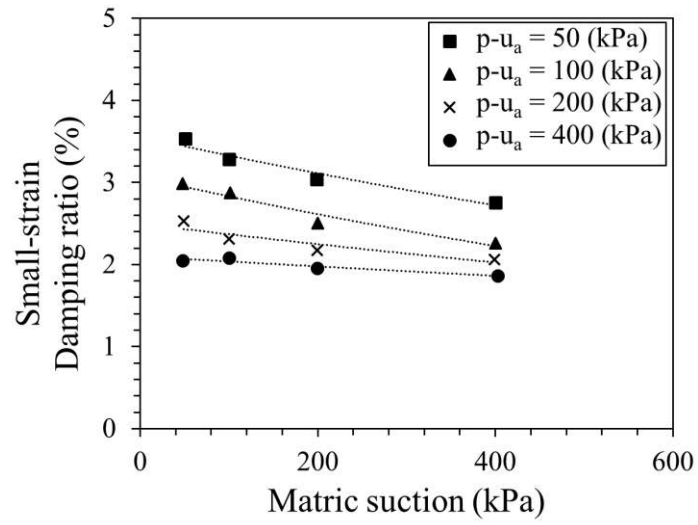
Figure 2-23. Small strain damping ratio variation with suction in suction control unsaturated silt (after Hoyos et al 2015).

CHAPTER 3

EXPERIMENTAL PROCEDURES

3.1. ABSTRACT

The experimental program in this study consisted of two series of bio-denitrification calibration tests and three series of undrained, strain-controlled, cyclic Direct Simple Shear (DSS) tests. The bio-denitrification calibration tests consisted of a series of batch column denitrification tests and a series of soil column denitrification tests to measure the efficiency and performance of denitrification process given different geo-environmental conditions. The cyclic DSS tests involved three series of undrained strain-controlled tests on samples prepared with MIPS, tensiometric suction control, and wet-compaction saturation methods to evaluate the impact of degree of saturation and desaturation method on dynamic response of soil. Following sections describe the materials tested, experimental setup, sample preparation, and testing protocols employed in this study to perform the experimental investigation.

3.2.   BIO-DENITRIFICATION CALIBRATION TESTS

In order to explore the effects of different factors on MIPS, batch and soil column experiments were conducted using a pure culture of denitrifying bacteria. The aim of the batch experiments was to explore the feasibility of controlling gas generation through initial nutrient content. The tests were performed using a mineral medium with different initial concentrations of nitrate and ethanol while measuring the rate of nitrate ($NO3^-$) and nitrite ($NO2^-$) reduction, and nitrogen (N2) production. The soil column experiments evaluated the effects of different compositional and geo-environmental conditions on gas bubble generation and transport inside the soil. Media with different initial conditions were prepared and the degree of saturation was measured to assess changes in rate and final gas generation. The initial conditions were nutrient concentration, pH, and temperature. Additionally, the implementation of a favorable medium and different soil types allowed for independent assessment of the effects of soil matrix and stresses on the attainable degree of saturation and efficiency of gas generation.

3.2.1. Bacterial cultivation and growth media

Paracoccus denitrificans (ATCC 17741), a gram-negative non-motile nitrate-reducing bacterium was used to perform denitrification experiments. The freeze-dried organism was inoculated on a sterilized nutrient agar plate (ATCC medium #3) and the inoculated plate was aerobically incubated at 26°C for 48 hours. Cells from colonies were then grown anaerobically in 100 mL of sterile liquid medium using a sterilized 750 mL reaction vessel. The medium contained 2.0 g KNO_3 and 8.0 g nutrient broth (Difco—Fisher Scientific) in 1 L deionized water. In order to be consistenct in all experiments, the final optical density (OD_{600}) of the inoculum was tested to be the same (~0.22).

A liquid mineral medium was used for denitrification tests. The liquid medium contained 1.5 mM K_2HPO_4, 0.5 mM KH_2PO_4, 0.2 mM NH_4Cl, 0.004 mM $FeSO_4$, $7H_2O$, 0.04 mM $MgSO_4$, $7H_2O$, 0.9 mM $CaCl_2·2H_2O$, and supplemented with ethanol as the electron donor and KNO_3 as the electron acceptor. Different concentrations of ethanol and nitrate at a constant C:N ratio of 1.1:1 were provided in order to obtain the target volumes of biogenic gas. The medium was inoculated with bacterial inoculum and purged with ultra-high pure nitrogen gas for 30 minutes to remove dissolved oxygen (Butler et al. 1994).

3.2.2. Batch experiments

Batch denitrification tests were conducted in 250 mL sterilized reaction vessels with a sampling port at the bottom cap and a gas measurement port at the top cap (Figure 3-1a). The reaction vessels contained 5 mL bacterial inoculum and 195 ml of the mineral medium with two different initial concentrations of ethanol and KNO_3. The initial concentrations of KNO_3 were 2.65 and 20 mM. The cylindrical vessels were sealed by screwing the caps using three threaded rods and were purged by nitrogen gas to remove oxygen in the headspace and placed in an incubator at 26°C. A control test was also conducted with the same medium without the bacterial inoculum.

Measurements of pH were made at the beginning and the end of the experiments. Gas volume and production rate were measured by connecting the top cap port to a manometer. When the gas was generated, it produced pressure in the headspace of the reaction vessels which could change the water level in the manometer. The volume and rate of gas generation were obtained by opening the top cap port at time intervals and recording the water level in the manometer. Nitrate and nitrite concentrations and removal rate were measured by collecting 1 mL samples from the bottom cap port at time intervals. Diluted liquid samples were filtered, and nitrate and nitrite

concentrations were analyzed using a HACH DR/1900 Spectrophotometer with a detection limit of 1 to 60 mg/L NO_3^- and 0.05 to 2 mg/L NO_2^-.
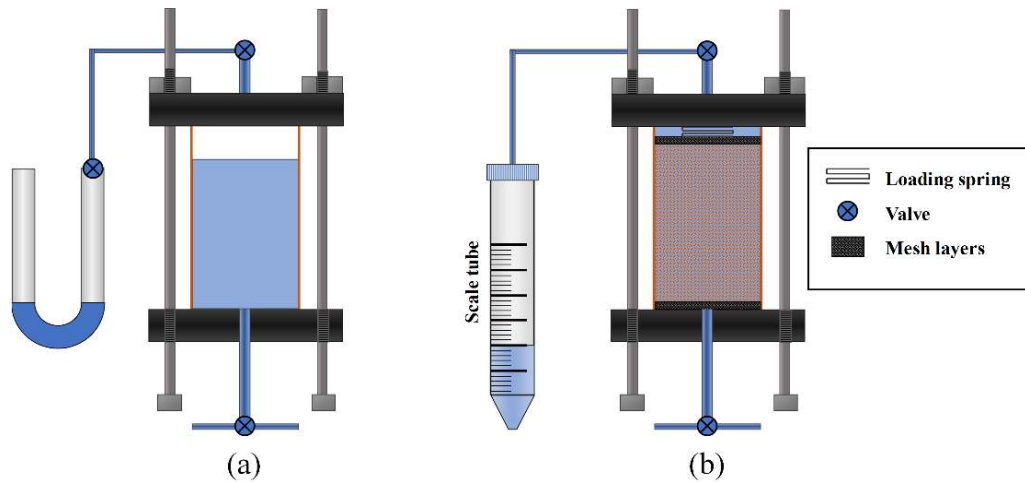
Figure 3-1. Schematic of the reaction vessels for (a) batch experiments and (b) soil experiments (Mousavi et al. 2019).

3.2.3. Soil experiments

Denitrification experiments using *P. denitrificans* were performed in the same reaction vessels as those of batch experiments with two internal mesh layers to prevent soil escape (Figure 3-1b). Four different soils were chosen to study the effects of soil type on denitrification process: (1) Ottawa F-75 sand: a fine poorly-graded sand; (2) sil-co-sil: a silica silt; (3) natural alkaline sand; and (4) natural acidic sand. Sands with various percentages of fines were prepared by mixing Ottawa sand and silica silt. Physical properties of the soils are presented in Table 3-1 with grain-size distribution shown in Figure 3-2 (ASTM D 422).

Soil specimens were prepared using specific amounts of dry soil or soil mixture, air pluviated (Vaid and Negussey 1988) into the reaction vessels to reach target void ratios (0.58, 0.66, and 0.73). The target effective stress was applied by placing a spring on top of the metal

mesh and screwing the caps to compress the spring. An approximately 40 kPa effective stress was applied by inducing a specific deformation to the spring. The carbon dioxide gas (CO_2) saturation method was used to ensure that the samples were completely saturated and anaerobic (Chaney et al. 1979). CO_2 was passed through the specimens for about 20 minutes to replace the air. Then, the samples were flushed from the bottom by the same media as in the batch experiments with different concentrations of nitrate and ethanol. The media had a volume three times the pore volume to ensure saturation. The specimens were placed in an incubator at the desired temperature. Gas volume and production rate were measured by connecting the top cap port to a scale tube. When the gas is generated, it causes the water to flow out of the sample. The accumulated water volume in the scale tube was recorded to obtain the gas volume and production rate.

Table 3-1. Physical properties of soils.

Soil type	Soil type				
	USCS soil classification	Coefficient of curvature, C_c	Coefficient of uniformity, C_u	Specific gravity, G_s	D_{50}
Ottawa F-75 sand	SP	1.74	1.08	2.65	0.19
95%OS+5%silt	SP-SM	0.73	2.04	2.65	0.19
85%OS+15%silt	SM	-	-	2.65	0.16
70%OS+30%silt	SM	-	-	2.65	0.12
Acidic sand	SW	1.2	6.1	2.6	0.5
Alkaline sand	SP	0.9	4.1	2.63	0.56
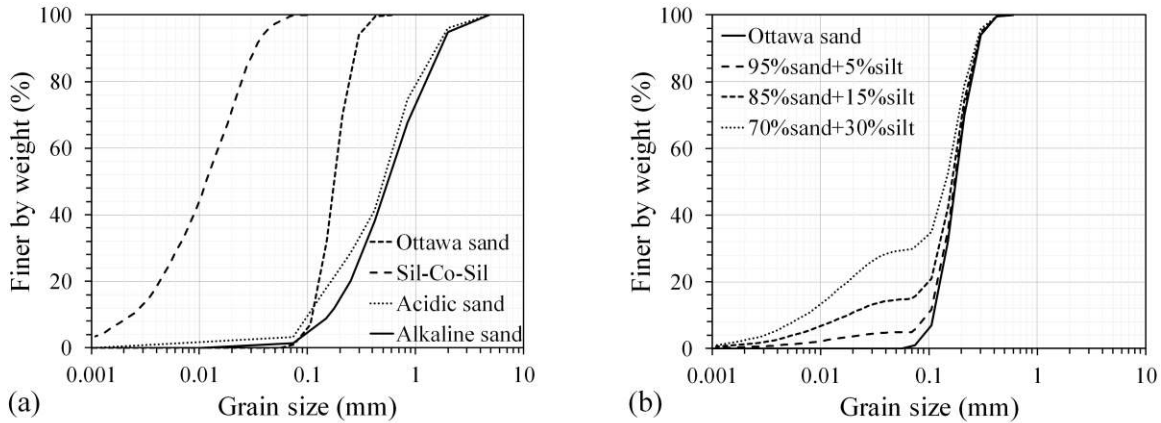
Figure 3-2. Grain size distribution of (a) four tested soils (b) silty sands with different silt contents (Mousavi et al. 2019).

3.3. CYCLIC DIRECT SIMPLE SHEAR TESTS

3.3.1. DSS apparatus

Direct Simple Shear apparatus is a convenient tool for studying and evaluating soil behavior under dynamic loading. This is due to its replication of seismic free-field motion in shear at smaller scale. The advantage of this test compared to other laboratory methods is that it best represents a soil element subjected to "simple shear" loading condition. The main configuration of most direct simple shear apparatuses contains the same mechanical movements and measurements. These systems often keep a constant vertical pressure applied to the top of the specimen while a horizontal static or cyclic shear load is applied to the sample. Then, the corresponding forces and displacements are measured. The variations between these systems are often in the sample containment methods and dimensions. Early developments with DSS involved modifying the soil chambers to be encased in rings (SGI) (Kjellman 1951), hinges (Cambridge device) (Budhu 1984) , or wire-reinforced membranes (NGI) (Airey and Wood 1987).

60

UNH's custom-made DSS system, upgraded for application of a wider shear strain range, houses the soil sample cell based on SGI-DSS configuration in which Teflon-coated aluminum rings and membrane confine the soil. The schematic of the system and specimen cell is shown in Figure 3-3. The machine was modified by incorporating axis translation/tensiometric techniques for suction-controlled testing, as well as adapted for biogas production processes. In order to conduct suction controlled tests, the bottom platen was modified by installing a 50-kPa HAEV disc for tensiometric suction control. The water flux through the ceramic disc was controlled by DigiFlow pump developed by GEOTAC (Houston, Texas). The flow pump enabled precise control of the flow rate and pore water pressure. The pore water pressure was monitored by a Validyne (Northridge, California) differential pressure transducer (DPT) located at the bottom platen external port. Vertical and horizontal loading was controlled through a pneumatic piston and a hydraulic actuator. The horizontal actuator range can produce stable displacements corresponding to strains of 0.001-1% for a 1-inch-tall soil sample. Vertical and horizontal dispacements were monitored through a series of Linear variable differential transformers (LVDT) located on top cap and to bottom platen, respectively. More details on the DSS components, functions, and capabilities are provided in Miller (1994) and Le (2016).
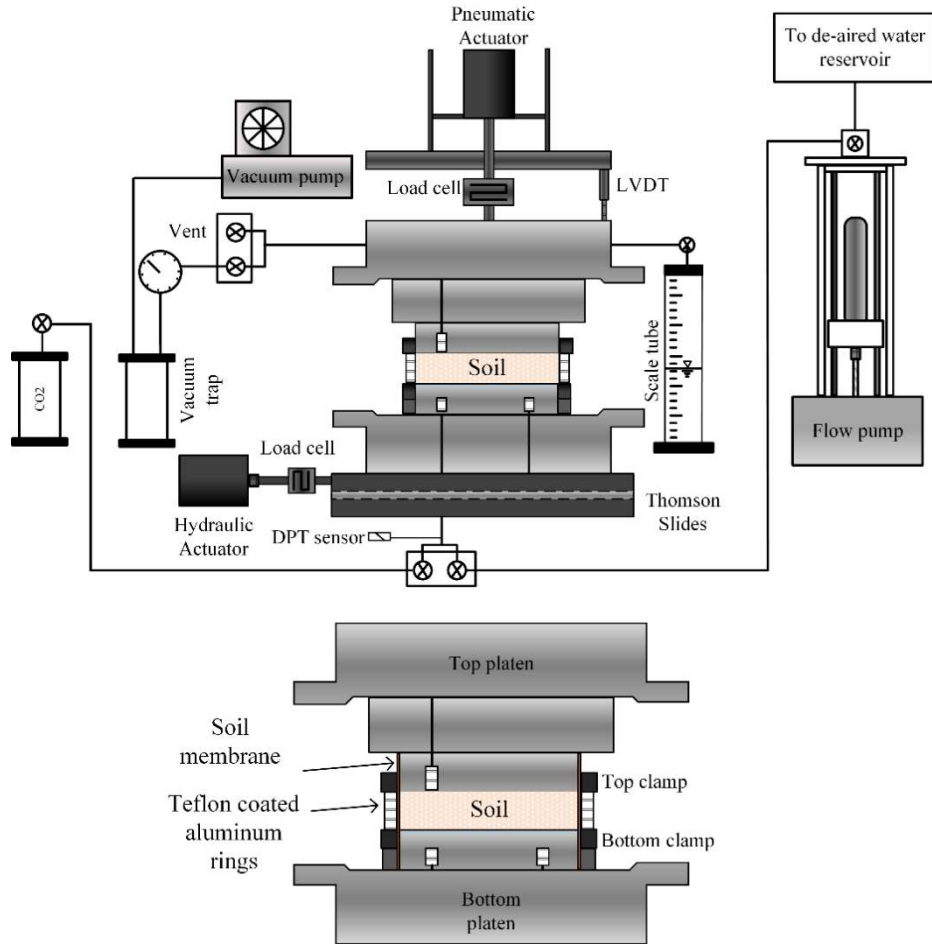
Figure 3-3. Schematic of the modified direct simple shear system and specimen cell at UNH.

3.3.2. Tested materials

Soils tested in this study consisted of reconstituted specimens of sands with different silt contents. The use of sand with different fines content enabled assessment of the impact of degree of saturation on dynamic properties of soils for a wide range of suction levels. The specimens were formed by mixing F-75 Ottawa sand, a uniformly distributed fine sand, and Sil-Co-Sil 52 silt, a non-plastic silica silt, at various fines content (FC); i.e., 0 (clean sand), 10%, and 20% of the

mixture's total weight. Table 3-2 and Figure 3-4 present the physical properties and grain-size distribution of the tested soils, respectively.

Table 3-2. Physical properties of the tested soils.

Property	Soil		
	Ottawa sand	FC= 10%	FC= 20%
Coefficient of curvature, C_c	1.74	1.27	-
Coefficient of uniformity, C_u	1.08	2.7	-
D_{10} (mm)	0.12	0.07	0.01
Specific gravity, G_s	2.65	2.65	2.65
Void ratio limits, e_{min}, e_{max}	0.49, 0.80	0.35, 0.79	0.3, 0.78
USCS soil classification	SP	SP-SM	SM
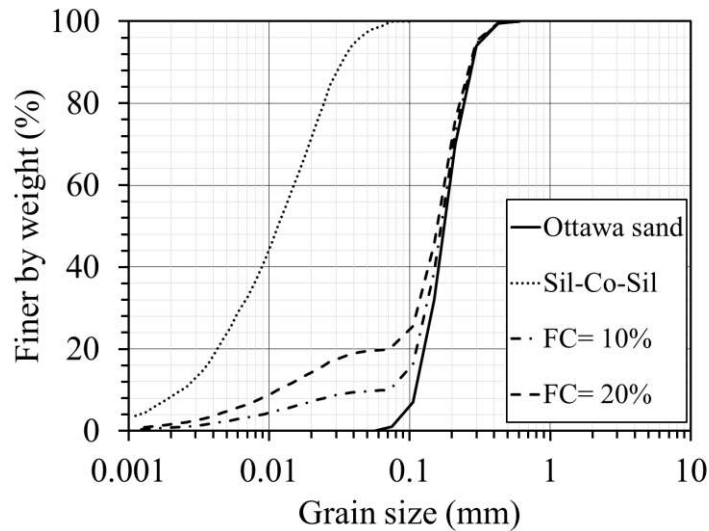
Figure 3-4. Grain size distribution of the tested soils.

3.3.3. Laboratory testing protocols

The testing program for evaluation of dynamic response of unsaturated and partially saturated soils consisted of three series of undrained strain-controlled tests on sand and silty sand samples. Three methods were implemented in this study to capture the different states of saturation discussed in chapter 2. Following sections are intended to describe the implemented procedures to prepare samples for cyclic testing in each method.

Sample preparation and full saturation:

Sample preparation involved a two-layer under-compaction method (Ladd 1978), where the first layer is compacted to a lower density to obtain specimens with uniform density. In this regard, the volume of dry soil required to reach the target relative density is calculated using the phase relationship and by considering the volume of DSS soil cell. Then, each layer was compacted to reach a final relative density of $D_r \approx 55\%$. The final specimen dimensions were 10.2 cm in diameter and ~2.5 cm in height. Before saturation, samples were percolated with carbon dioxide gas (CO_2) for about 20 minutes to ensure full saturation (Chaney et al. 1979). The full saturation of specimens was achieved by flushing de-aired water through the specimen and applying backpressure in incremental steps with pore pressure parameter (B-value) check to dissolve entrapped air. After full saturation, the samples were flushed with de-aired water again to remove the dissolved air and the samples were consolidated at a vertical stress of σ_v= ~50 kPa and an initial pore water pressure of u_w= ~0 kPa. The following sections describe two methods, MIPS and suction control techniques, used to desaturate specimens after their full saturation. The wet-compaction method which involves the preparation of specimens at their as-compacted degree of saturation is also described.

MIPS technique for desaturation of samples:

Saturated soil samples were desaturated using microbial denitrification process, where pore water was replaced by a solution medium containing a mixture of (a) *Paracoccus denitrificans* (ATCC 17741) bacteria; and (b) the nutrient medium containing the mineral salts and ethanol and nitrate at different concentrations while C:N ratio was kept constant (i.e. 1.1:1) for any degree of saturation. Dissolved oxygen was removed by inoculating the nutrient medium with bacterial inoculum and purging it with ultra-high purity nitrogen gas for about 30 minutes (Butler et al. 1994). The solution with three times volume of the soil samples' pore volume was flushed through to achieve full solution replacement. The volume of gas generated in this process was measured using a scale tube connected to the top cap and recording the expelled water as a result of gas formation in the soil pores. Then, the final gas volume was used in estimating the achieved degree of saturation. Details of bio-denitrification process were provided in section 3.2.

Suction control through tensiometric technique:

After full saturation and consolidation of samples at σ_v= ~50 kPa, the tensiometric suction control technique was used to desaturate the specimens. In order to reach the target degree of saturation or suction level, negative pore water pressure in small incremental steps was induced by utilizing the flow pump. In this regard, water was withdrawn from the bottom of the soil specimen by the operation of the flow pump in the withdrawal mode while the top of the specimen was connected to the ambient air. The difference in pressure at the bottom (water) and at the top (air) of the specimen (i.e., matric suction) was measured with the differential pressure transducer. Because the pressures are induced at the boundaries, the system needs to equilibrate throughout the soil to give reasonably uniform matric suction. The equilibrium was achieved when the suction remained constant with negligible outflow of water for at least 10 hours. This methodology has been reported

to represent a compromise between the practical testing time and the equilibration of flow in the specimen (Khosravi and McCartney 2011; Khosravi et al. 2016). The flow pump recorded the amount of drained water from the sample during equilibration which resulted in a precise control of the degree of saturation with time and induced suction. The suction level and degree of saturation at the equilibrium was recorded to obtain SWRC data. The degree of saturation at each equilibrium point was calculated using the volume of expelled water measured by the flow pump and specimen pore volume calculated based on phase relationships. More details about suction-controlled testing using the UNH DSS setup is provided in Le (2017).

Wet-compaction technique:

This method uses the compaction of soil at different water contents (Frost and Park 2003). The two-layer under-compaction method was also adopted to prepare silty sand specimens with different as-compacted saturation levels. Set amounts of water were added to soil mixtures and the materials were cured in a sealed chamber for at least one day to maintain homogenous water content. The target as-compacted degree of saturation was achieved by compacting the moisture-conditioned specimens to similar $D_r = 55\% \pm 5\%$.

DSS cyclic tests

After preparation of soil samples with the desired degrees of saturation or suction levels, cyclic shear strains were applied to the samples using the DSS apparatus. The cyclic tests were conducted in undrained conditions and under constant shear strain levels. All the tests were conducted at 0.1Hz frequency and variable cycles of loading. Variable shear strain amplitudes ranging from 0.01 to 0.4% were applied to the specimens and the response was recorded during and after cyclic testing. Induced shear displacements, induced vertical loads, induced horizontal loads, pore pressures, and vertical displacements were measured during the cyclic testing. Vertical

displacement was also measured after cyclic testing where drainage was allowed for reconsolidation of samples.

3.3.4. Data reduction and analysis

Previous studies using the UNH DSS reported a horizontal movement in the top table (attached to the top of the sample cell) during cyclic loading. The top movement is to be corrected to obtain the net displacement of the sample. Le (2016) performed a series of calibration tests, shown in Figure 3-5 and obtained a function for the calibration of top table movement, D_T, based on induced displacement on bottom table, D_B (Equation (3-1)). The net horizontal displacement is obtained by subtracting the D_T from D_B.
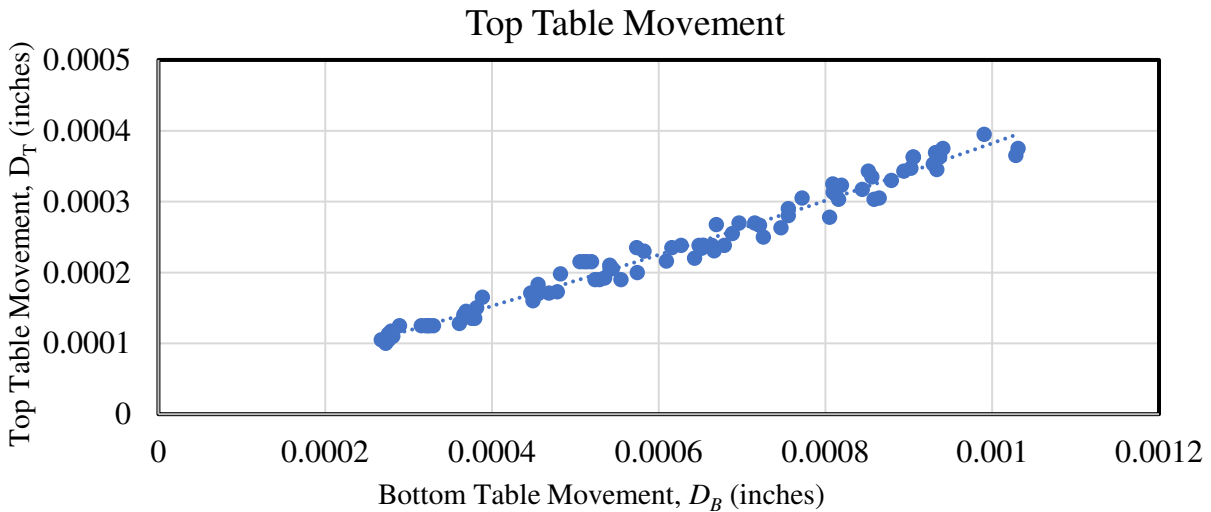
Figure 3-5. Top table movement calibration results (Le 2016)

$$D_T = 55.4D_B^2 + 0.3D_B + 0.00002 \qquad (3\text{-}1)$$

In addition, the measured horizontal load is to be corrected for a friction between sliding components in the DSS. This is performed by using a calibration function that relates net displacement of a sample containing only water to the horizontal pressure response. The calibration function developed by Le (2016) was used to reduce the data for friction.

$$F_H = -46619D_{net}^2 + 0.3D_{net} + 0.0133 \tag{3-2}$$

where D_{net} is the net displacement in inch and F_H is the horizontal friction pressure in psi.

The reduced data including induced horizontal displacement and load, vertical displacement and load, and pore pressure response were used for data analysis. The raw data was filtered using a Butterworth high pass filter for removing possible noises in the data. The reduced horizontal loads were divided by the cross-sectional area of the specimens to obtain the induced shear stresses. Induced horizontal shear strains were calculated by dividing net horizontal displacements by the samples' height. The induced volumetric strains, assumed to be equal to the vertical strains given the constant cross-sectional area in DSS test, were calculated by dividing the vertical deformation by the samples' initial height during both the cyclic tests as well as after the reconsolidation of samples. The secant shear modulus (called shear modulus, G, in this study) at each cycle of loading was obtained from shear stress–strain response of the specimens which typically follows a hysteresis loop (Kramer 1996), as shown in Figure 3-6. The shear moduli were obtained by calculating the slope of a line connecting the minimum and maximum shear strains and the corresponding shear stresses (Kramer 1996) (i.e., line B-B' in Figure 3-6). The damping ratio was obtained by computing the ratio of dissipated energy (i.e., area of hysteresis loop) to total energy (i.e., area of triangles OAB and OA´B´ in Figure 3-6) using Equation (3-3).

$$D = \frac{1}{2\pi}\left(\frac{Area\ of\ hysteresis\ loop}{Area\ of\ traingles\ OAB\ and\ OA'B'}\right) \tag{3-3}$$
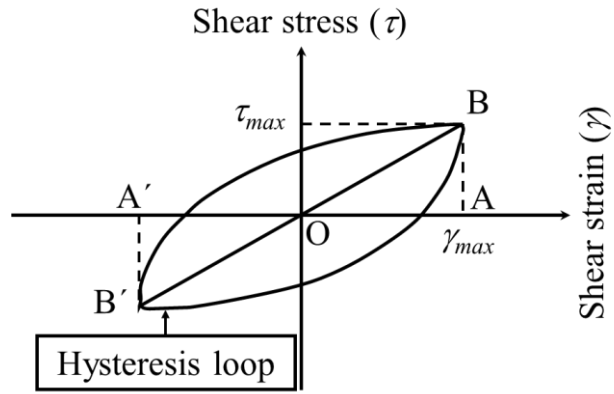
Figure 3-6. A generic strain-stress hysteresis loop.

CHAPTER 4

COMPOSITIONAL AND GEO-ENVIRONMENTAL FACTORS IN MICROBIAL INDUCED PARTIAL SATURATION

4.1.   ABSTRACT

Introducing gas bubbles in saturated soils, even by very small amounts, will increase the liquefaction resistance, especially useful around existing structures. Bio-denitrification through dissimilatory reduction of nitrate to nitrogen gas has been recently implemented as an alternative desaturation technique. In this study, a number of compositional, mechanical, and environmental factors were examined to assess their effects on efficiency of treatment system and retainability of gas bubbles in the soil. Results from denitrification gas generation tests with different initial nutrient concentrations were compared with the expected values predicted from bioenergetic calculations. Soil density, fines content, and overburden stress affected the treatment efficiency and retainability of gas bubbles. Lower degrees of saturation with higher efficiencies could be attained in soils with higher density, fines content, or overburden stresses. However, the results suggested that gas accumulation in pore space is not unlimited. Substantial gas loss from the soil

surface resulted in reduction in treatment efficiency, explained through the effects of potential gas transport mechanisms, i.e. capillary invasion and fracture opening.

4.2.   INTRODUCTION

Induced partial saturation (IPS) has become popular in geotechnical and geo-environmental engineering to enhance undrained shear strength and liquefaction resistance of soils (Chaney et al. 1979; Yoshimi et al. 1989; Okamura and Noguchi 2009; Rebata-Landa and Santamarina 2011; Eseller-Bayat et al. 2013; He et al. 2013; O'Donnell et al. 2017a), decrease primary consolidation settlement (Puzrin et al. 2011), control the hydraulic conductivity of soils (Dror et al. 2004) , and/or promote in situ bioremediation (Fry et al. 1997). Specifically, IPS is an attractive, and non-disruptive alternative option to other conventional earthquake-induced liquefaction mitigation methods such as densification and cementation. Previous research has shown that even a small reduction in soils' degree of water saturation can significantly reduce the excess pore pressure generation and consequently reduce soils' susceptibility to liquefaction (Chaney et al. 1979; Yoshimi et al. 1989; Okamura and Noguchi 2009; Rebata-Landa and Santamarina 2011; Eseller-Bayat et al. 2013; He et al. 2013; O'Donnell et al. 2017a). Induced partial saturation can also enhance the shear strength by generating capillary suction forces (Mousavi and Ghayoomi 2018, 2020a).

Historically, several techniques have been implemented to reduce the liquefaction potential through induced partial saturation. Okamura et al. (2006) showed that sand compaction piles would introduce pressurized air into ground and lower the degree of saturation to less than 77%. Electrolysis of water was proposed by Yegian et al. (2007) to generate oxygen and hydrogen gases in saturated soil specimens. Their experimental results indicated that the electrolysis of water led to reduction in the degree of saturation from 100 to 96.3%. Yegian et al. (2007) also adopted a

drainage and recharge method to reduce the degree of saturation by trapping air bubbles into the soil pores. This method showed a uniform reduction in the degree of saturation up to a limited value of 82-86%. An in-situ investigation by Okamura et al. (2011) demonstrated that pressurized air injection could potentially reduce the degree of saturation to between 68 and 98%. Eseller-Bayat et al. (2013) utilized sodium perborate monohydrate chemical compound, to generate oxygen bubbles in sand specimens. Uniform degrees of saturation ranging from 40 to 100% were achieved based on the initial mass of sodium perborate. The long-term sustainability of gas bubbles inside the soil has also been previously studied. Field investigations by Okamura et al. (2006) demonstrated that air bubbles introduced by application of sand compaction piles in soil deposits remained for several years. Eseller-Bayat et al. (2013) examined the durability of partial saturation under hydrostatic, upward flow and horizontal base excitation conditions, showing that the degree of saturation changed only slightly for a sufficient period of time (~115 weeks).

More recently, a technique to implement anaerobic microbial respiration to induce partial saturation for liquefaction mitigation was proposed by Rebata-Landa and Santamarina (2012). Rebata-Landa and Santamarina (2012) reviewed CO_2, H_2, CH_4, and N_2 as the most common biogenic gases found near the surface. Nitrogen gas (N_2) produced by denitrification, a microbial-mediated anaerobic dissimilatory reduction of nitrate, presents a highly suitable biogenic gas since it is neither explosive nor greenhouse; it is chemically inert and has very low solubility in water. Microbial Induced Partial Saturation (MIPS) using denitrification offers the following advantages: (1) it introduces a non-disruptive, cost-effective method, which could potentially be used under or around existing infrastructure; (2) it forms comparatively uniform distribution of bubbles in saturated soil if nutrient liquid is injected in relatively homogeneous soil with consistent bacterial cell distribution; and (3) interestingly, biological denitrification can also induce calcium carbonate

(CaCO$_3$) precipitation and enhance soils' hydro-mechanical properties through cementation (O'Donnell et al. 2017a; O'Donnell et al. 2017b; Pham et al. 2016; van Paassen et al. 2010).

Rebata-Landa and Santamarina (2012) assessed the feasibility of MIPS using a denitrifying bacterial inoculum and a favorable nutrient medium. Different soil types were treated with the media to capture the effect of fines content and soil matrix on production and retention of gas bubbles. The results showed that sands with little to no fines may fail to trap bubbles while more stable degrees of saturation could be achieved when the fines content increases. A similar observation was reported by Istok et al. (2007) where a maximum desaturation of 23% was achieved when enough nutrients were provided to desaturate a coarse-grained soil. He et al. (2013) utilized a nutrient medium and produced enough biogenic gas within days to reduce the degree of saturation of sand down to 80-95%. He et al. (2013) manifested a linear correlation between the gas production and the initial nitrate concentration; thus, the degree of saturation can be adjusted by controlling the nitrate content. The results, however, contrasted with that of Rebata-Landa and Santamarina (2012) and Istok et al. (2007) where a limited reduction in the degree of saturation was observed due to compositional constrains (e.g. gas escape from pore throats).

In addition, although these studies were insightful to feasibility of MIPS as a liquefaction mitigation strategy they were mostly conducted in favorable environmental conditions; thus, they delineated limited knowledge about compositional and environmental constraints. However, the effects of environmental factors such as pH and temperature on denitrification including the process rate and metabolic end products have been discussed (Parkin et al. 1985; Saggar et al. 2013; Saleh-Lakha et al. 2009). It is generally reported that in soils with lower pH and temperature denitrification occurs at lower rate with higher intermediate by-products (e.g. N$_2$O) (Saggar et al. 2013). This study investigates how different compositional factors (i.e. grain size and soil density),

environmental factors (i.e. pH and temperature), and geostatic effective stress may affect the effectiveness and success of MIPS. This involves a set of batch and soil column denitrification experiments with different initial conditions.

4.3. EXPERIMENTAL INVESTIGATION PROGRAM

In order to explore the effects of different geo-enviornmental factors on efficiency of MIPS, batch and soil column experiments were conducted using a pure culture of denitrifying bacteria. The aim of the batch experiments was to explore the feasibility of controlling gas generation through initial nutrient content. The soil column experiments evaluated the effects of different compositional and geo-environmental conditions on gas bubble generation and transport inside the soil. The experimental procedures and material used for batch and sand column tests were described in section 3.2 and a brief review of experimental program is provided in the following sections.

4.3.1. Batch experiments

Batch denitrification tests were conducted in 250 mL reaction vessels contained 5 mL bacterial inoculum and 195 ml of the mineral medium with KNO_3 concentrations of 2.65 and 20 mM. A control test was also conducted with the same medium without the bacterial inoculum. Measurements of pH were made at the beginning and the end of the experiments. Gas volume and production rate were measured by connecting the top cap port to a manometer shown in Figure 3-1. In addition, nitrate and nitrite concentrations and removal rate were measured at time intervals.

4.3.2. Soil Experiments

Denitrification experiments were performed in four different soils. Sands with various percentages of fines were prepared by mixing Ottawa sand and silica silt. Physical properties of the soils are

presented in Table 3-1 with grain-size distribution shown in Figure 3-2 (ASTM D 422). Soil

specimens with different initial conditions were prepared to examine the effects of different

compositional and geo-environmental factors on MIPS treatment process. A compilation of tested

specimens and initial conditions are presented in Table 4-1. The method for sample preparation

and testing procedure was described in section 3.2.3.

Table 4-1. Bio-denitrification soil columns' initial conditions.

Specimen #	Soil type	Initial void ratio	Initial overburden stress, σ' (kPa)	Initial pH/ incubation Temperature (°C)	Initial nitrate concentration (mM)
1,2,3,4,5	Clean Ottawa sand	0.66	0	~7.1/26	2.5,5,10,20,50
6,7,8,9	Ottawa sand+5%silt	0.66	0	~7.1/26	5,10,20,50
10,11,12,13,14	Ottawa sand+15%silt	0.66	0	~7.1/26	2.5,5,10,20,50
15,16,17	Ottawa sand+30%silt	0.66	0	~7.1/26	10,20,50
18,19	Clean Ottawa sand	0.73	0	~7.1/26	5,20
20,21	Clean Ottawa sand	0.58	0	~7.1/26	5,20
22,23	Clean Ottawa sand	0.66	40	~7.1/26	20,50
24,25	Ottawa sand+15%silt	0.66	40	~7.1/26	20,50
26	Natural acidic sand	0.66	0	~5.3/26	5
27	Natural alkaline sand	0.66	0	~7.8/26	5
28	Clean Ottawa sand	0.66	0	~7.1/14	5

4.4. RESULTS AND DISCUSSION

4.4.1. Batch experiments

Results from batch experiments in terms of nitrate and nitrite concentration and volume of

generated gas from manometer readings are shown in Figure 4-1. The initial concentrations of

NO_3^- were 2.63 mM and 19.68 mM, which closely matched the target concentrations of 2.5 mM and 20 mM. The results indicated that NO_3^- reduction occurs in two steps; the reduction of nitrate to nitrite followed by the reduction of nitrite to nitrogen gas. The NO_3^- and NO_2^- were completely removed in both experiments and a considerable volume of biogenic gas was generated during the experiments. However, no changes were observed in manometer readings of the control test. The final generated gas volume in the batch experiment supplemented with 19.68 mM initial nitrate concentration (i.e., 35 cm^3) was approximately 7.5 times greater than the experiment with 2.63 mM initial nitrate concentration (i.e., 4.7 cm^3). This revealed the linkage between the volume of generated gas and the initial concentration of nitrate; thus, the generated gas volume could be adjusted by changing the initial nitrate concentration. A longer lag in gas generation was observed for the experiment with higher initial nitrate concentration. It is well known that NO_3^- has an inhibitory influence on reduction of N_2O to N_2 (Blackmer and Bremner 1978; Weier et al. 1993; Saggar et al. 2013), because the reduction of NO_3^- provides more energy from denitrification than the reduction of N_2O. The denitrification increased alkalinity in the batch experiments by reducing NO_3^- to N_2 (Table 4-2). The pH was elevated from 6.82 to 7.13 and 6.87 to 8.54 by reduction of 2.63 mM NO_3^- and 19.68 mM NO_3^-, respectively. The increase in pH and carbon dioxide production potentially provides a suitable geochemical condition to induce $CaCO_3$. The $CaCO_3$ precipitation can buffer the alkalinity produced as a result of denitrification and bind with soil particles that enhances its hydro-mechanical properties (Hamdan et al. 2017; O'Donnell et al. 2017b; Pham et al. 2017, 2018).

Table 4-2. Initial and final pH in the batch experiments.

Specimen #	Initial NO_3^- concentration (mM)	Initial pH	Final pH
1	2.63	6.82	7.13
2	19.68	6.87	8.54
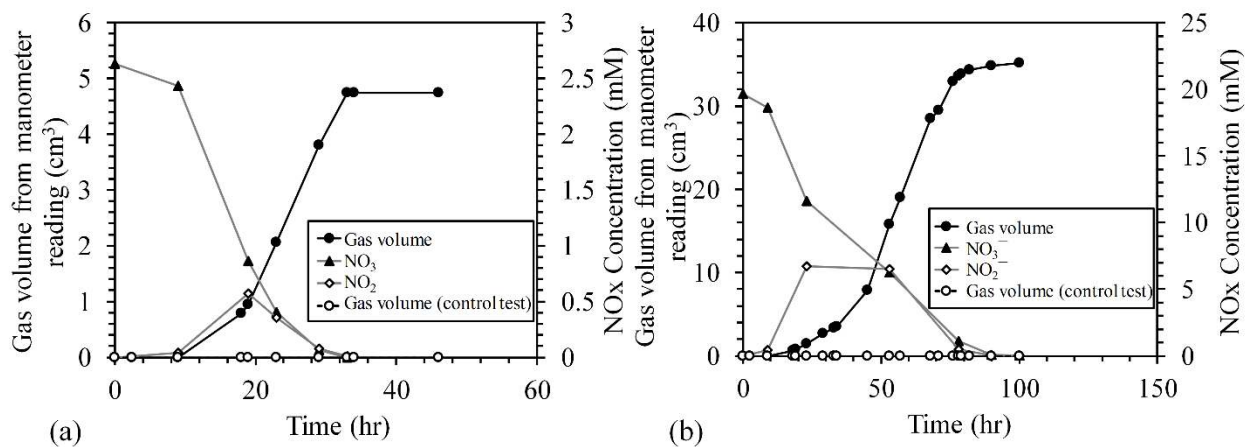
Figure 4-1. Nitrate and nitrite concentration and manometer readings (water level) from the batch experiments with a) 2.63 mM and b) 19.68 mM initial NO3⁻ concentration (Mousavi et al. 2019).

4.4.2. Soil experiments

**Effects of initial nitrate concentration and fines content:**

Figure 4-2 illustrates the effect of initial concentrations of nitrate on the attainable degree of saturation, S_r, of MIPS-treated soil specimens with different fines content. The tests were conducted on samples without any overburden stresses and with the same initial void ratios. Based on the stoichiometry from reduction of NO_3^- to N_2 (Equation 1 in Table 2-1), the expected nitrogen gas generation and subsequently the degree of saturation were predicted using the ideal gas law at

77

299°K assuming atmospheric pressure. Due to very low solubility of nitrogen gas in water under standard temperature and pressure (0.017g/l), it was assumed that most of the N_2 would form gas bubbles and other generated gases like CO_2 would remain into the solution because of their relatively high aqueous solubility (1.5g/l) (Istok et al. 2007; He et al. 2013).

Based on experimental measurements presented in Figure 4-2, the degree of saturation of MIPS-treated specimens was significantly influenced by the initial concentration of nitrate. Regardless of the specimens' fines content, an approximately linear decrease in the degree of saturation was observed when the initial concentration of nitrate was increased up to a critical degree of saturation. In this portion of the initial NO_3^--S_r curves, the S_r values corresponded well to the predicted values indicating that nitrate was completely reduced to nitrogen gas and all generated gas bubbles remained in the pores.
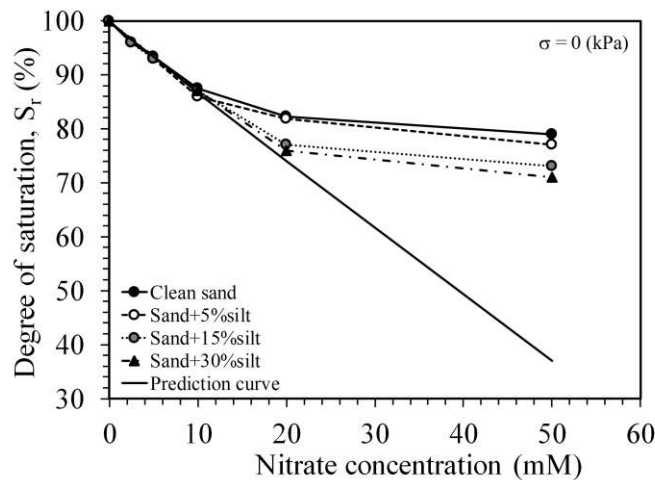
Figure 4-2. the effects of fines content and initial nitrate concentration on biogenic gas generation in soil experiments.

The linear trend in desaturation was followed by a gradual reduction in the rate of desaturation with increasing initial nitrate concentration where a non-linear relation between the initial NO_3^-

and S_r was observed. However, the magnitude of the reduction varied depending on the fines content and was lower at higher fines content. In the non-linear portion of the curves, a discrepancy was observed between the predicted and measured degree of saturations. The most likely reason for this discrepancy is the probable gas escape form the soil. Further gas generation beyond the critical degree of saturation increases the gas bubble pressure and results in capillary or fracture invasion of gas bubbles according to Equation (2-3) and (2-4). The gas invasion enables the gas bubbles to coalesce and form larger bubbles that could eventually rise toward the surface and escape from the soil. Gas clusters rising from the top cap port could be seen by naked eye after the critical degree of saturation which confirmed the fracturing/capillary invasion transport and escape of the bubbles from the soil. However, null to very small gas bubbles were observed in the linear portion of the curves.

In the non-linear portion of the curves, lower degrees of saturation could be achieved in specimen with considerable fines content (15 and 30%) which is a result of higher gas retention. The fine particles fill the pores between the sand particles; reduce the pore throat size and the mean particle size of the soil. This, as discussed earlier in the study, results in higher capillary forces which overcome the buoyancy forces and retain the bubbles inside the pores. The higher retention in specimen with considerable fines content could also be explained based on Equations (2-3) and (2-4). As the pore throat size and particle size decrease, generation of greater pressure is required for gas to invade a throat or fracture the soil. Therefore, it could be hypothesized the higher pressure required for gas transport through the surrounding throats would maintain the gas within the pore, increase its retention in the soil system. Increase in fines content also alters the favorable invasion mechanism from capillary invasion to fracture opening (Boudreau 2012; Jain and Juanes 2009), which can disturb the soil structure and lower the effectiveness of treatment process.

Effect of soil density:

In order to investigate the effects of soil density on gas retention of MIPS-treated specimens, clean sand samples with three different initial void ratios of 0.58, 0.66, and 0.73 were prepared. Figure 4-3 presents variations of S_r for sand specimens with different initial void ratios desaturated with two initial nitrate concentrations of 5 and 20 mM. For specimens with initial $NO_3^- = 5$ mM, the attainable S_r was not significantly affected by the initial void ratio. S_r of sand specimens at this nitrate concentration may not have reached the critical degree of saturation leading to less gas escape. For higher initial concentration of nitrate, the density of sand specimens influenced the reduction in the degree of saturation of the treated specimens. The degree of saturation decreased from 83 to 80% as the void ratio decreased from 0.73 to 0.58. This is due to higher retention of gas bubbles in denser sands. Such behavior could be also explained through Equation (2-1) where the required pressure for capillary invasion is reversely proportional to the radius of surrounding pore throats. As the soil density increases, the pore throat becomes smaller, increasing the required invasion pressure and causing higher gas retention within pores.
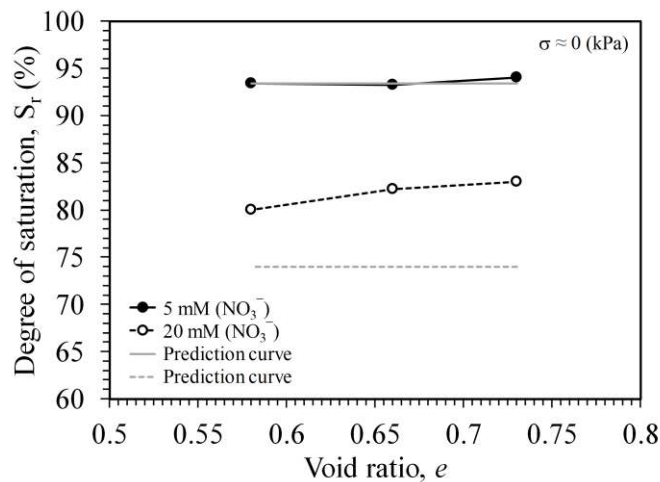
Figure 4-3. The effects of compaction (void ratio) on gas retention of microbial induced partially saturated specimens.

80

Effect of overburden stress:

The effect of overburden stress could be independently discussed for the linear and non-linear portions of nitrate concentration-degree of saturation plots in Figure 4-4. In the linear portion of the curves and before the critical degree of saturation, regardless of the soil type, increase in overburden stress had no effect on the gas retention of the specimens, where most generated gas had remained in the specimens. However, the overburden stress affected the range of linear portion and consequently the critical degree of saturation. This change was more pronounced in the clean sand specimens. It could be hypothesized that the change in the invasion mechanisms could be the most probable reason for this observation. According to Equations (2-3) and (2-4), at low confining stresses, the required gas pressure to fracture soils is lower and, depending on soil particle size, capillary invasion may become the dominant transport mechanism; similarly reported by other researchers (Boudreau 2012; Pham et al. 2016). For example, Pham et al (2016) utilized X-ray CT scanning for MIPS-treated sand specimens via denitrification. They observed that the gas bubble migration towards the sand column surface induced cracks at shallow depths causing fractures at low confinement stress. As the overburden stress increases, the pressure required for fracture opening increases as well Equations (2-4) and capillary invasion becomes the dominant gas transport mechanism. Thus, higher pressure required to invade a throat increases the gas retention of the soil.

The effect of overburden pressure on specimens' gas retention was also observed in specimens treated with high nitrate concentration. The attainable reduction in the degree of saturation of clean sand specimens increased by 49% when the overburden stress increased to 40 kPa. The effect of overburden stress became more pronounced as the fines content increased where the attainable degree of saturation increased by 56% as the overburden stress increased to 40 kPa.
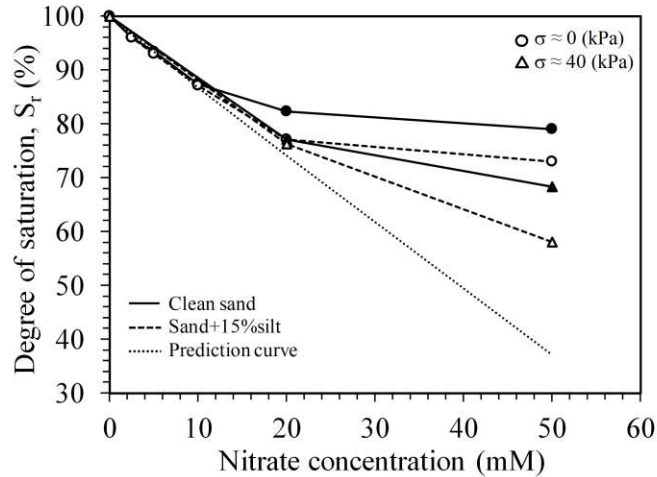
Figure 4-4. The variation of achieved degree of saturation versus Nitrate concentration for different overburden stresses.

Effects of soil pH and temperature:

The effects of pH and temperature on MIPS treatment of soil specimens via denitrification is demonstrated in Figure 4-5. Figure 4-5a illustrates the variation of the degree of saturation by time for three soil types with different initial pH but with the same initial void ratio. As shown in this figure, dissimilatory reduction of NO_3^- generated gas in the reaction vessels and reduced the degree of saturation over time. Regardless of the initial soil pH, a lag in gas generation was observed in all experiments. However, this lag increased as the soil pH decreased. While the natural alkaline sand and Ottawa sand were desaturated approximately over the same time period (33hr and 36hr, respectively), 67hr was required to reduce NO_3^- to biogenic gas for natural acidic sand as a reflection of both a longer lag phase and a slower rate of gas production. This observation is consistent with several studies that reported the decrease in denitrification rate in acidic soils (Parkin et al. 1985; Saleh-Lakha et al. 2009). Parkin et al. (1985) reported that for a reduction of soil pH from 6.02 to 4.08, denitrification rate and denitrification enzymes activity decrease by twofold and threefold, respectively. Saleh-Lakha (2009) established a 539-fold reduction in levels

of gene expression of *nirS* (gene for *nir* production) when pH reduced from 6 to 5. In addition to reduction in the denitrification rate, denitrification in the natural acidic soil produced a slightly lower volume of biogenic gas compared to the specimens with higher initial pH. Due to high solubility of N_2O in water compared with N_2, it could be hypothesized that $N_2:N_2O$ ratio experienced a slight increase as the soil pH decreased from 7.8 to 5.3.

The S_r versus time curve for Ottawa sand specimen incubated at 14°C is compared to that of 26°C in Figure 4-5b. Similar to the reduction in pH, a longer lag in gas generation was observed when the temperature decreased from 26 to 14°C. An approximately twofold decrease in the rate of the degree of saturation reduction was observed; i.e. from 0.28 %/hr to 0.11 %/hr as the temperature decreased from 26 to 14°C, respectively. However, a minimal change in the final degree of saturation was recorded, probably due to higher gas solubility and lower gas volume at lower temperature. The results confirmed the effectiveness of denitrification as a viable soil desaturation method for the range of temperature used in this research.
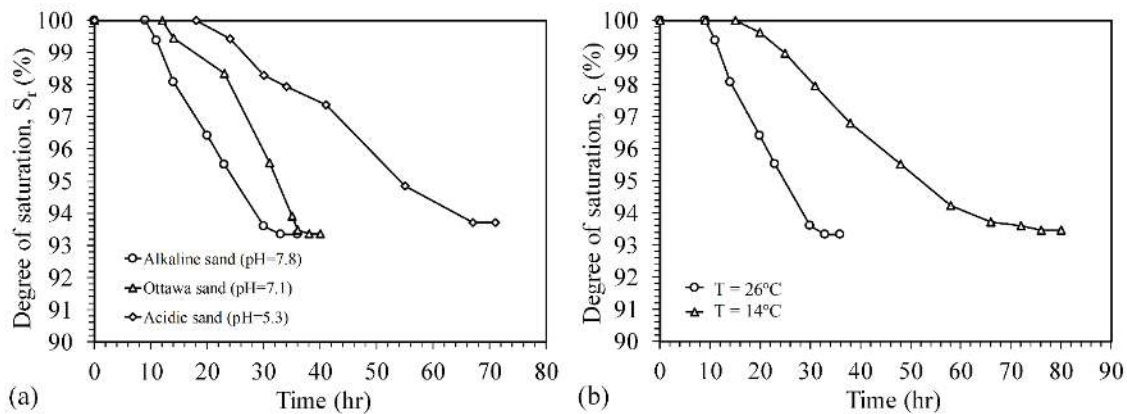
Figure 4-5. The variation of the degree of saturation with time in microbial induced partially saturated soils a) with different pH and b) at different temperatures.

4.5. MIPS TREATMENT EFFICIENCY AND CRITICAL DEGREE OF SATURATION

Based on the experimental results, it was observed that the compositional and environmental factors could affect the efficiency of the treatment system. The treatment efficiency, η, could be defined as the ratio of expected (i.e., predicted using the stoichiometry of reactions) reduction in the degree of saturation from fully saturated condition (i.e., $S_r =1$) to the experimentally measured reduction in the degree of saturation, as follows:

$$\eta = \frac{(1 - S_{r,measured})}{(1 - S_{r,expected})} \times 100 \qquad (4\text{-}1)$$

The variations of η versus nitrate concentrations for specimens with different initial compositional and environmental conditions are presented in Figure 4-6. For specimens with void ratios lower than 0.73 and regardless of fines content, an approximately 100% treatment efficiency was observed when the nitrate concentration was lower than 5 mM (Figure 4-6a). The efficiency of the treatment system was decreased at higher initial concentrations of nitrate. For example, the treatment efficiency of the clean sand specimens decreased to 68% and 33% when the initial nitrate concentration was increased to 20 and 50 mM, respectively. While 20 mM initial nitrate reduced the clean sand's degree of saturation by 17.8%, only 3% reduction in S_r was observed when 30 mM more nitrate was added to the initial nitrate concentration. As a result, higher nitrate concentrations do not necessarily lead to more reduction in the degree of saturation as generated gas could escape from the soil. This observation is consistent with several studies which reported a plateau in the reduction of degree of saturation (Istok et al. 2007; O'Donnell et al. 2017a; Rebata-Landa and Santamarina 2012). At high concentrations of nitrate, higher treatment efficiencies were observed in the specimens with higher fine contents and densities. For example, the treatment

efficiency of sand containing 30% silt with 20 mM initial nitrate concentration was 92%, which was 22% higher than that of clean sand. Among the environmental and mechanical factors, overburden stress had the most influence on the efficiency (Figure 4-6b). The efficiency of the treatment system for silty sand specimen with initial NO_3^- = 50 mM increased from 43 to 67%, when the overburden stress increased from 0 to 40kPa. Despite their significant effects on denitrification rate, η was only slightly affected by pH and temperature.

The critical (or attainable) degree of saturation could be defined as the degree of saturation at which further gas generation results in gas escape from the soil where less significant changes in degree of saturation could be achieved by addition of nutrients. The critical S_r in this study was defined as the degree of saturation at which the efficiency of the treatment system becomes lower than 80%. Similarly, the required nitrate concentration to reduce S_r to the critical S_r could be defined as the critical nitrate concentration. The critical nitrate concentration corresponds to the level of initial nitrate concentration at which addition of more nitrate would not lead to significant changes in S_r. Figure 4-7 presents the variations of critical S_r with different compositional and environmental factors. Figure 4-7a shows the effects of silt content and effective stress on the critical degree of saturation. The critical S_r is less affected by low silt content (5%), however, lower critical S_r could be attained when sand specimens contained considerable amounts of fines (more than 5%). The critical S_r in specimens under higher effective stress were lower for entire range of the silt content (Figure 4-7a). Thus, lower degree of saturations could be reached in soils under higher effective stresses (i.e. at greater depths). The critical S_r versus void ratio curve also shows lower attainable degree of saturation in soils with high densities.

The efficiency and critical degree of saturation are of great importance for the design of both MIPS and MICP via denitrification treatment systems. Although studies on pore pressure response

have shown that partial saturation even with a small amount of gas (about 4-7% of pore water volume) would completely mitigate liquefaction (Mousavi and Ghayoomi 2019, 2020a), further reduction in degree of saturation could improve the soil resistance against earthquake induced deformations (He et al. 2013, Mousavi and Ghayoomi 2018). In addition, high initial nitrate concentration is required to introduce suitable condition for calcite precipitation and effective improvement of soils by MICP treatment. However, from the results presented in Figure 4-6 and Figure 4-7, it could be concluded that the initial nitrate concentration and desired S_r must be limited based on the soil type and depth. Lower degrees of saturation could be reached in soils with higher densities and overburden stresses. Both MIPS and MICP treatment are expected to be more effective in soils containing fines relative to clean sands since treatment media with higher nitrate concentrations could be injected and lower degree of saturations could be achieved in these soils. However, injection of media containing nitrate higher than the critical nitrate concentration not only reduce the efficiency of the system but may also result in disrupting the soil structure by fracturing the soil.
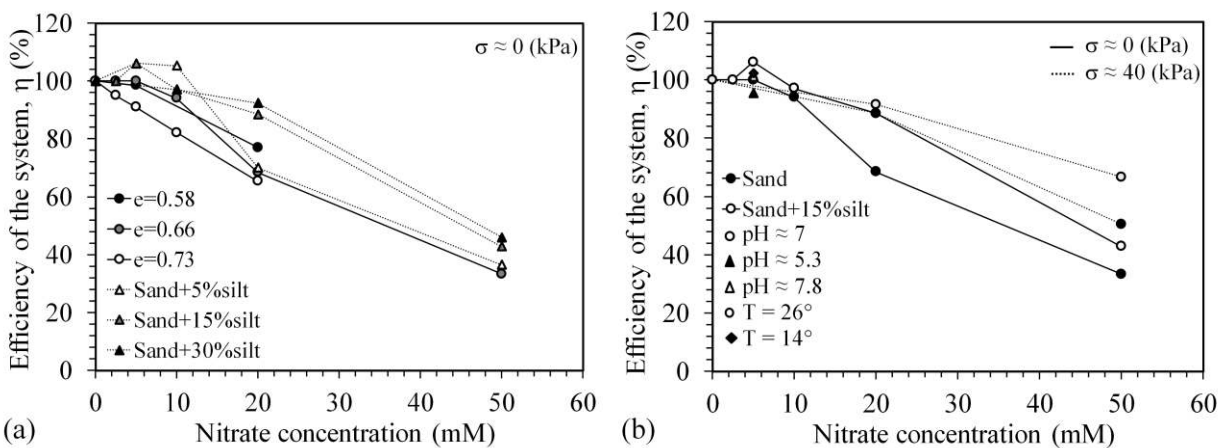
Figure 4-6. The variation of efficiency of microbial induced partial saturation with nitrate concentration under different a) compositional (void ratio and fines content) and b) environmental (pH and temperature) and mechanical (overburden stress) conditions.
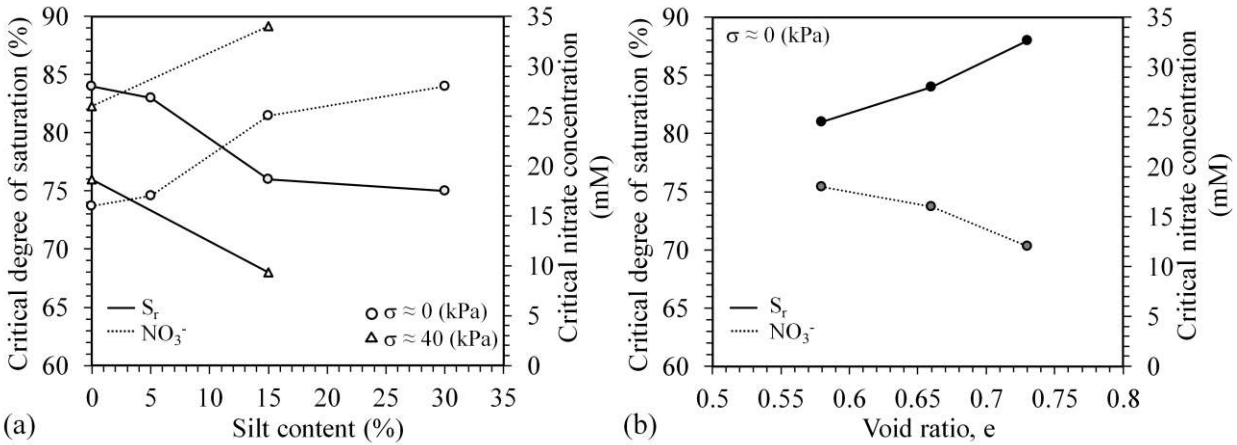
Figure 4-7. The variation of critical degree of saturation and nitrate concentration in microbial induced partially saturated soils with a) different silt content and effective stress and b) different void ratio.

4.6.　CONCLUSIONS

Denitrification experiments with various initial nutrient concentrations were conducted to evaluate the impact of a number of compositional, mechanical, and environmental factors on the efficiency of the treatment system and retainability of gas bubbles in the soil. Results from batch experiments revealed that the volume of gas generation could be adjusted by changing the initial nitrate and ethanol concentrations. High initial nitrate concentration not only resulted in generation of substantial volume of gas, but also elevated pH levels providing a suitable condition for potential calcite precipitation.

Results from soil experiments indicated that substantial gas loss from the soil surface restricts further gas accumulations inside the pores at high initial nitrate concentrations. Two potential gas transport mechanisms, capillary invasion and fracture opening, were hypothesized to be the main reason for this loss. Lower degrees of saturation were attained in soils with higher density,

87

overburden stress, or fines content. Despite the significant effect of environmental factors, i.e. temperature and pH, on denitrification rate, they were found to have minimal effect on final desaturation level for the range of values in this study. The initial nitrate concentration and compositional and mechanical factors were found to impact the efficiency of the treatment system. Results of this study suggested that the efficiency could be controlled by adjusting the initial nitrate concentration based on the soil type and loading conditions.

CHAPTER 5

LIQUEFACTION MITIGATION OF SANDS WITH NON-PLASTIC FINES VIA MICROBIAL INDUCED PARTIAL SATURATION

5.1.   ABSTRACT

A review of liquefaction case histories shows that sand deposits containing some fines were common in past liquefaction events. While current liquefaction mitigation measures are mostly applicable to clean sands or at open sites, development of non-disruptive techniques applicable for sands containing fines is critical. This study examines the application and performance of Microbial Induced Partial Saturation (MIPS) for liquefaction mitigation of sand with various silt content. The investigation consisted of a set of undrained strain-controlled cyclic Direct Simple Shear (DSS) tests on untreated and MIPS-treated samples. Experimental results suggest that considerably high excess pore pressure can be developed in untreated clean and silty sand specimens depending on induced shear strain. Regardless of fines content and induced shear strain, MIPS-treated samples with only 4-5% reduction in degree of saturation from full saturated state did not liquefy. A semi-empirical equation was adopted to predict the excess pore pressure

generation in partially saturated conditions. The model is able to reasonably predict the excess pore pressure generated in both clean and silty sands with variable degrees of saturation.

5.2.   INTRODUCTION

Catastrophic consequences of liquefaction have led to social and economic disruption during most moderate to large earthquakes (Seed et al. 1989; Huang and Wang 2016). Ground improvement techniques can be used to prevent this damage or to reduce its extent by strengthening soils around or adjacent existing infrastructure, as well as open sites. However, current liquefaction mitigation measures are mostly applicable to open sites, being disruptive, or expensive for application near existing structures (Eseller-Bayat et al 2013). Further, most of conventional and recently developed techniques are only validated for clean granular soils and are restricted either in application or performance for soils with fines (Thevanayagam and Martin 2002).

Previous research efforts have revealed that saturated sands containing non-plastic or low-plastic fines (silts) are also highly susceptible to liquefaction (Youd and Bennett 1983; Polito and Martin 2001; Hazirbaba and Rathje 2010; Sadrekarimi 2013; Porcino and Diano 2017). Experimental research on silty sands with a constant void ratio indicated that their cyclic resistance decrease as the silt content increases up to about 25-45% (Polito and Martin 2001; Dash and Sitharam 2009; Porcino and Diano 2017). A review of static and earthquake-induced liquefaction case histories also shows that sand deposits containing some fines were common in past liquefaction events (Youd and Bennett 1983; Boulanger et al. 1998; Bray et al. 2004; Orense et al. 2011). While past studies mainly focused on liquefaction potential of silty sands, limited investigations have been performed on the development of suitable techniques for their liquefaction mitigation. Existence of fines in granular soils can significantly alter their hydro-mechanical characteristics including their permeability and shear strength (Lade et al. 1998;

90

Thevanayagam et al. 2002; Wood and Maeda 2008; YANG and WEI 2012; Yang and Liu 2016).

Specifically, fine particles can lower the permeability of sands by several orders of magnitude, which in turn render the effectiveness of conventional liquefaction mitigation techniques through application (e.g., in densification and grouting techniques) or performance (e.g., in drainage techniques) (Thevanayagam and Martin 2002). Therefore, development of non-disruptive liquefaction remedial techniques that are also compatible with the hydro-mechanical characteristics of silty sands (e.g., low permeability) is of critical concern.

In recent years, researchers have explored non-disruptive (or less-disruptive) measures for liquefaction mitigation of silty sands such as nanoparticles grouting (Huang and Wang 2016) and Microbial Induced Calcite Precipitation (Zamani and Montoya 2019). Induced Partial Saturation (IPS) is another technique that can potentially enhance the liquefaction resistance of silty sands. Previous studies have revealed that inducing partial saturation, even in minute amount, can significantly increase the cyclic resistance of liquefiable soils (Chaney et al. 1979; Yoshimi et al. 1989; Okamura and Soga 2006; Yegian et al. 2007; Unno et al. 2008). Several methods have been developed to induce partial saturation in soils. Such methods either use immiscible displacement of gas, which leaves a residual volume of gas behind (e.g., gas injection, drainage and recharge) (Yegian et al. 2007; Okamura et al. 2011) or are based on exsolution of gas from liquid due to supersaturation (e.g. by chemical reaction, pressure drop, and microbial activity) (Fry et al. 1997; Eseller-Bayat et al. 2013; Mousavi and Ghayoomi 2019). Although the methods in the first category can successfully reduce the degree of saturation, they may not offer effective and non-disruptive measures for silty sands. For example, soil drainage and recharge method induces deformation due to the changes of stress while gas injection may cause non-uniform distribution due to the percolation of air bubbles along preferential paths. Further, gas injection may not be

91

applicable for sands containing fines since high gas pressure, required to overcome pores' entry capillary pressure, may exceed the inter-particles contact stresses, which would disrupt the soil matrix by fracturing the soil (Okamura et al. 2011). Gas exsolution techniques are more suitable in terms of application as they are less-disruptive and can be implemented in a wide range of soils as the soil is desaturated by the expansion of bubbles inside the pore space. Specifically, these methods can be more effective for liquefaction mitigation of silty sands compared to clean sands where experimental studies revealed that sands with higher fines content can retain more gas bubbles for longer periods of time (Rebata-Landa and Santamarina 2011; Mousavi et al. 2019).

The exsolution of gas can occur in-situ through decomposition of organics by microbes in soil pores. Rebata-Landa and Santamarina (2012) proposed Microbial Induced Partial Saturation (MIPS), which utilizes microbial anaerobic respiration to produce biogenic gas. Results of shake table tests showed more than 50% reduction in the generated excess pore pressure within desaturated clean sands when the degree of saturation was lowered to 95-80% (He et al. 2013). Biological denitrification can also induce calcium carbonate ($CaCO_3$) precipitation and enhance soils' hydro-mechanical properties through cementation (van Paassen et al. 2010; O'Donnell et al. 2017a; b; Pham et al. 2017). Although past research has examined MIPS method's effectiveness for liquefaction mitigation of clean sands, no study has investigated its performance and application for sands containing fines.

This chapter describes an experimental investigation on the effect of MIPS on liquefaction resistance of sands containing various non-plastic fines (silt) content. The experimental program consisted of a set of cyclic Direct Simple Shear (DSS) tests on MIPS-treated samples with different degrees of saturation under variable induced shear strain levels. The performance of MIPS

treatment against liquefaction was evaluated by comparing excess pore pressure generation as a quantifiable parameter to monitor the onset of liquefaction under dynamic loading.

5.3. MECHANISMS OF EXCESS PORE PRESSURE GENERATION IN PARTIALLY SATURATED SOILS

The mechanisms of excess pore pressure generation in partially saturated soils was elaborated in section 2.7.2 and two possible mechanisms by which induced biogenic gas bubbles can improve the liquefaction resistance of soils were identified (Okamura et al. 2006). The first mechanism is where existence of bubbles lowers bulk stiffness of pore fluid so that the soil system can reduce its volume with less excess pore pressure generation during cyclic loading. In the second mechanism, suction induced due to development of air-liquid-solid interfaces could increase inter-particle forces and consequently enhance the liquefaction resistance of soils (Unno et al. 2008; Okamura and Noguchi 2009; Tsukamoto et al. 2014; Zhang and Muraleetharan 2018; Mele and Flora 2019; Tsukamoto 2019). Specifically, suction could lead to significant increase in liquefaction resistance of sands containing considerable fines (Okamura and Noguchi 2009; Tsukamoto et al. 2014). Therefore, MIPS could be highly suitable in silty sands in terms of performance.

5.4. EXPERIMENTAL INVESTIGATION PROCEDURES

In order to assess the suitability of MIPS treatment for liquefaction mitigation of silty sands, a series of strain-controlled cyclic direct simple shear tests were conducted on fully saturated and MIPS-treated partially saturated sand and silty sand samples with different degrees of saturation. The soils used for experimental investigation, sample preparation, and experimental program was discussed in section 3.3. Table 5-1 presents a summary of specimens' initial conditions and

experimental program. Results of cyclic tests were interpreted in terms of excess pore water pressure, shear modulus, and induced vertical deformation to assess the effect of desaturation on excess pore pressure generation in treated soils. The excess pore pressure was monitored to interpret the state of liquefaction during cyclic testing of MIPS-treated and untreated specimens. The state of liquefaction in this study is defined as the excess pore pressure ratio, r_u, reaching 1. The vertical deformation was measured during the cyclic tests as well as after reconsolidation of the sample by using a vertical LVDT, and the total vertical deformation was calculated by summation of the two values.

Table 5-1. Experimental program of cyclic DSS test.

test number #	Fine content, FC (%)	Degree of saturation, S_r (%)	Shear strain amplitude, γ (%)
1-4	0	100	0.005, 0.025, 0.1, 0.3
5-13	0	95-89-82	0.025, 0.1, 0.3
14-17	10	100	0.005, 0.025, 0.1, 0.3
18-26	10	95-88-80	0.025, 0.1, 0.3
27-31	20	100	0.005, 0.015, 0.025, 0.1, 0.3
32-40	20	96-88-79	0.025, 0.1, 0.3

5.5.   EXPERIMENTAL RESULTS

Experimental results from undrained strain-controlled DSS tests are presented in terms of excess pore pressure generation and excess pore pressure ratio history with loading cycles. Example results from cyclic DSS tests on an untreated ($S_r = 100\%$) and a MIPS-treated ($S_r = 89\%$) clean sand samples subjected to a constant 0.3% shear strain level are presented in Figure 5-1. It should be noted that degrees of saturation reported in this study are initial degrees of saturation before

94

cyclic loading. For the untreated samples, induced shear strains progressively increased pore pressure until the excess pore pressure reached the applied vertical effective stress (Figure 5-1a). Due to excess pore pressure generation, a regressive trend was observed in induced shear stresses with loading cycles (Figure 5-1b). In comparison, pore pressure of MIPS-treated sample shown in Figure 5-1 (c) was less affected by cyclic loading, where only 11 kPa excess pore pressure was generated after 20 cycles of loading. This indicates a significant increase in liquefaction resistance of desaturated sands compared to fully saturated sands. The shear stress versus number of cycles, *N*, curve also confirms this where no meaningful softening in the induced shear stress was observed over cycles of loading (Figure 5-1d).
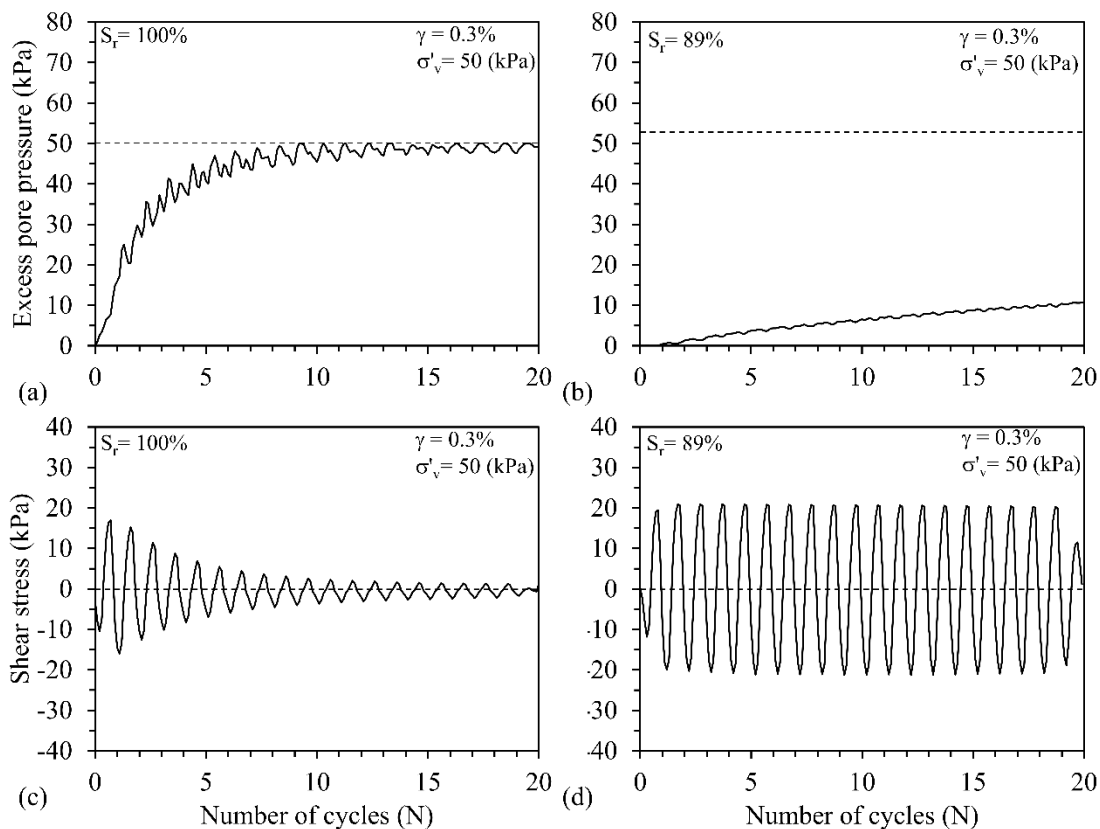
Figure 5-1. Typical experimental results from cyclic DSS tests on (a,b) a fully saturated and (c,d) a MIPS treated clean sand specimen.

5.5.1. Effects of silt content on pore pressure generation characteristics of fully saturated specimens

Cyclic DSS tests on fully saturated sand specimens with various FC, prepared at a pre-loading relative density of approximately 55%, allowed for independent assessment of the effects of fines content on excess pore pressure during cyclic loading. The tests were conducted at various strain levels for 20 cycles of loading. Figure 5-2 illustrates the excess pore pressure ratio versus the cycles of loading for $\gamma = 0.1\%$ and $\gamma = 0.3\%$. At the shear strain of 0.1%, the pore pressure histories showed higher excess pore pressure generation in clean sand specimens compared to silty sand specimens. For example, a clean sand specimen experienced an excess pore pressure ratio as high as 0.95 after the end of 20 loading cycles where r_u was only increased up to 0.70 and 0.55 in silty sand specimens with FC=20% and FC=10%, respectively (Figure 5-2a). Regardless of induced shear strain amplitude, lower pore pressure was generated in silty sand specimen with FC=10% compared to clean sand and FC=20% silty sand specimens. For specimens tested at the largest strain level both clean sand and FC=20% silty sand specimens liquefied after less than 10 cycles of loading. However, the silty sand specimen with FC=10% did not liquefy until about 15 cycles of loading were applied to the specimen (Figure 5-2b).
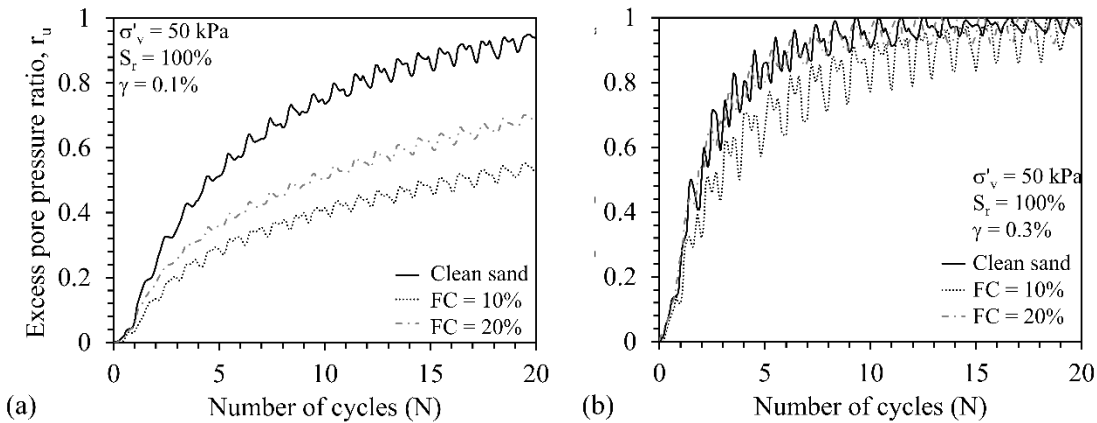
Figure 5-2. Excess pore pressure generation histories for specimens at constant $D_r \approx 55\%$ with different fines content under constant induced shear stain levels of (a) $\gamma = 0.1\%$ and (b) $\gamma = 0.3\%$.

Figure 5-3 illustrates a comparison between the results obtained in this study with those reported in literature from silty sand specimen tested at a constant relative density. The results obtained in this study indicated an initial decrease in r_u with increasing FC from 0 to 10%, and then an increase in r_u with increasing silt content to 20% (Figure 5-3a). The trends in r_u with silt content observed in this study is in agreement with results of cyclic DSS tests conducted on silty sand specimens at a constant $D_r = 50\%$ reported by Hazirbaba and Rathje (2009). The observed trends can be explained by considering the effect of FC on soil skeleton. At low fines content, fine particles fill the inner void spaces between sand grains until the pore space is filled with fine particles. Further increase in FC results in a transition in mechanical behavior of soil from a sand dominated behavior to a fines' dominated behavior (Thevanayagam and Mohan 2000; Polito and Martin 2001; Hazirbaba and Rathje 2009). Thus, the trends illustrated in Figure 5-3 can be attributed to change in mechanical behavior of sand by addition of fines. In terms of cyclic resistance, data from cyclic triaxial tests on silty sand specimen at constant relative density reported by Polito and Martin (2001), Singh (1994), and Kokusho (2007) were considered (Figure

97

5-3b). According to Figure 5-3b, most of the data obtained from cyclic stress-controlled tests revealed a decrease in cyclic resistance of the sand and silt mixture by increasing the fines content which is not in agreement with strain-controlled tests data. It should be noted that a decrease in cyclic resistance corresponds to an increase in excess pore pressure generation and vice versa. The reason for the discrepancy may be explained by considering the difference between soil response subjected to cyclic stress-controlled versus strain-controlled tests. Previous research indicated that the excess pore pressure generation in saturated sands is highly influenced by cyclic strains induced by an earthquake rather than cyclic stresses (Dobry et al. 1982). The presence of fines can significantly affect soil shear stiffness (Iwasaki and Tatsuoka 1977; Salgado et al. 2000; Carraro et al. 2009; Yang and Liu 2016; Goudarzy et al 2018) and consequently induced strains in a cyclic stress-controlled test. Thus, silty sand specimens may be subjected to different strain levels depending on their silt content in a cyclic stress-controlled test as opposed to cyclic strain-controlled test and have different cyclic response.
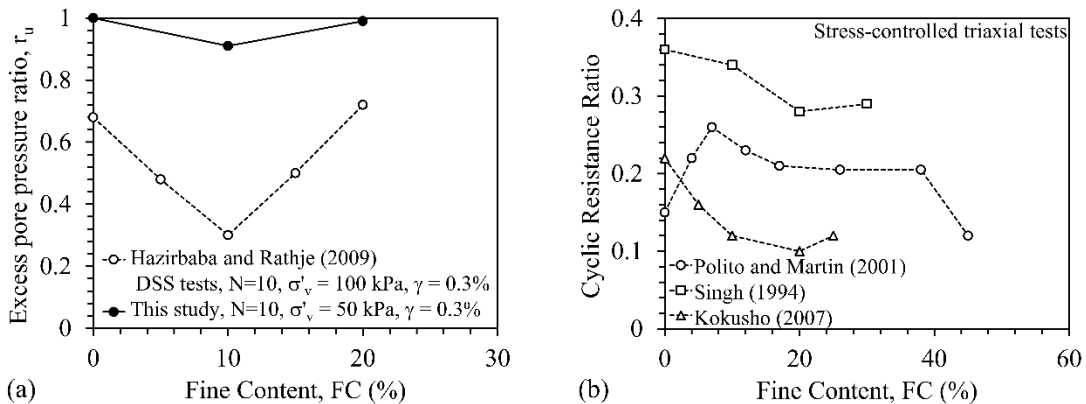
Figure 5-3. Results of previous (a) strain-controlled and (b) stress-controlled tests on excess pore pressure generation and cyclic resistance of sands with different FC at a constant relative density.

98

5.5.2. Effects of MIPS treatment on pore pressure generation characteristics of clean sand

A comparison of the excess pore pressure ratio histories in tests on MIPS-treated and untreated sand specimens with various degrees of saturation and at 0.1% and 0.3% shear strain levels are shown in Figure 5-4. It should be noted that test results at smaller shear strain levels are not shown here as relatively low pore pressure values were generated. At 0.1% shear strain level, MIPS treatment led to a substantial reduction in pore pressure generation when the degree of saturation was only decreased to 95% from full saturation (Figure 5-4a). The same behavior was observed when the clean sand samples were tested at 0.3% shear strain level, where desaturation to 95% degree of saturation in clean sand specimen reduced the excess pore pressure ratio to less than 0.6 at the end of cyclic loading (Figure 5-4b). This trend continued with reduction in excess pore pressure ratios by more than 79% for sands at S_r=89% compared to full saturation. However, further reduction in the degree of saturation had less effect on excess pore pressure generation, as only 4% reduction in r_u was observed when S_r decreased from 89 to 82%. Similar observation has been reported in the literature where a small reduction in degree of saturation (around 10%) is enough to significantly improve the liquefaction resistance of clean sands at modest strain levels (Okamura and Soga 2006; He et al. 2013; O'Donnell et al. 2017a).
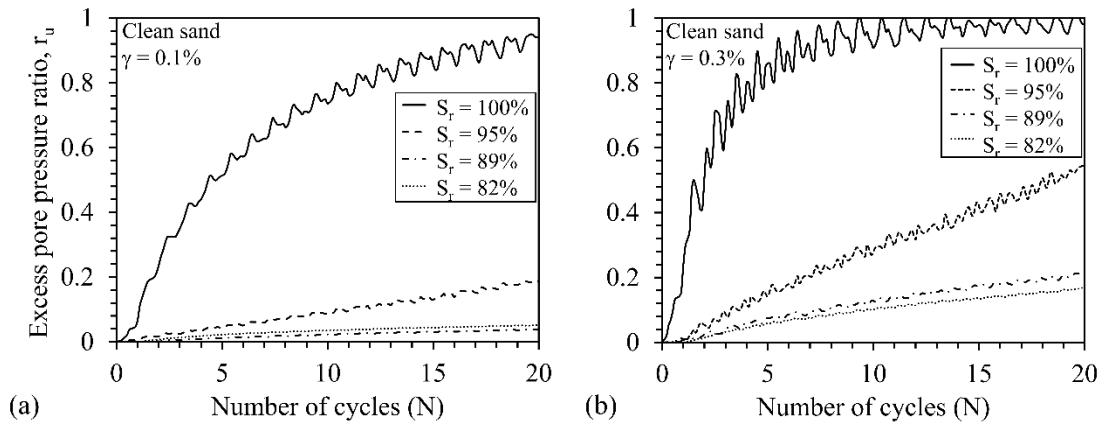
Figure 5-4. Excess pore pressure generation ratio histories of MIPS treated and untreated clean sand specimens with various degrees of saturation at (a) γ = 0.1% and (b) γ = 0.3%.

5.5.3. Effects of MIPS treatment on pore pressure generation characteristics of silty sand

Figure 5-5 presents variations of the excess pore pressure ratio with the degree of saturation for sand specimens with different silt contents. The excess pore pressure ratio was obtained from the maximum pore pressure generated at 20 cycles of loading under 0.1% and 0.3% shear strain levels. Similar to clean sand specimens, silty sand specimens did not liquefy even though S_r was merely decreased by about 5% from full saturation. This indicated that MIPS can also effectively reduce excess pore pressure generation in silty sand. For tests under 0.1% strain level and regardless of fines content, 5% reduction in S_r was enough to substantially reduce r_u. Further desaturation at this strain level had a slight effect on excess pore pressure generation. However, clean sand and silty sand specimens subjected to γ=0.3% produced considerable excess pore pressure at S_r = 95-96%, even though they did not liquefy. This indicated that although small reduction in the degree of saturation might be enough to adequately reduce excess pore pressure of soils subjected to less intense shakings, higher volume of biogas may be required in more intense shakings to prevent soil softening due to high excess pore pressure generation.

100
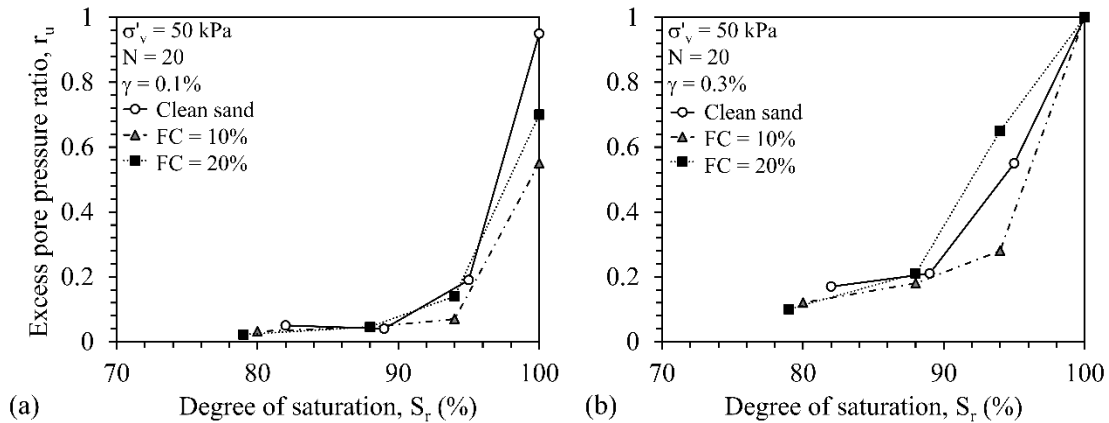
Figure 5-5. Variations of the excess pore pressure ratio histories with degree of saturation for sand specimens with different silt contents at (a) γ = 0.1% and (b) γ = 0.3%.

5.5.4. Effects of MIPS treatment on shear stiffness of clean sand and silty sand

Previous investigations have indicated that several factors including shear strain level, soil type, void ratio, effective mean confining stress, stress history, and degree of saturation can affect dynamic shear stiffness of soils (Seed and Idriss 1970; Hardin and Drenvich 1972; Oztoprak and Bolton 2013; Le and Ghayoomi 2017). Pore pressure generation during cyclic loading affects the soil shear stiffness by reducing the effective stress and consequently the developed shear stress (as can be seen in Figure 5-1b). This prevents the independent assessment of the effects of suction on soil's shear stiffness. Therefore, the shear modulus of specimens was only obtained for the smallest shear strain level ($\gamma = 0.025\%$) as minimal pore pressures were generated at this strain level.

Figure 5-6 presents the variations of the secant shear modulus, G, with the degree of saturation for sand specimens with different silt contents. The secant shear modulus was calculated for the second cycle of loading at $\gamma = 0.025\%$. It is noteworthy that the shear modulus for the first cycle was not reliable as this cycle was set up for ramp up in the actuator control system. Regardless of the degree of saturation, results showed a softer soil response in specimens with

101

higher silt content; specimens with FC=20% having the smallest shear modulus. This observation is in agreement with previous studies where lower small strain and strain dependent shear modulus were reported for silty sands comparing to the ones in clean sands (Iwasaki and Tatsuoka 1977; Salgado et al. 2000; Carraro et al. 2009; Yang and Liu 2016; Goudarzy et al 2018).

For clean sand specimens, reduction in the degree of saturation (to the extent tested in this study) did not lead to significant change in shear modulus of clean sand. A slight increase (about 4%) in shear modulus was observed when the degree of saturation was reduced to 82% from initial saturation. However, the effect of desaturation was more significant in silty sand specimens. This could be expected since higher suction levels can be developed in finer soils for the same degree of saturation. The S_r-G of silty sand specimens showed an increasing trend in shear modulus with a decrease in the degree of saturation. The results indicated up to 20% increase in shear modulus of desaturated silty sand specimens with FC=10% compared to fully saturated one. MIPS treatment of silty sand specimens with FC=20% resulted in 32% increase in shear modulus when S_r was reduced to 79%.
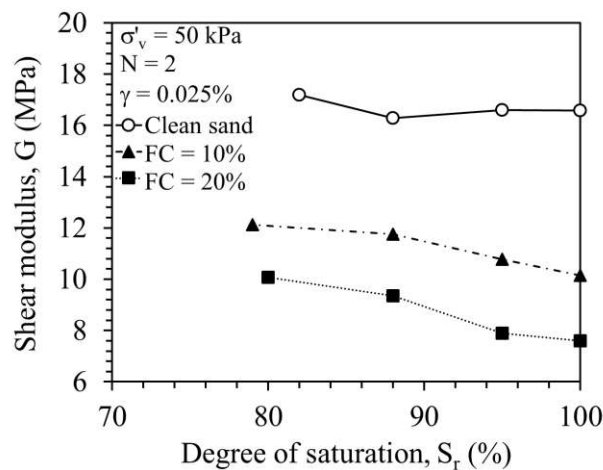
Figure 5-6. Variations of the secant shear modulus with degree of saturation for sand specimens with different silt contents.

5.5.5. Effects of MIPS treatment on volumetric deformation of clean sand and silty sand

Figure 5-7 presents the variation of induced volumetric strain ratio in MIPS treated soils to fully saturated soils $(\varepsilon_{vd,MIPS}/\varepsilon_{vd,sat})$ for samples with various silt contents and subjected to 0.3% shear strain level. It is noteworthy that since all tests were conducted in undrained condition, the induced volumetric strains were calculated after reconsolidation of sample at the end of cyclic loadings. Regardless of the fines content, the data in Figure 5-7 show no clear trend of $\varepsilon_{vd,MIPS}/\varepsilon_{vd,sat}$ with the degree of saturation. This is in agreement with previous studies on volumetric deformation of partially saturated soil with high levels of saturation (i.e., $S_r > 60\%$) subjected to constant shear strain tests (Duku et al. 2008; Yee et al. 2013). For example, Yee et al. (2013) conducted strain-controlled DSS tests on sand and silty sand samples with different silt contents and plasticity and reported no significant effect of S_r on volumetric deformation of soils when $S_r > 60\%$. Therefore, it can be concluded that for the range of saturation tested in this study (i.e., $S_r > 79\%$) and the method of desaturation and testing implemented, the degree of saturation does not significantly affect the volumetric deformation of silty sands.
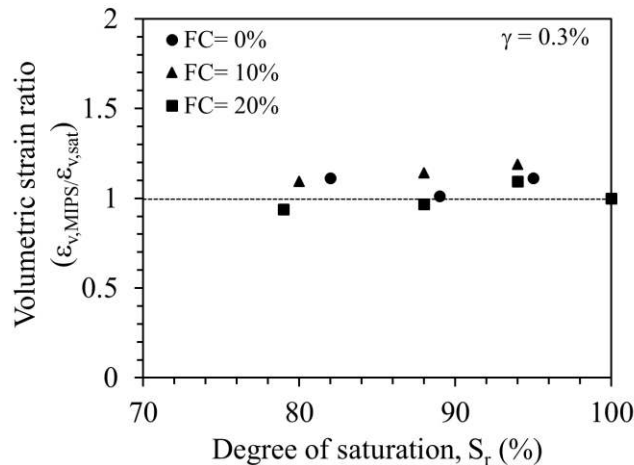
Figure 5-7. Variations of the volumetric strain ratio with the degree of saturation.

5.6. ANALYSIS AND DISCUSSION

5.6.1. Effects of shear strain and fines content on excess pore pressure

Dobry (1985) compiled data from laboratory experiments on seven sands where the tests were conducted on undisturbed as well as remolded samples at varying effective confining stresses from 25 to 200 kPa and relative densities from 20-80% for 10 cycles of loading. They demonstrated a clear relation between cyclic shear strain amplitude and pore pressure response and revealed that all the data fall within a narrow band when the pore pressure response is plotted against cyclic shear strain. The results obtained from fully saturated tests in that investigation were utilized to study the application of this band when non-plastic fines are added to sand (Figure 5-8). Results from this study confirm the significant effect of induced shear strain on pore pressure generation of fully saturated specimens. Regardless of fines content, the excess pore pressure data appears to fall within the bounds proposed by (Dobry 1985). This suggests that the upper and lower bounds for clean sands over a wide range of shear strains can encapsulate most of the data points. The results also suggested that there is a shear strain level below which no excess pore pressure was generated. This shear stain level, which is referred to as threshold shear strain, γ_{tvp} (Dobry et al. 1982) appears to be around 0.01 to 0.015 % for clean sand. This is consistent with $\gamma_{tvp} = 0.01\%$ reported by Dobry et al. (1982) for clean sands. The excess pore pressure ratio values at $\gamma = 0.025\%$ were lower for silty sand than the one for clean sand specimens, which indicates that higher magnitudes of γ is required to develop pore pressure in silty sands. Therefore, γ_{tvp} is expected to be higher for silty sands than clean sand. This is in agreement with the reported values by Hazirbaba and Rathje (2009).

Although strain-controlled cyclic tests on sands and silty sands provide a fundamental approach to study and compare their excess pore pressure generation, the lower pore pressures

generated in silty sand specimens compared to clean sand do not indicate their lower potential to liquefaction in a seismic event. As presented in Figure 5-8, the induced shear strain level significantly influences the excess pore pressure in sands and silty sands. However, the induced strain level in a seismic event is reversely proportional to the soil shear stiffness ($\gamma = \tau/G$). Considering this fact and from experimental results presented in Figure 5-8, higher induced shear strain levels are expected in silty sands than in sands subjected to the same cyclic stress amplitudes since addition of non-plastic fines results in significant reduction in shear modulus of mixture. This can be confirmed with observed lower cyclic stress resistance of silty sands than sands in stress-controlled tests reported by other researchers (Figure 5-3b).
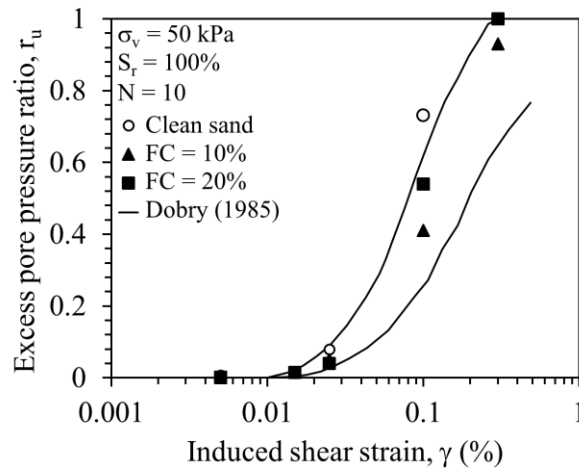
Figure 5-8. r_u variation with induced shear strain amplitude at 10 cycles of loading obtained in this study compared with the upper and lower bound curves proposed by Dobry (1985) for clean sands.

5.6.2. Effects of bulk modulus of fluid and suction on pore pressure response

In order to better interpret the results, experimental data should be examined within the context of unsaturated soil mechanics. Figure 5-9 presents conceptual MIPS treated soil models at two

105

different ranges of degree of saturation; i.e. partially saturated soils with S_r approximately above 95% and unsaturated soils with S_r approximately below 95%. At degrees of saturation approximately higher than 95%, the induced biogenic gas bubbles are present as discrete tiny gas bubbles located within soil pores (Figure 5-9a). Theoretical and experimental investigations (Finno et al. 2017) have shown that discrete gas bubbles at this state do not develop inter-particle suction; thus, they would have minor effects on shear stiffness of desaturated samples. However, further gas generation can result in development of inter-particle forces (suction) within the three-phase material system (Figure 5-9b). It is well established that suction can affect shear modulus of soils and result in stiffer soil response (e.g., Dong et al. 2016; Ghayoomi et al. 2017). This effect is expected to be more significant in fine grained soils and at lower degrees of saturation since higher suction levels can be developed in soils with finer grain size, which consequently result in stiffer soil response. This explains why desaturation resulted in more substantial impact on shear modulus of silty sands compared to clean sands. From the results presented in Figure 5-6, MIPS treatment of sands containing considerable amounts of fines and bringing the saturation levels lower than 95% led to increase in shear modulus due to the induced suction.
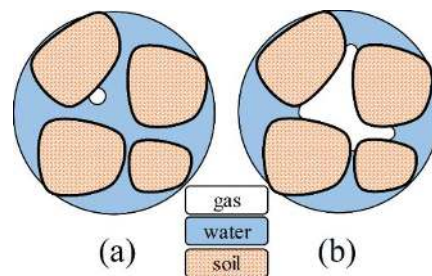
Figure 5-9. Conceptual gas-water-soil particle interaction at (a) high degrees of saturation and (b) lower degrees of saturation.

The theoretical formulation of Martin et al. (1975) (Equation (2-18)) provides a simple and strong basis to discuss the impact of bulk modulus of fluid and suction on pore pressure response of MIPS treated soils. Based on this formulation, excess pore pressure generation in soils is mainly governed by induced volumetric strains and bulk modulus of pore fluid. Previous studies have revealed that volumetric deformation of soils can be significantly affected by the level of saturation due to the development of inter-particle suction (Ghayoomi et al 2013; Yee et al. 2013). However, this behavior has been reported to be more pronounced in soils with mid- to low-range degrees of saturation (e.g., $S_r < 60\%$). Therefore, degree of saturation did not show its effect on volumetric deformation data in Figure 5-10. Based on this observation, it can be concluded that the variation of pore fluid bulk modulus is the dominant factor governing the excess pore pressure generation in MIPS treated soils for the range of saturations tested in this study. This is also evident from pore pressure data in Figure 5-5, where although they are different in magnitudes, r_u-S_r curves for clean sand and silty sand samples follow a relatively similar trend, indicating the dominant role of fluid bulk modulus.
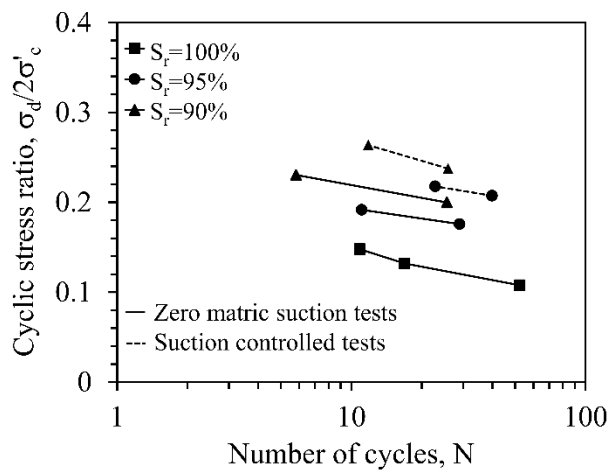
Figure 5-10. Effect of matric suction and fluid bulk modulus on liquefaction resistance of silt specimens (after Okamura and Noguchi 2009).

5.6.3. Prediction of excess pore pressure generation in partially saturated soil

On the basis of observations from seven series of undrained cyclic strain-controlled direct simple shear, cyclic triaxial, and cyclic torsional shear tests, and Martin et al. (1975)'s theoretical formulation (Equation 2-18), Dobry et al. (1985) derived a simple model to predict the excess pore pressure ratio in fully saturated soils. The proposed model was subsequently modified by Vucetic and Dobry (1986) in the following form:

$$r_{u,N} = \frac{p \times f \times N \times F \times (\gamma - \gamma_{tvp})^s}{1 + f \times N \times F \times (\gamma - \gamma_{tvp})^s} \tag{5-1}$$

where, f is dimensionality factor and can be assumed as 1 or 2, depending on whether pore pressure is induced by one-or two-directional shaking. F, p, and s are fitting parameters which depend on volumetric deformation potential of soils and can be obtained by laboratory data-based fitting attempts. In the absence of laboratory data, the model's fitting parameters can be derived using empirical equations. Carlton (2014) compiled laboratory data for different soils and developed empirical correlations for the curve fitting parameters F and s. The parameter F is reversely proportional to the shear wave velocity of soil and takes the following functional form:

$$F = 3810 \times V_s^{-1.55} \tag{5-2}$$

where V_s is the shear wave velocity of fully saturated soil. Equation (5-2) indicates that the parameter F is a function of soil shear stiffness and decreases as the stiffness increases. The fitting parameter s is proportional to fines content and can be presented as follows:

$$s = (FC+1)^{0.1252} \tag{5-3}$$

which indicates that s increases as the fines content increases. Further, laboratory data from different types and relative densities of sands indicate that values for the parameter p vary between ±7.1% of 1, and is often set to 1 for practical purposes (Hashash 2009).

The applicability of this model has been verified by several authors and it has been utilized in a number of effective-stress based nonlinear ground response analysis software such as D-Mod, D-Mod_2, and Deepsoil (Matasovic and Vucetic 1993; Matasovic 2006; Hashash 2009; Cetin and Bilge 2012). In addition, the model in Equation (5-1) was validated in this study and used to predict the excess pore pressure generation in fully saturated sand and silty sand. In this regard, a dimensionality factor $f = 1$ was used in the model and the fitting parameters were obtained by fitting the predicted values to the fully saturated experimental data using a least square fitting method. A summary of fitting parameters obtained for different fines contents is presented in Table 5-2. Estimated values of the excess pore pressure ratio (Equation (5-1)) were plotted versus the values of induced shear strain in Figure 5-11. The data points in this figure represent the measured values of r_u, while the curves are the prediction of r_u for induced shear strain values ranging from threshold shear strain to 1%. The r_u values estimated using Equation (5-1) and those measured experimentally during undrained cyclic loading relatively correspond well. The obtained parameters for clean sand were also employed to investigate the model capability to predict the values of r_u in similar clean sand material reported in literature. Figure 5-11(a) presents laboratory triaxial pore pressure data reported by Dobry (1985) for silica sand with $D_r = 40\%$ and mean effective stress of 95 kPa subjected to 10 cycles of loading. A relatively acceptable prediction of reported r_u values was observed in this figure by comparing them to those predicted by Equation (5-1).

Table 5-2. r_u **prediction model parameters.**

Fines content, FC	Model parameter			
(%)	p	F	s	γ_{tvp}, (%)
0	1.07	9.88	1.65	0.011
10	1.13	3.52	1.75	0.013
20	1.06	12.1	2.05	0.016

(a)   (b)
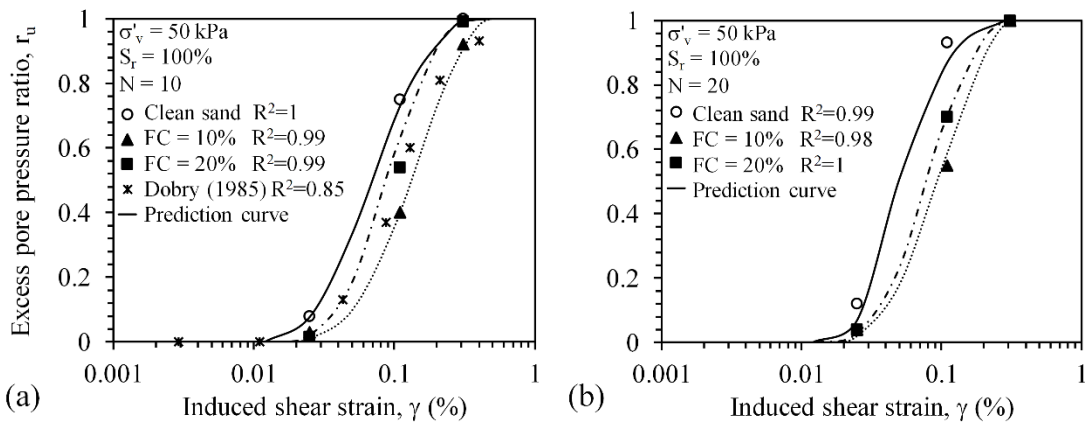
Figure 5-11. Comparison of r_u from experimental results and Dobry (1985) laboratory data to model (Equation (9)) predictions at (a) N = 10 and (b) N = 20 at initial saturation condition.

Although Equation (5-1) has shown to be capable of estimating r_u in fully saturated soils, it does not directly consider the effect of S_r on excess pore pressure generation; even though this was considered in the theoretical formulation by Martin et al. (1975). In their theoretical formulation (Equation (2-18)), Martin et al. (1975) showed that excess pore pressure generation is proportional to bulk modulus of pore fluid. As discussed earlier, the bulk modulus of pore fluid is highly governed by soil degree of saturation (Equation (2-19)). To capture the effect of partial saturation on the excess pore pressure generation, Equation (2-18) was modified by implementing

110

the effect of the ratio of fluid bulk modulus in partially saturated condition to the one in fully saturated soil into Equation (2-18), as follows:

$$r_{u,N} = \frac{\dfrac{K_f}{K_{f_0}} \times p \times f \times N \times F \times (\gamma - \gamma_{tvp})^s}{1 + \dfrac{K_f}{K_{f_0}} \times f \times N \times F \times (\gamma - \gamma_{tvp})^s}$$

(5-4)

In this equation, $K_{f,0}$ is the initial pore fluid bulk modulus at which the fitting parameters are obtained and K_f is the bulk modulus of pore fluid in partially saturated condition. The methodology to obtain proposed equation's parameters relies on undrained stain-controlled test on saturated samples. Overall, the parameters that are needed to solve the evolution of r_u during cyclic loading include: the fitting parameters (p, F, s) and the threshold shear strain value obtained from cyclic tests on saturated samples at various shear strain amplitudes as well as K_f and K_{f0} calculated from Equation (2-19). As the direct measurement of degree of saturation in a nearly saturated sample is difficult, the initial bulk modulus of pore fluid can be indirectly calculated from B-value or p-wave measurements (Yoshimi et al. 1989; Rebata-Landa and Santamarina 2012; Eseller-Bayat et al. 2013; He et al. 2013). Thus, the K_f/K_{f0} ratio can be formulated in following form:

$$\frac{K_f}{K_{f_0}} = \frac{1}{m - (m-1)S_r}$$

(5-5)

where m depends on initial fluid bulk modulus and can be obtained from laboratory tests on saturated and unsaturated soils. In order to examine the applicability of the proposed equation for prediction of r_u in a partially saturated state, the fitting parameters obtained for fully saturated samples and Equation (5-5) with m=667 (corresponding to the B-value in saturated tests) were used in Equation (5-4) and compared with the experimental r_u data obtained from cyclic tests on microbially induced partially saturated samples.

111

Figure 5-12 shows the suitability of the model to predict the experimental trends in r_u with the degree of saturation for the specimens at different fines contents subjected to different shear strain levels and number of cycles. As presented in this figure, the model predicted a dramatic drop in the excess pore pressure ratio of sand and silty sand specimens as the degree of saturation decreases which followed by a gradual decrease in r_u with further reduction in degree of saturation; a behavior which was found consistent with the experimental results as presented in Figure 5-12. Regardless of the degree of saturation, the model predicted higher r_u in samples subjected to higher number of cycles and shear strain levels. The results have high coefficient of determination (R^2) values, confirming the model's adequacy to predict the experimental data.
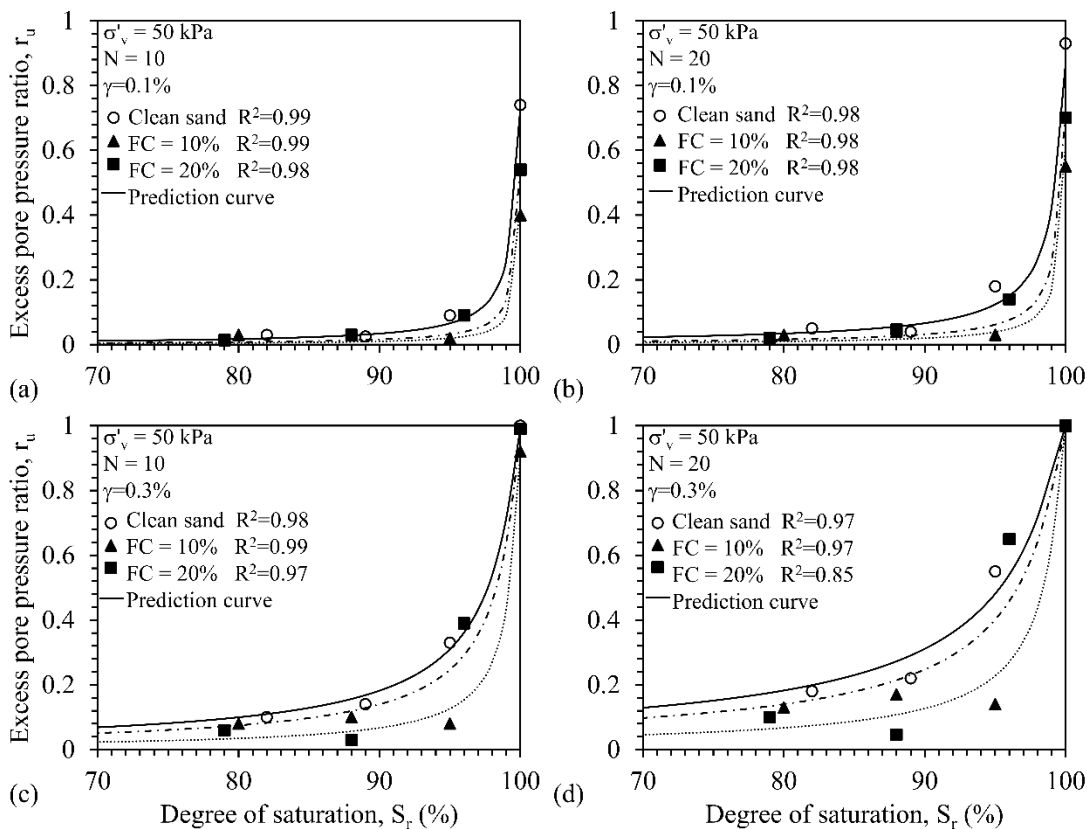
Figure 5-12. Comparison of r_u from experimental results to proposed model predictions at (a) N=10 & γ=0.1%, (b) N=20 & γ=0.1%, (c) N=10 & γ=0.3%, and (d) N=20 & γ=0.3%.

In order to further validate the model, its capacity to predict the r_u-S_r trends was examined using experimental data by He et al. (2013). They performed shaking table experiments with an instrumented laminar box and conducted a series of cyclic tests on saturated and MIPS treated sands. The frequency of shaking was around 2 Hz and the maximum induced horizontal shear strain on top of the sample was around 0.25%. The tests were conducted on sands with relative densities approximately ranging from 30 to 60% and at $S_r=$ 100, 95, 90, and 80%. Figure 5-13 presents data obtained from cyclic tests on sand samples with relative densities ranging from 30 to 60% located at one-third depth of sample from soil surface. The r_u value at each saturation level represent mean r_u value of repeated tests. Similar to the results presented in this study, the experimental r_u data reported by He et al. (2013) revealed a sharp drop in r_u with a slight decrease in degree of saturation followed by a gradual decrease in r_u with a further decrease in S_r. The proposed equations and values by Carlton (2014) were employed to obtain the parameters in Equation (5-4). The shear wave velocity of soil at 0.1 m depth was estimated given the soil density (ρ=1.8 to 2 g/cm^3):

$$V_s = \sqrt{\frac{G_{\max}}{\rho}} \tag{5-6}$$

where the small strain shear modulus, G_{max}, is estimated from the empirical relationship proposed by Seed and Idriss (1970):

$$G_{\max} = 218.2 K_{2(\max)} (\sigma'_0)^{0.5} \tag{5-7}$$

where $K_{2(max)}$ is a fitting parameter and varies from about 34 to 52 for sand with relative density of 30 to 60%, respectively and σ'_0 is the mean effective stress. V_s values were estimated using Equation (13), and the parameter F was found 5.5 and 8 for samples with $D_r=$ 30% and 60%, respectively, using Equation (5-2). Since the r_u data for different shear strain amplitudes were not

available, the threshold shear strain was assumed to be the same as that of clean sand in this study (i.e., γ_{tvp}= 0.01%). The parameters s= 1, p= 1, and f= 1 were used for the one-dimensional tests conducted on the clean sand specimens. The K_f /K_{f0} ratio for different degrees of saturation was obtained using Equation (5-5) with m= 667. The proposed model was found to provide an acceptable prediction of r_u data at different degrees of saturation for data reported by He et al. (2013) (Figure 5-13). The proposed predictive relation performed relatively well for the limited soils and initial conditions presented in this study; however, further experimental data can be used to verify its suitability in other circumstances.
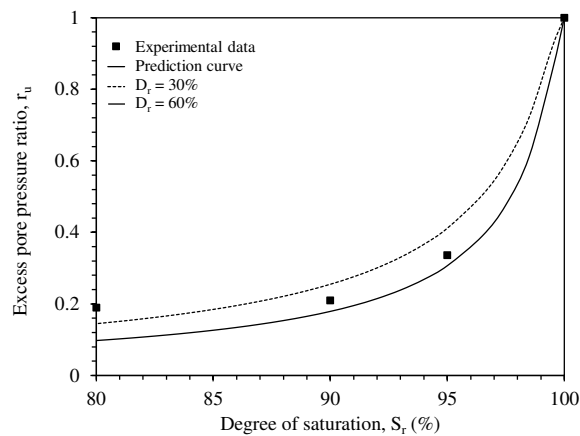
Figure 5-13. Comparison of model predictions with r_u data from He et al. (2013).

5.7.   CONCLUSIONS

This study investigated the application and performance of MIPS treatment for liquefaction mitigation of silty sands. Regardless of fines content, results showed considerable excess pore pressure generation in untreated specimens subjected to undrained strain-controlled cyclic loading. However, the magnitude of the generated excess pore pressure was highly governed by the level

114

of induced shear strain. In general, lower excess pore pressure was generated in silty sand specimens in comparison with clean sand tested under the same initial conditions (i.e. D_r, S_r, and effective vertical stress). Regardless of fines content, significantly smaller r_u was obtained when S_r was merely reduced to 95-96% from desaturation through MIPS treatment. A semi-empirical model was adopted to capture the impact of partial saturation on r_u of sands and silty sands. The model has the capability of capturing the impacts of fluid bulk modulus reduction in desaturated soils on r_u. The capability of the model was evaluated by comparing the r_u values obtained from experiments in this study as well as data reported in literature and the values predicted by the model. The model was found to satisfactorily capture the trends in the r_u measurements for different degrees of saturation in this study. Specifically, the model was capable of capturing the dramatic drop in r_u with the degree of saturation reduction as observed in the experimental results.

CHAPTER 6

SEISMIC COMPRESSION OF UNSATURATED SILTY SANDS: A STRAIN-BASED APPROACH

6.1. ABSTRACT

The vast majority of surface structures are located on or surrounded by unsaturated soil deposits and may suffer excessive settlement during earthquakes. However, the fundamental understanding of the mechanisms by which the degree of saturation impacts volumetric deformation of soils during seismic loading is still not mature. Consequently, it is critical to develop and calibrate seismic compression models while considering these mechanisms. The objective of this study is to experimentally investigate the impact of degree of saturation, fines content, and desaturation technique on seismic compression of sand and silty sands. The experimental program involved undrained cyclic direct simple shear tests on specimens prepared using suction control and wet-compaction techniques. A strain-based predictive model was adapted and modified to capture the observed trends in the seismic compression of soils with the different degrees of saturation. The suitability and applicability of the model were verified by comparing the measured and estimated compression values in this study with ones reported in the literature for other soils and desaturation approaches.

6.2.　INTRODUCTION

Seismically induced volumetric deformation of unsaturated soil layers has been recognized as a major cause of damage to infrastructure during past earthquakes (Stewart et al. 2001, 2004). In the past decades, extensive research has been conducted to understand the mechanisms of seismic soil settlement and factors affecting its magnitude in saturated and unsaturated soils (Silver and Seed 1971; Lee and Albaisa 1974; Tokimatsu and Seed 1987; Pradel 1998; Ghayoomi et al. 2013; Yee et al. 2014; Zeybek and Madabhushi 2019; Rong and McCartney 2020). While early studies mostly focused on soils in either fully saturated or dry conditions, in recent research, the attention has shifted to the impact of degree of saturation on seismic settlement (Whang et al. 2004; Ghayoomi et al. 2011; Yee et al. 2014; Zeybek and Madabhushi 2019; Rong and McCartney 2020). Although previous investigations have provided valuable insights on the impact of degree of saturation on settlement of unsaturated soils, results were often inconsistent, which requires further examination and a more unified formulation.

Duku et al. (2008) performed strain-controlled cyclic simple shear (CSS) tests on sixteen sandy soils with various degrees of saturation, prepared using the wet-compaction method, and reported no meaningful trend in seismic compression with the degree of saturation. On the other hand, centrifuge tests on unsaturated clean Ottawa sand, desaturated using steady state infiltration or capillary ascending methods, indicated that the degree of saturation can significantly impact the seismically induced settlement of sand layers (Ghayoomi et al. 2011, 2013; Mirshekari and Ghayoomi 2017; Borghei et al. 2020). Similar observations were also made by Le and Ghayoomi (2017) and Rong and McCartney (2020) who performed drained strain-controlled CSS tests on unsaturated clean sand samples with suction control. This disagreement has also been reported for soils containing considerable amounts of fines. For example, Whang et al. (2004) conducted strain-

117

controlled CSS tests on four fill materials having fines content, *FC*= 40-50% with plasticity indices, *PI*= 2-15. Samples with different as-compacted degrees of saturation ranging from 54 to 91% were prepared and subjected to cyclic loadings. They observed significantly lower volumetric strains in specimens having water contents higher than the optimum value in comparison with the specimens compacted at water contents lower than the optimum. In contrary, Yee et al. (2014) reported no significant effect of as-compacted degree of saturation on seismic compression of low plastic silty sands (0<PI<9) when S_r> 60%, regardless of fines content and soil plasticity. However, the compression in most of the specimens with the degree of saturation between 0 to 60% was lower than that of the dry specimens.

A wealth of literature on dynamic response of unsaturated soils unanimously confirms the significant impact of degree of saturation on small strain as well as large strain dynamic shear modulus of soils (Mancuso et al. 2002; Sawangsuriya et al. 2009; Hoyos et al. 2015; Dong and Lu 2016; Ghayoomi et al. 2017; Ng et al. 2017; Khosravi et al. 2018; Mousavi and Ghayoomi 2018, 2020a). Thus, one would expect that this change of stiffness, to some extent, would influence the seismic compression. The inconsistency reported in previous works could be attributed to different factors such as the sample preparation method (e.g., wet-compaction versus suction control) and the testing protocol (e.g., stress-controlled versus strain-controlled). For example, in several studies on seismically induced volumetric deformation, the target degree of saturation was achieved through tamping the soil with different water contents at constant dry density or relative density, which may have led to different soil structures and dynamic response (Qian et al. 1991; Kim et al. 2003). Consequently, the changes in soil structure could have rendered the independent evaluation of the impact of degree of saturation on the compression. This emphasizes the need for an experimental study which independently investigates the role of degree of saturation and the

method by which the water content is controlled on the volumetric deformation of soils. Results of such experiments must be employed to calibrate and update the available models for estimation of seismic compression.

The objective of this study is to investigate the effect of degree of saturation and the desaturation technique on the seismic compression of sand and silty sands. First, undrained, strain-controlled cyclic tests were conducted on soil specimens prepared using suction control technique. Then, additional specimens with the same relative density and degree of saturation were prepared using wet-compaction technique and were subjected to cyclic loading. This enabled independent evaluation of the impact of desaturation method on seismic compression. Existing predictive models were adapted and modified to capture the observed trends in the seismic compression of soils with different degrees of water saturation.

6.3.   EXPERIMENTAL PROGRAM

In addition to DSS tests on MIPS treated samples described in previous chapter, two series of undrained, strain-controlled, cyclic DSS tests were performed on silty sand specimens with different degrees of saturation to assess the impact of saturation and testing approach on seismically induced volumetric deformation. The first set included cyclic DSS tests on suction-controlled unsaturated soils achieved using the tensiometric technique. Sands with different silt contents were used to capture a wide range of suction levels. Suction-controlled tests closely mimic the natural moisture movement in soils while enabling independent evaluation of degree of saturation without altering its structure. The second set involved cyclic DSS tests on silty sand specimens prepared using wet compaction method at target degrees of saturation. Comparisons of these tests will reveal the impacts of degree of saturation, the technique to control the saturation level, and fines content on seismic settlement in soil layers. Table 6-1,6-2, and 6-3 present

119

summaries of experimental program of this study. Details of tested soils, sample preparation, and experimental testing procedures are provided in chapter 3.

Table 6-1. Experimental program of cyclic DSS tests on MIPS treated soils.

test number #	Fine content, FC (%)	Degree of saturation, S_r (%)	Shear strain amplitude, γ (%)
1-4	0	100	0.005, 0.025, 0.1, 0.3
5-13	0	95-89-82	0.025, 0.1, 0.3
14-17	10	100	0.005, 0.025, 0.1, 0.3
18-26	10	95-88-80	0.025, 0.1, 0.3
27-31	20	100	0.005, 0.015, 0.025, 0.1, 0.3
32-40	20	96-88-79	0.025, 0.1, 0.3

Table 6-2. Experimental program of cyclic DSS tests on suction-controlled soils.

test number #	Fines content, FC (%)	Degree of saturation, S_r	Shear strain amplitude, γ (%)
1	0	0.99	0.01, 0.2
2-4	0	0	0.01, 0.2
5	0	0	0.4
6	0	0	0.1
7-11	0	0.6-0.45-0.33-0.31-0.15	0.01, 0.2
12-14	0	0.26	0.025, 0.4
15	10	0	0.01, 0.1, 0.2, 0.4
16	10	0.28	0.01, 0.1, 0.2, 0.4
17	20	0	0.025, 0.1, 0.2, 0.4
18	20	0.79	0.025, 0.1, 0.2, 0.4
19	20	0.49	0.025, 0.1, 0.2, 0.4
20	20	0.33	0.025, 0.1, 0.2, 0.4

Table 6-3. Experimental program of cyclic DSS tests on wet-compacted soils.

test number #	Fines content, FC (%)	Degree of saturation, S_r	Shear strain amplitude, γ (%)
1	20	0.8	0.025, 0.1, 0.2, 0.4
2	20	0.5	0.025, 0.1, 0.2, 0.4
3	20	0.35	0.025, 0.1, 0.2, 0.4
4	20	0.33	0.025, 0.1, 0.2, 0.4

6.4. EXPERIMENTAL RESULTS

6.4.1. SWRCs of the tested soils

The soil-water retention data was obtained by drying initially fully saturated samples using suction control tensiometric technique. Figure 6-1 presents soil-water retention data and SWRCs of the tested specimens along with the SWRC of Ottawa sand specimens with initial conditions similar to clean sand in this study reported in (Ghayoomi et al. 2011). According to Figure 6-1, an increase in matric suction results in reduction in specimens' degree of saturation. However, the rate of changes differed depending on the silt content, i.e., lower rates of reduction in degree of saturation were observed in specimens with higher fines content. This is due to higher capillary rise and consequently water retention ability of fines material compared to coarse soils. The SWRCs of tested specimens were obtained by fitting estimated values of the van Genuchten SWRC model (Equation (6-1)) to the experimental data for each soil. Details of SWRC model is provided in chapter 2.

$$S_e = \frac{S - S_r}{1 - S_r} = (\frac{1}{1 + (\alpha\psi)^n})^m \tag{6-1}$$

In this regard, residual degree of saturation values of 0.05, 0.1, and 0.15 were assumed for specimens having 0, 10, and 20% fines content, respectively. van Genuchten SWRC model's

fitting parameters α and n were obtained by least square fitting method and values are reported in Table 6-4.

Table 6-4. van Genuchten SWRC parameters for tested soils.

Parameter	Soil		
	Ottawa sand	FC= 10%	FC= 20%
Van Genuchten's α (kPa^{-1})	0.25	0.20	0.09
Van Genuchten's n	6	3.5	2.5
Residual degree of saturation, S_r	0.08	0.18	0.2
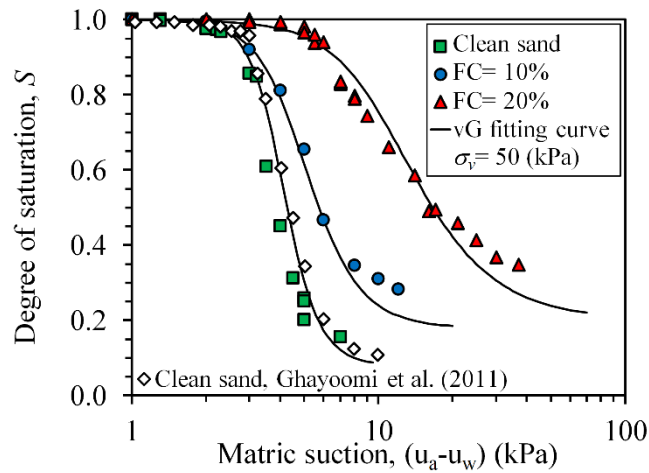
Figure 6-1. SWRCs of the tested specimens

6.4.2. Cyclic DSS tests results

Example results of cyclic DSS tests on a dry and a suction-controlled unsaturated silty sand (FC= 20%) having an initial $S_r = 0.49$, both subjected to 15 cycles of sinusoidal shear strains with an amplitude of 0.2% are presented in Figure 6-2. A slight increase in the measured maximum shear

122

stress was observed with cycles of loading (Figure 6-2 a and b). The induced shear strains gradually increased the cumulative volumetric strains, ε_v (Figure 6-2 c and d). Positive volumetric strain reflects compression in this study.
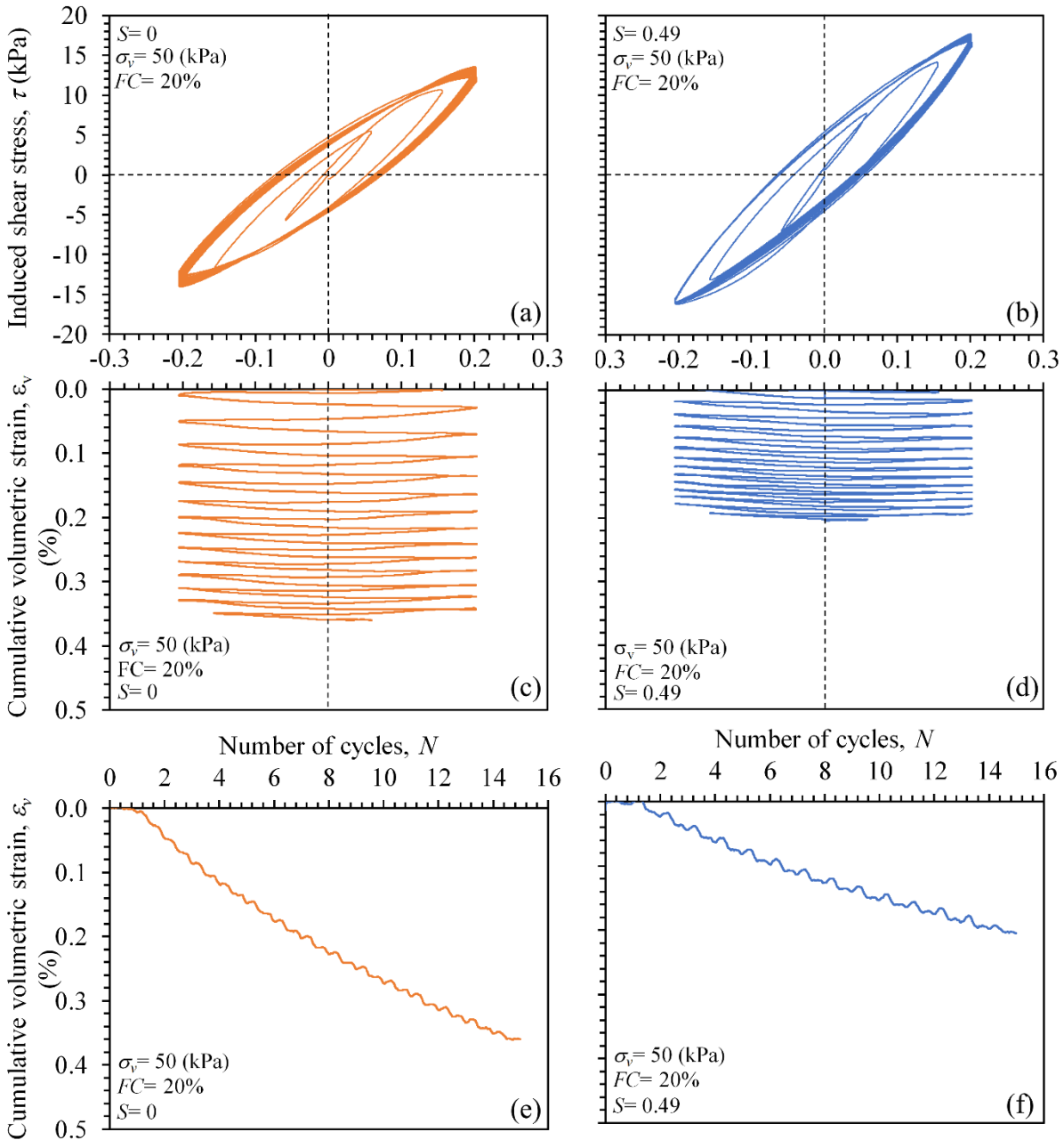
Figure 6-2. Typical experimental results from cyclic DSS tests on (a,c,e) a dry and (b,d,f) an unsaturated silty sand specimen.

6.4.3. Volumetric deformation of dry specimens

Cyclic DSS tests on dry sand specimens with various FC, prepared at a pre-loading relative density of approximately 55%, allowed for independent assessment of the effects of fines content and induced shear strain amplitude on the volumetric strain. The tests were conducted at various strain levels for 15 cycles of loading and results are presented in Figure 6-3. A strong relationship was observed between ε_v and the shear strain amplitude which is in agreement with previous findings that the volumetric strain in soils is highly affected by the magnitude of the induced shear strain (Silver and Seed 1971; Hsu and Vucetic 2004; Duku et al. 2008; Yee et al. 2014). No considerable plastic volumetric strain was observed at shear strain amplitudes less than approximately 0.02%. This is within the range of threshold shear strain (i.e., 0.01-0.03%) reported for sands (Hsu and Vucetic 2004). For a given shear strain level higher than γ_{tv}, the volumetric strain increased with the fines content. Similar observations were made by Whang et al. (2005) who investigated the effect of non-plastic fines on seismic compression of sands. This is explained by considering the effect of fines on sand structure where the addition of fines leads to a transition in mechanical behavior of the soil from a sand dominated behavior to a fines' dominated behavior (Thevanayagam and Mohan 2000; Polito and Martin 2001). The results also corresponded well with the data reported by Duku et al. (2008) who conducted cyclic DSS tests on dry clean sand specimens with similar initial conditions (i.e., $D_r = 60\%$, $\sigma'_v = 50$ kPa).
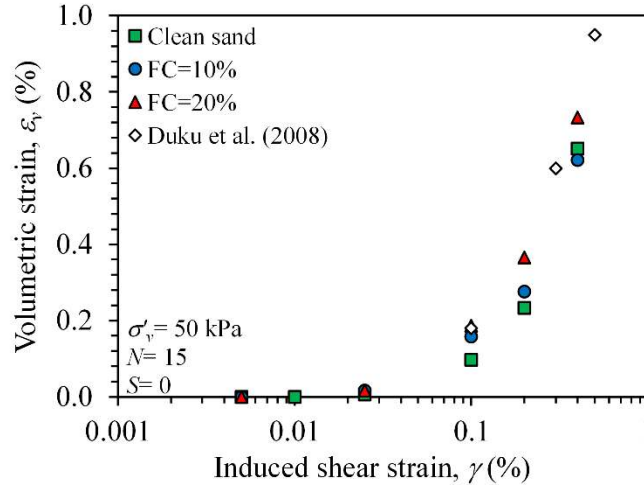
Figure 6-3. Variations of volumetric strain with induced shear strain amplitude at 15 cycles of loading obtained from cyclic DSS tests on dry sand and silty sand specimens in this study (Data represent the mean values) compared with those reported by Duku et al (2008).

6.4.4. Volumetric deformation of suction-controlled unsaturated specimens

Figure 6-4 presents the variation of $\varepsilon_{v,unsat}/\varepsilon_{v,dry}$ values with the degree of saturation as well as matric suction for specimens prepared with suction control under 0.1, 0.2, and 0.4% shear strains. Experimental volumetric deformation measurements indicated a decrease in $\varepsilon_{v,unsat}/\varepsilon_{v,dry}$ with decreasing the degree of saturation from fully saturated to approximately $S=0.3$, followed by an increase in $\varepsilon_{v,unsat}/\varepsilon_{v,dry}$ with further decrease in the degree of saturation (Figure 6-4 a, c, e). This impact was more pronounced for sands with higher fines contents where the induced volumetric strain of silty sand with FC=20% decreased by almost 75% in the specimen with $S=0.33$ compared to that in the dry specimen (e.g., Figure 6-4c). This is due to higher matric suction developed in silty sands than in sands at the same degree of saturation (i.e., as shown in Figure 4), which resulted in stiffer soil response. The results also indicated a strong correlation between induced volumetric strains and the matric suction level (Figure 6-4 b, d, f). For both clean sand silty sand specimens, $\varepsilon_{v,unsat}/\varepsilon_{v,dry}$ initially decreased as the matric suction increased from zero suction at fully saturated condition. Then, the clean sand specimens followed a subsequent increase in $\varepsilon_{v,unsat}/\varepsilon_{v,dry}$ with an

125

increase in matric suction after the corresponding value of *S*≈ 0.3. Similar observations were reported by Ghayoomi et al. (2011) and Yee et al. (2014). Overall, the results signify the importance of incorporating both the degree of saturation and matric suction in seismic compression prediction models.
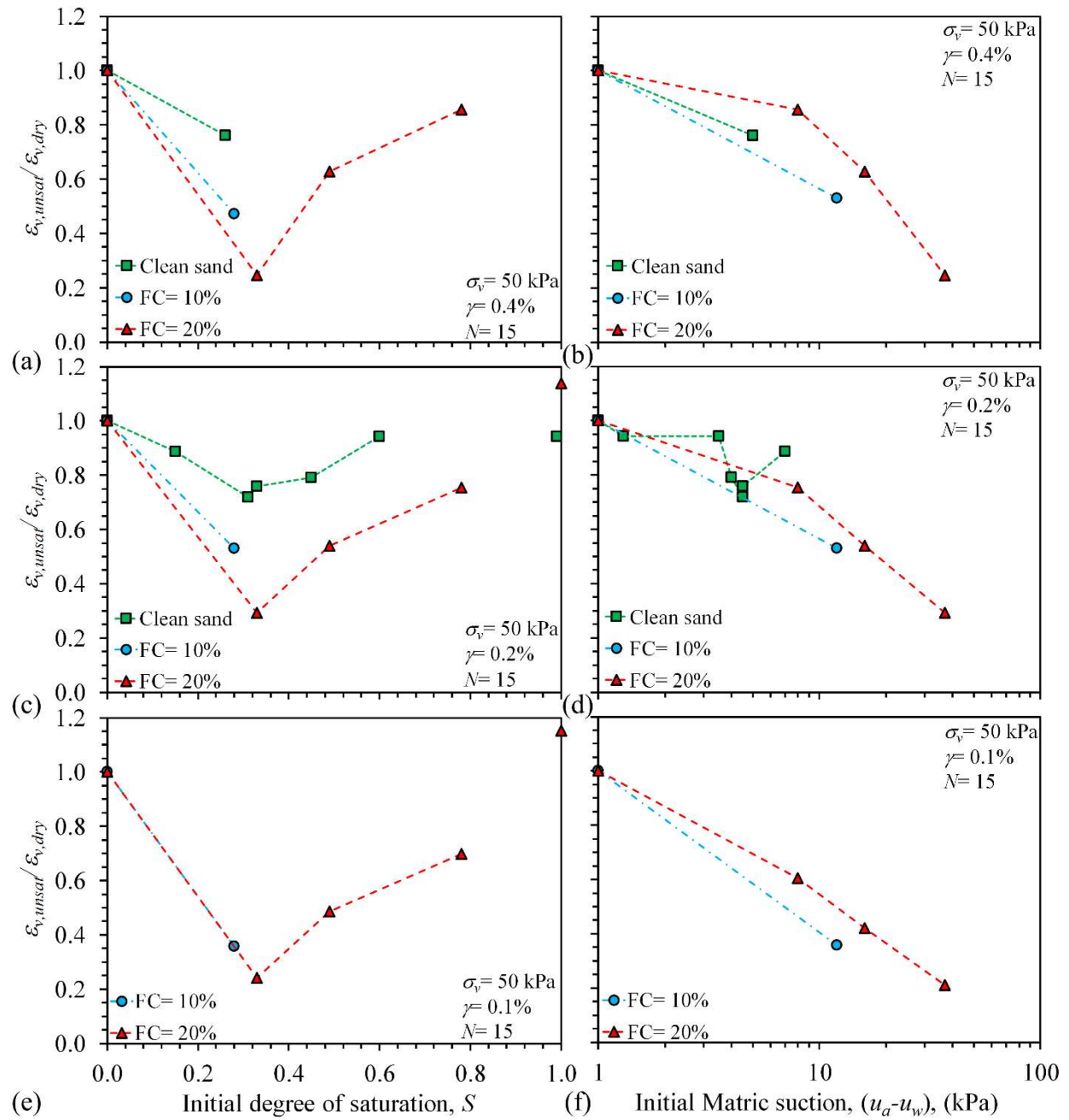
Figure 6-4. Variations of volumetric strain with induced shear strain amplitude at 15 cycles of loading obtained in this study (Data represent the mean values).

126

6.4.5. Impact of desaturation approach on the volumetric deformation

In order to evaluate the impact of the desaturation approach, results of cyclic tests on specimens with FC= 20% prepared through suction control were compared with those prepared through wet compaction (Figure 6-5). In addition, results of cyclic test on desaturated silty sand samples using Microbial Induced Partial Saturation (MIPS) method discussed in previous chapter and reported by Mousavi and Ghayoomi (2020) and wet compacted silty sands reported by Yee et al. (2013) are also populated in Figure 6-5 (a,b), respectively. Induced partial saturation results in the reduction of degree of saturation in soils below the ground water level through entrapment of gas bubbles inside the pore space and has been investigated as an effective measure for liquefaction mitigation (Okamura et al. 2011; Eseller-Bayat et al. 2013; Mousavi and Ghayoomi 2019; Mousavi et al. 2019). In order to compare the results in a consistent manner, the mean values of volumetric strain of repeated tests on unsaturated soils with similar degrees of saturation but different shear strain amplitudes with approximately similar degrees of saturation were normalized by their corresponding ε_v in dry condition. The volumetric strain data from bio-desaturated samples revealed minimal impact of desaturation on volumetric deformation of soils (Figure 6-5a). The comparison of $\varepsilon_{v,unsat}/\varepsilon_{v,dry}$ data from cyclic tests on specimens prepared using suction control and wet compaction techniques indicates similar trends in $\varepsilon_{v,unsat}/\varepsilon_{v,dry}$ versus S for low to intermediate degrees of saturation ($S<\sim 0.6$). However, for the degrees of saturation greater than 0.6, $\varepsilon_{v,unsat}/\varepsilon_{v,dry}$ of wet-compacted soils, in general, resulted in higher volume change than that of the dry specimens. This behavior was also observed in the results of cyclic tests on natural soils reported by Yee et al. (2013) (Figure 6-5b).

127
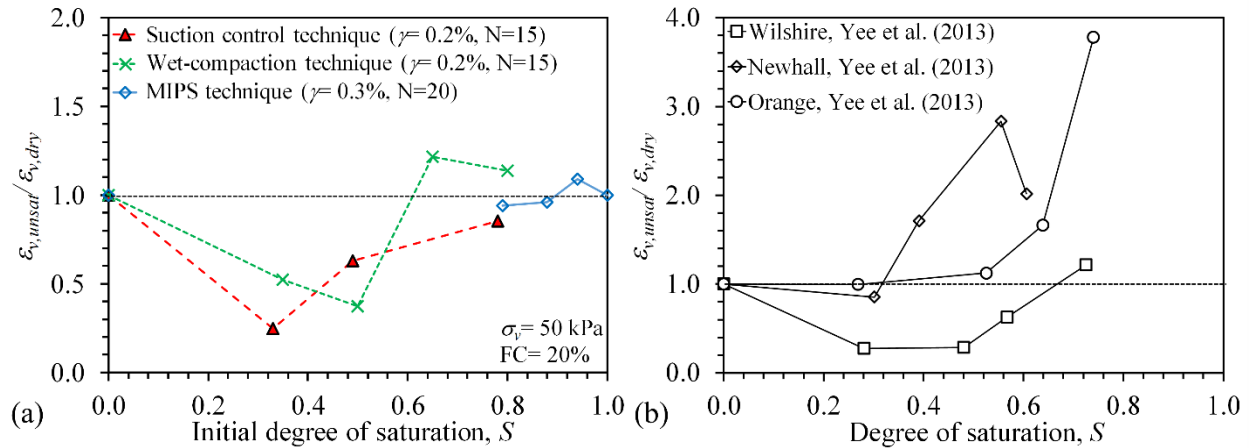
Figure 6-5. Variations of normalized volumetric strains with degree of saturation.

Two potential mechanisms may be responsible for the different trends observed between the volumetric deformation of samples desaturated through suction control, wet compaction, and MIPS methods. First, this difference may be attributed to the different soil structures, the energy absorbed during compaction, and their corresponding effects on dynamic properties of soil (Qian et al. 1991; Kim et al. 2003). During sample preparation using wet-compaction method, it is likely that soil samples compacted at high degrees of saturation near their optimum compaction moisture content may experience significantly lower energy level than dry or unsaturated soils with low or intermediate degrees of saturation and, consequently, possess less stable structures. The impact of the stability of soil structure on its volumetric deformation can indirectly be confirmed by considering the volumetric behavior of re-sheared versus virgin-sheared specimens. Experimental results by Yee et al. (2013) indicated that soils subjected to re-(cyclically)shear strains show significantly lower volumetric deformations than virgin-sheared specimens (i.e., almost one-quarter), although they had similar initial conditions (i.e., density, saturation, vertical stress). Second, wet compaction and MIPS treatment may lead to a different state of saturation than the one achieved through suction-control, even though they possess the same degree of saturation.

128

Although compaction at low degrees of saturation would result in formation of interconnected air-filled pores, compaction of soils with high water contents may lead to entrapment of air in pores. Similarly, MIPS process leads to formation of occluded gas bubbles in soils. In this case, occluded gas bubbles at high degrees of saturation may not result in development of inter-particle suction (Finno et al. 2017; Mousavi et al. 2019, 2020). Therefore, although suction-controlled, MIPS-treated, and wet-compacted samples may have the same degrees of saturation, it is likely that occluded gas bubbles do not impact the inter-particle stresses and the volumetric deformation of soils under similar seismic demands.

6.5. THEORETICAL FORMULATION

The analysis of seismic volumetric deformation of soils requires an appropriate seismic demand and volumetric strain material model parameters. Although different parameters such as cyclic stress ratio (CSR), excess pore pressure ratio, and factor of safety against liquefaction (F_L) are commonly used to interpret the seismic settlement in soils, experimental results from this study and previous research suggest that the amplitude of the induced shear strain and the number of strain cycles are the two most critical parameters (Silver and Seed 1971; Tokimatsu and Seed 1987; Ishihara and Yoshimine 1992; Hsu and Vucetic 2004; Yee et al. 2014). The best evidence would be the approximately similar seismic settlement in dry and fully saturated soil samples tested under strain-controlled condition with similar shear strain. However, the definition of an equivalent shear strain amplitude in stress-based seismic analysis may not be readily available and require approximate iterative procedures. For unsaturated soils, with the degree of saturation low enough not to cause significant excess pore pressure generation, the equivalent induced shear strain amplitude can be defined using the equivalent linear framework. Ghayoomi et al. (2013) synthesized the laboratory results by Lee and Albaisa (1974) and showed that seismic compression

is the dominant settlement mechanism when $r_u < 0.2$, and its magnitude may be estimated using a volumetric strain material model.

In order to develop a volumetric strain model, the model originally developed by Yee et al. (2014) was considered as a starting point since it is calibrated using a rich dataset (Yee et al. 2014). As discussed in chapter 2, the model has the following form:

$$\varepsilon_{v-compression} = a \, [\gamma_e - \gamma_{tv}]^b (K_{FC})(K_{\sigma,\varepsilon})(C_N)(K_S) \tag{6-2}$$

where γ_{tv} is volumetric threshold shear strain below which cyclic loading does not result in permanent volumetric deformation (Hsu and Vucetic 2004), a and b are fitting parameters, and K_{FC}, $K_{\sigma,\varepsilon}$, C_N, and K_S are reduction factors for fines content, overburden stress, number of cycles, and degree of saturation, respectively. Yee et al. (2014) reported no significant impact of degree of saturation on the compression for sands with FC< 10% and incorporated a step function for the impact of water saturation in the model; i.e., Equation (6-3):

$$K_S = \begin{cases} -0.017S + 1 & (S < 30\%) \\ 0.5 & (30\% \leq S < 50\%) \\ 0.05S - 2 & (50\% \leq S < 60\%) \\ 1 & (S > 60\%) \end{cases} \tag{6-3}$$

where, K_s is the ratio of volumetric strain in unsaturated soil with a given degree of saturation, S, to that of the dry soil (i.e., $\varepsilon_{v,unsat}/ \varepsilon_{v,dry}$). It is noteworthy that Equation (6-3) did not capture the trends of seismic compression with the degree of saturation in one of the three soils tested by Yee et al. (2014) and provided a very approximate estimate for the other two. Also, the model indicates that the volumetric strain material characteristics is only a function of degree of saturation.

However, experimental results from the current study suggested that volumetric strain material characteristics of unsaturated soils is affected by both the degree of saturation and the developed matric suction value. Therefore, Equation (6-3) may not be able to capture the impact of matric suction on volumetric behavior of unsaturated soils under seismic loading. To address

130

this issue, a new reduction factor was defined to simultaneously incorporate the impact of the degree of saturation and the matric suction in VSMM, and Equation (6-3) was modified as follows:

$$\varepsilon_{v-compression} = a \, [\gamma_e - \gamma_{tv}]^b (K_{FC})(K_{\sigma,\varepsilon})(C_N)(K_{S,\psi}) \tag{6-4}$$

where $K_{S,\psi}$ is the new reduction factor considering the impact of degree of saturation and matric suction on seismic compression, which is defined as:

$$K_{S,\psi} = \begin{cases} S^\beta & (S > S_{min}) \\ \dfrac{S_{min}^\beta - 1}{S_{min}} S + 1 & (S < S_{min}) \end{cases} \tag{6-5}$$

where β is the material specific parameter relating the impact of suction to volumetric straining in unsaturated soils and S_{min} is the degree of saturation at which the volumetric strain in unsaturated soil reaches its minimum value. Based on the experimental results, it was considered that further reduction in degree of saturation from S_{min} results in a linear increase in $K_{S,\psi}$ from S_{min}^β to 1. The synthesis of the results from this study, Ghayoomi et al (2011), Whang et al. (2005), and Yee et al. (2014) would recommend $S_{min} \approx 0.3$.

6.6.   ANALYSIS AND DISCUSSION

In order to evaluate the suitability of Equation (6-4) to capture the trends observed in the experimental results, the estimated values of ε_v were first compared to the results of experiments on dry samples. In this regard, parameter $b = 1.2$ was used as suggested by Yee et al. (2014), and parameter $a = 1.52$ was obtained using the equation suggested by Yee et al. (2014):

$$a = a_1 \exp{(a_2 D_r)} \tag{6-6}$$

where parameter $a_1 = 5.38$ and parameter $a_2 = -0.023$. The reduction factor for number of cycles was obtained using the equation proposed by Yee et al. (2014):

$$C_N = R(LnN) + c \tag{6-7}$$

where $R = Ln(\gamma_e - \gamma_{tv}) + 0.26$ and $RLnN + c = 1 - (RLn(15))$. The parameter $C_N = 1$ was obtained for 15 cycles of loading. The reduction factor $K_{\sigma,\varepsilon}$ was also found using the proposed equation by Yee et al. (2014):

$$K_{\sigma,\varepsilon} = (\frac{\sigma_v}{p_a})^{-0.29} \tag{6-8}$$

where p_a is the atmospheric pressure. $K_{\sigma,\varepsilon} = 1.22$ was obtained for 50 kPa overburden stress using Equation (6-8) and $K_{S,\psi} = 1$ was considered for dry samples. Yee et al. (2014) proposed the following equation for estimation of the impact of FC on seismic compression of clean sands containing low plastic fines:

$$K_{FC} = \begin{cases} 1 & (FC < 10\%) \\ e^{-0.042(FC-10)} & (FC = 10\% - FC_L) \\ 0.35 & (FC \geq FC_L) \end{cases} \tag{6-9}$$

where FC_L (in percent) is the limiting fines content at which the mechanical behavior of the soil transitions from a course dominant behavior to a fine dominant behavior (~35% for sands tested by Yee et al. 2014) and K_{FC} is the ratio of volumetric strains of soils with a given fines content to the volumetric strain of clean sand (i.e., $K_{FC} = \frac{\varepsilon_{v,FC\geq0}}{\varepsilon_{v,FC=0}}$).

Yee et al. (2014) indicated that Equation (6-9) was not able to capture the trends in ε_v with fines content for sands containing non-plastic silt. Thus, in this study K_{FC} was treated as fitting parameter to fit estimated values of Equation (6-4) to the experimental results for silty sands using least-square regression. $K_{FC} = 1$ and 1.2 were found to provide the best fit to the experimental data for sands with FC= 10% and 20%, respectively. Using these parameters, comparisons between the experimental results and the estimated values of ε_v for dry specimens with different fines content are plotted in Figure 6-6 as a function of the amplitude of induced shear strain. The comparisons

indicated that Equation (6-4) may provide a very good estimate of seismic compression in dry soils

and is capable of capturing the non-linear evolution of ε_v with the induced shear strain.
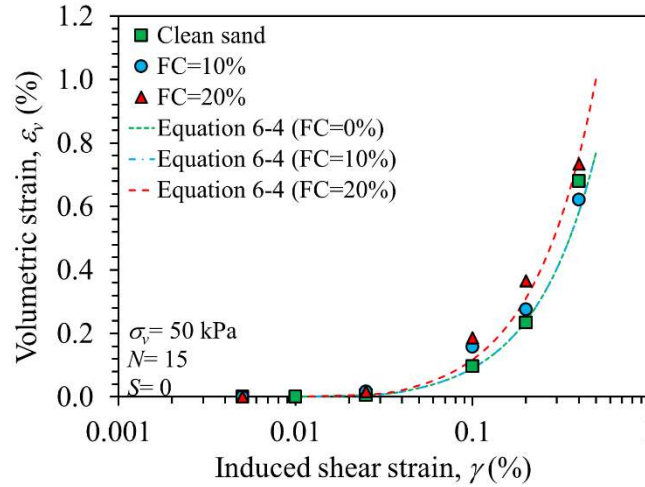
Figure 6-6. Experimental trends in ε_v with induced shear strain in comparison with Equation (6-4) predictions for dry samples.

The experimental data for unsaturated soils were used to calibrate the newly defined

reduction factor, $K_{S,\psi}$. The least square regression technique was used for the determination of

parameter β in Equation (6-5) for each test. Using sands with different fines content enabled an

independent investigation of the impact of suction on the parameter β for a wide range of matric

suction levels at a given degree of saturation. Regardless of the amplitude of induced shear strain,

a relatively strong correlation observed between matric suction and $K_{S,\psi}$ at a given degree of

saturation (Figure 6-7a); suggesting a linear relationship between $K_{S,\psi}$ and $log(1/\psi)$. The

magnitude of matric suction developed at a given degree of saturation in silty sand mainly depends

on pore size distribution. In the van Genutchen (1980) SWRC model, the correlation between the

magnitude of suction and pore size distribution is described through parameter n_{vG}:

$$\frac{1}{\psi} \propto S^{\frac{1}{n_{vG}-1}} \tag{6-10}$$

From Equation (6-5) and (6-10) it can be concluded that the parameter β is correlated to n_{vG}:

$$\beta \propto \frac{1}{n_{vG}-1} \qquad (6\text{-}11)$$

From this line of logic, the possible correlation between SWRC parameter n_{vG} and parameter β was investigated. The results indicated that $1/(n_{vG}\text{-}1)$ values from SWRC data and the estimated values of parameter β may fall on a single line (Figure 6-7b). Therefore, the correlation between the two can be expressed as:

$$\beta = \frac{f_1}{n_{vG} - 1} + f_2 \qquad (6\text{-}12)$$

The experimental results obtained from this study suggest approximate values of $f_1 = 1.5$ and $f_2 = 0$.

(a)

(b)
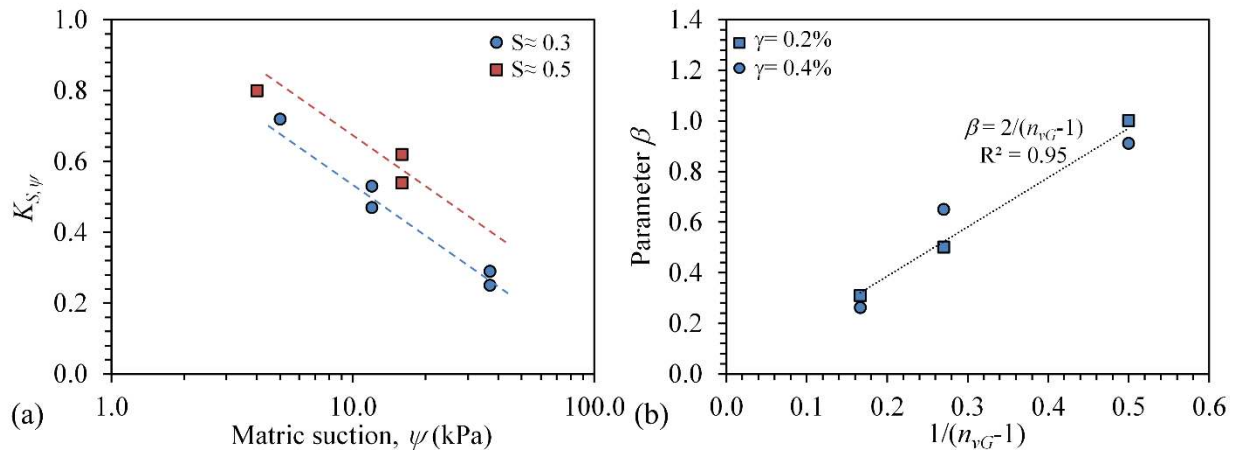
Figure 6-7. (a) Correlation between matric suction and $K_{S,\psi}$ and (b) relationship between parameter β and $1/(n_{vG}\text{-}1)$.

Figure 6-8 illustrates comparisons between $\varepsilon_{v,unsat}/\varepsilon_{v,dry}$ obtained from the experiments and those predicted using Equation (6-4). The general trends in $\varepsilon_{v,unsat}/\varepsilon_{v,dry}$ with the degree of saturation predicted by the proposed reduction factor fits very well with the experimental results. Specifically, the newly defined reduction factor $K_{S,\psi}$ was able to predict greater impact of degree

of saturation on volumetric deformation of sands with higher fines content. The model was also

able to capture different trends in $\varepsilon_{v,unsat}/\varepsilon_{v,dry}$ for the degrees of saturation above and below S_{min}.
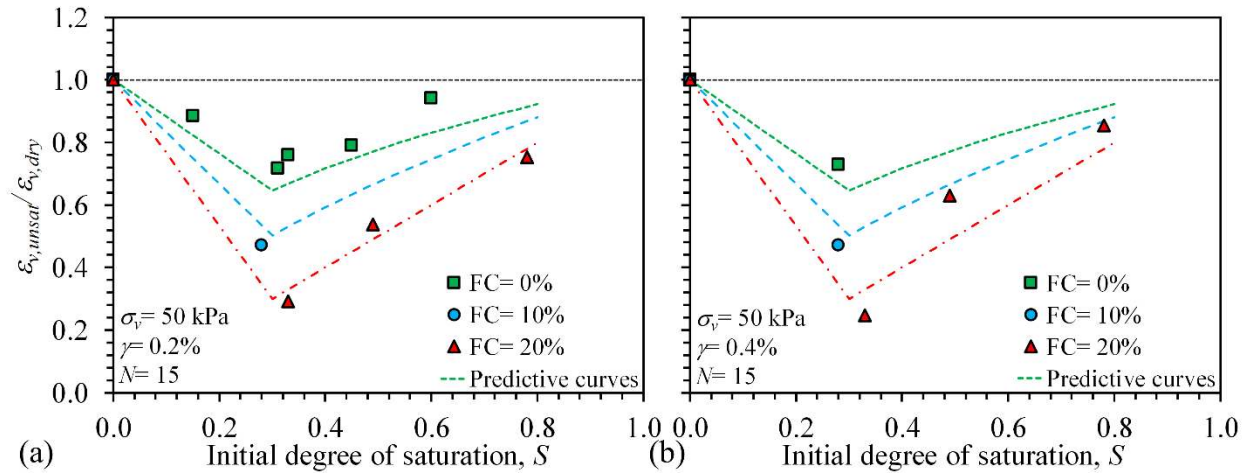
Figure 6-8. Comparisons of experimental trends in ε_v with degree of saturation with Equation (6-4) predictions.

It should be emphasized that Equation (6-4) estimates the seismically induced volumetric

settlement of soils under a certain induced shear strain amplitude. As discussed earlier in this study,

the degree of saturation may also impact the induced shear strain amplitude through suction-

induced hardening or excess pore pressure softening. Therefore, the trends in $\varepsilon_{v,unsat}/\varepsilon_{v,dry}$ of soils

with the degree of saturation are most valid when the specimens are subjected to identical induced

shear strain amplitudes. Elevated stiffness in unsaturated soils due to the developed matric suction

is likely to decrease the induced shear strains and consequently the seismic compression. Equation

7 was generally developed for soils that are not prone to excess pore pressure generation; the

excessive settlement due to the strain softening may be estimated by the methods such as the one

proposed by Ghayoomi et al. (2013). However, for strain-controlled tests where the amount of

shear strain amplitude is constant, Equation (6-4) may be used to estimate the volumetric strain

potential of soils with any degree of saturation. Figure 6-9 compares the predicted $\varepsilon_{v,unsat}/\varepsilon_{v,dry}$ values using Equation (6-4) and those measured experimentally using suction control and MIPS methods. The comparisons of model predictions and experimental data for nearly and fully saturated soils indicates that the model is able to approximate the volumetric strain potential of the soils subjected to similar strain-based seismic demand, regardless of the degree of saturation range (Figure 6-9a). In general, Equation (6-4) predictions fall below the experimental data for soils desaturated using MIPS method. Experimental $\varepsilon_{v,unsat}/\varepsilon_{v,dry}$ data from MIPS tests displayed closely in Figure 6-9b appear to be independent of the magnitude of degree of saturation. This is likely due to the minimal impact of entrapped air developed via MIPS as opposed to negative pore pressure generated via suction control on soil inter-particle forces. Thus, for soils with entrapped air bubbles, $K_{S,\psi}$ may be assumed to be 1, if Equation (6-4) is to be used.
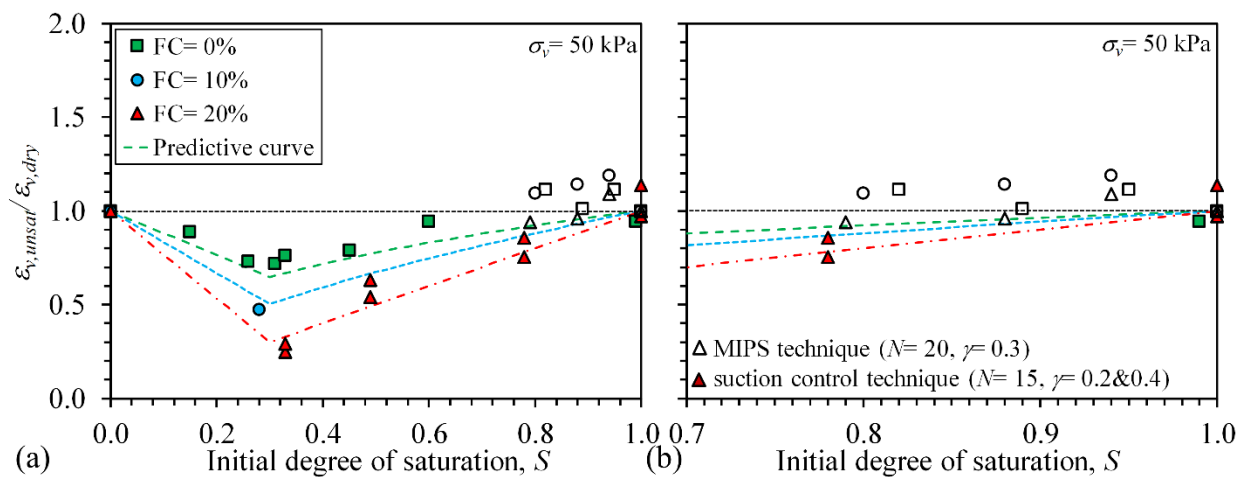
Figure 6-9. Comparisons of the model predictions of ε_v with experimental data obtaied in this study and those reported by Mousavi and Ghayoomi (2020).

6.7. CONCLUSIONS

This chapter described a series of strain-controlled, cyclic DSS tests on unsaturated sand and silty sands prepared using suction control as well as wet compaction techniques. The results of the

136

experiments revealed the significant impact of the degree of saturation and methods of desaturation on seismic settlement. Suction control tests indicated that a reduction in the degree of saturation from full saturation results in a reduction in the volumetric strains of specimens during cyclic loading, down to a minimum value. Further reduction in the degree of saturation, however, would result in the recovery of volumetric strain values to those of dry samples. Based on the results of this study and previously reported data, this minimum value is believed to occur at a degree of saturation of about 0.3. Similar trends were observed in samples prepared via wet-compaction method having degrees of saturation lower than approximately 0.6. Wet-compacted samples with degrees of saturation higher than 0.6 showed significantly higher volumetric strains comparing with the specimens prepared using suction control technique.

Insights gained from these experimental observations, theoretical considerations, and previous investigations led to the identification of critical contributors in seismic volumetric deformation behavior of unsaturated soils. On such basis, a strain-based seismic compression model was adapted and modified to estimate the compression of sands and silty sands in unsaturated conditions by incorporating the seismic demand and volumetric strain material parameters. Similar volumetric deformation magnitudes in nearly saturated and dry samples suggested that seismic induced shear strains and number of cycles of loading are unique parameters for describing the seismic demand. Degree of saturation and matric suction were identified as key parameters affecting both seismic demand and volumetric strain material characteristics of soil. A new reduction factor was introduced to capture the impact of the saturation level and matric suction on the volumetric deformation. The comparison between the model predictions and experimental data indicated the suitability of the model in estimating the seismic compression of unsaturated soils, especially in low to intermediate degrees of saturation.

137

CHAPTER 7

IMPACT OF THE STATE OF SATURATION AND DEGREE OF SATURATION ON DYNAMIC PROPERTIES OF SILTY SANDS

7.1. ABSTRACT

Dynamic soil properties including shear modulus and damping ratio are key components controlling mechanisms of wave propagation and seismic induced settlement in soils. During the last few decades, extensive research has been conducted to address issues related to the seismic performance of geosystems. Previous studies revealed that soil's degree of saturation can have a significant impact on its dynamic properties. However, they mostly focused on small strain dynamic response of unsaturated soils above the ground water table. The soil below the ground water can also have a degree of saturation below 100%, however, the existence of air bubbles in this condition results in different state of saturation than that of unsaturated soil. This study investigates the impact of degree of saturation, the technique to achieve it, state of saturation, and fines content on shear modulus and damping ratio of sand and silty sands. This involved three series of cyclic direct simple shear tests on samples desaturated using microbial partial saturation, suction control, and wet-compaction techniques. The strain-controlled DSS tests with variable

amplitudes of shear strain were imposed on soil specimens with different degrees of saturation in undrained conditions. Results showed significant impact of fines content on dynamic properties of sand. Further, shear modulus of unsaturated samples was consistently higher than those of dry ones. In comparison with dry samples, lower damping ratio values were observed in unsaturated samples tested using suction control technique. The impact of desaturation was higher in sands containing higher fines content. A meaningful difference was observed between shear moduli of specimens prepared using MIPS, suction control, and wet-compaction methods. In general, for similar degree of saturation and initial conditions, samples prepared with suction control technique with negative pore water pressure had higher shear modulus than those prepared with MIPS and wet-compaction techniques.

7.2. INTRODUCTION

Unsaturated soils are widely available in shallow ground above the water table, where their strength and stiffness are controlled and impacted by inter-particle suction forces (Jafarzadeh and Sadeghi 2012; Ghayoomi et al. 2013, 2017; Oh and Vanapalli 2014; Hoyos et al. 2015; Dong et al. 2016; Khosravi et al. 2016b; a, 2017; Mirshekari and Ghayoomi 2017; Borghei et al. 2020; Zhang and Lu 2020). Air bubbles can also be entrapped below the ground water table as a result of gas exsolution (e.g., pore fluid pressure drop, bio-respiration) or immiscible displacement (e.g., drainage and imbibition, gas injection). These bubbles, even in minute amounts, can significantly affect undrained dynamic soil response, including the excess pore pressure generation (Yoshimi et al. 1989; Unno et al. 2008; Okamura et al. 2011; Rebata-Landa and Santamarina 2011; Eseller-Bayat et al. 2013; He et al. 2013; Tsukamoto et al. 2014; Mele et al. 2019; Mousavi and Ghayoomi 2020a). Taking advantage of this effect, Induced Partial Saturation (IPS) techniques such as the use of biogenic gas generation have been explored as an effective means to mitigate liquefaction.

These soils have different state of saturation compared to unsaturated soils above the ground water since the existence of occluded bubbles in the pore space may not affect inter-particle suction stress (Finno et al. 2017; Mousavi and Ghayoomi 2018; Mousavi et al. 2020).

A vast majority of geotechnical infrastructures rest on or are surrounded by unsaturated and partially saturated soils where the degree of saturation and state of saturation can significantly impact their dynamic properties. Soils' dynamic properties including shear modulus and damping ratio are key parameters in design and performance evaluation of geotechnical systems. In particular, the analysis of earthquake wave propagation and seismically induced settlement in soils rely on a precise estimation of dynamic soil properties (Yee et al. 2014; Mirshekari and Ghayoomi 2017; Zeybek and Madabhushi 2017; Borghei et al. 2020). Centrifuge tests by Mirshekari and Ghayoomi (2017) indicated that unsaturated soils may increase the amplification of seismic motions due to altered dynamic properties of soil. In addition, the increased soil stiffness may result in a reduction of induced shear strains and consequently volumetric deformations in unsaturated soils (Ghayoomi et al. 2013; Yee et al. 2014; Borghei et al. 2020; Rong and McCartney 2020). The majority of models for the prediction of seismic compression in partially saturated and unsaturated soils rely on accurate estimation of shear modulus in soils.

Past research mainly focused on small strain behavior or strength evaluation, failure mechanisms, and liquefaction assessment of partially saturated and unsaturated soils in limit state. There is a lack of fundamental understanding and mechanical framework to evaluate the impact of degree of saturation and state of saturation on dynamic properties of soils. Specifically, despite their beneficial use for liquefaction mitigation, IPS soils may still suffer excessive settlement due to seismic compression and also alter the wave propagation mechanisms. Therefore, there is a pressing need to evaluate dynamic properties of soils in a three-phase media with different states

140

of saturation. This study experimentally evaluates the air-water-solid particle interaction effects on the dynamic properties of soils in the context of unsaturated soil mechanics.

7.3. EXPERIMENTAL INVESTIGATION

The work involved sets of undrained cyclic direct simple shear (DSS) tests to impose different dynamic loading conditions on soils with different saturation levels. The degree of saturation was controlled through (1) generation of biogenic gas using microbial induced partial saturation (MIPS) method; (2) controlling suction by incorporating tensiometric technique in unsaturated soils; and (3) wet-compaction. Sandy soils with different silt contents were used to investigate the extent to which desaturation affects the dynamic response, given the fines content. Table 7-1, Table 7-2, and Table 7-3 present summaries of experimental program used in this chapter. Details of tested soils, sample preparation, experimental testing procedures, and data analysis approach are provided in chapter 3.

Table 7-1. Experimental program of cyclic DSS tests on MIPS treated soils.

test number #	Fine content, FC (%)	Degree of saturation, S_r (%)	Shear strain amplitude, γ (%)
1-4	0	100	0.005, 0.025, 0.1, 0.3
5-13	0	95-89-82	0.025, 0.1, 0.3
14-17	10	100	0.005, 0.025, 0.1, 0.3
18-26	10	95-88-80	0.025, 0.1, 0.3
27-31	20	100	0.005, 0.015, 0.025, 0.1, 0.3
32-40	20	96-88-79	0.025, 0.1, 0.3

Table 7-2. Experimental program of cyclic DSS tests on suction-controlled soils.

test number #	Fines content, FC (%)	Degree of saturation, S_r	Shear strain amplitude, γ (%)
1	0	0.99	0.2
2-4	0	0	0.2
5	0	0	0.4
6	0	0	0.1
7-11	0	0.6-0.45-0.33-0.31-0.15	0.2
12-14	0	0.26	0.025, 0.4
15	10	0	0.1, 0.2, 0.4
16	10	0.28	0.1, 0.2, 0.4
17	20	0	0.025, 0.1, 0.2, 0.4
18	20	0.79	0.025, 0.1, 0.2, 0.4
19	20	0.49	0.025, 0.1, 0.2, 0.4
20	20	0.33	0.025, 0.1, 0.2, 0.4

Table 7-3. Experimental program of cyclic DSS tests on wet-compacted soils.

test number #	Fines content, FC (%)	Degree of saturation, S_r	Shear strain amplitude, γ (%)
1	20	0.8	0.025, 0.1, 0.2, 0.4
2	20	0.65	0.025, 0.1, 0.2, 0.4
3	20	0.5	0.025, 0.1, 0.2, 0.4
4	20	0.35	0.025, 0.1, 0.2, 0.4

7.4.   EXPERIMENTAL RESULTS AND DISCUSSIONS

7.4.1. Dynamic properties of dry samples

Figure 7-1 presents the variations of shear modulus and damping ratio values with number of

cycles, *N*, for dry sand specimens with different silt contents subjected to constant shear strain

amplitudes of 0.025, 0.2%, and 0.4%. The G and D values for the first and last cycles were excluded from the data as these cycles were set up for ramp up and ramp down in the actuator control system. According to experimental data, cyclic straining of specimens at shear strain amplitudes of 0.1% and 0.4% gradually increased the shear modulus of specimens with increasing N (almost 10% increase in G after 14 cycles of loading). However, no meaningful trend was observed in G versus N for specimens subjected to $\gamma = 0.025\%$. The change in shear modulus with number of cycles can be attributed to the compaction and rearrangement of soil particles under cycles of loading. This also explains no significant change in G with N observed for the smallest γ, as this level of strain most likely does not induce significant plastic deformations in soils. Regardless of the magnitude of shear strains, damping ratio decreased as N increased as result of soil stiffening.

Comparisons between samples with different silt contents indicated a reduction in soil stiffness with an increase in silt content. For example, for $\gamma = 0.2\%$, specimens containing 10% and 20% silt had approximately 20% and 40% lower shear modulus than clean sand. These trends are in agreement with previous studies who reported decrease in small strain shear modulus of sands with increasing fines content (Iwasaki and Tatsuoka 1977; Salgado et al. 2000; Carraro et al. 2009; Goudarzy et al. 2018; Yang et al. 2018). The reason for this observation is the alteration of soil skeleton with the addition of FC. For low fines content (i.e., FC< ~30-50%) the fine particles mostly are positioned in the pore space between larger soil grains. In this case, load transfer mechanism and mechanical behavior of the mixture is mainly controlled by coarser grains (Salgado et al. 2000; Thevanayagam and Mohan 2000; Polito and Martin II 2001; Thevanayagam et al. 2002; Hazirbaba and Rathje 2010). Accordingly, lower stiffness of mixture compared to base sand is expected since a lower portion of soil resist against shearing. However, the impact of fines

content on shear modulus of sand became less pronounce as the induced shear strain amplitude increased. The reason for this observation is the change in the load transfer mechanism with increasing shear strain. The increase in shear strain and movement of soil particles results in contribution of fine particles floated in pore space. Consequently, higher portion of soil particles resist against shearing of soil which results in elevated shear stiffness of the soil. This behavior is confirmed by previous studies who compared the results of small strain and triaxial shearing tests for sands with variable fines contents. For example, Salgado et al. (2000) reported a considerable increase in friction angle of sands with the addition of fines whereas small strain shear modulus of sands dramatically decreases with even a small increase in fines content.

The change in sand structure with the addition of fines also significantly impacted damping ratio. While addition of fines resulted in an increase in damping ratio of sand subjected to the smallest shear strain, it had an opposite effect on damping ratio of samples subjected to larger amplitudes of shear strain ($\gamma = 0.2\%$ and 0.4%), i.e., the damping ratios were generally lower in sands with higher FC. This can be attributed to contribution of initially non-active fines in soil shearing at larger strains, as discussed above.

As discussed previously, dynamic shear modulus and damping ratio in soils are dependent on the amplitude of induced shear strain. Figure 7-2 illustrates the trends in the magnitude of G and D with the amplitude of induced shear strain for the three soils in dry condition. Results presented in Figure 7-2a indicate similar trends in G-γ to what has been reported for dry soils; the shear modulus was found to increase nonlinearly, for this range of strain amplitudes, with a decrease in γ. However, the rate of the increase followed different trends for sands with variable fines content. This is due to alternation of fines role in dynamic soil response with the increase in

144

shear strain amplitude, as discussed earlier. The D values also exhibit an increasing trend with increasing γ, as commonly is reported for dry soils (Menq 2003).
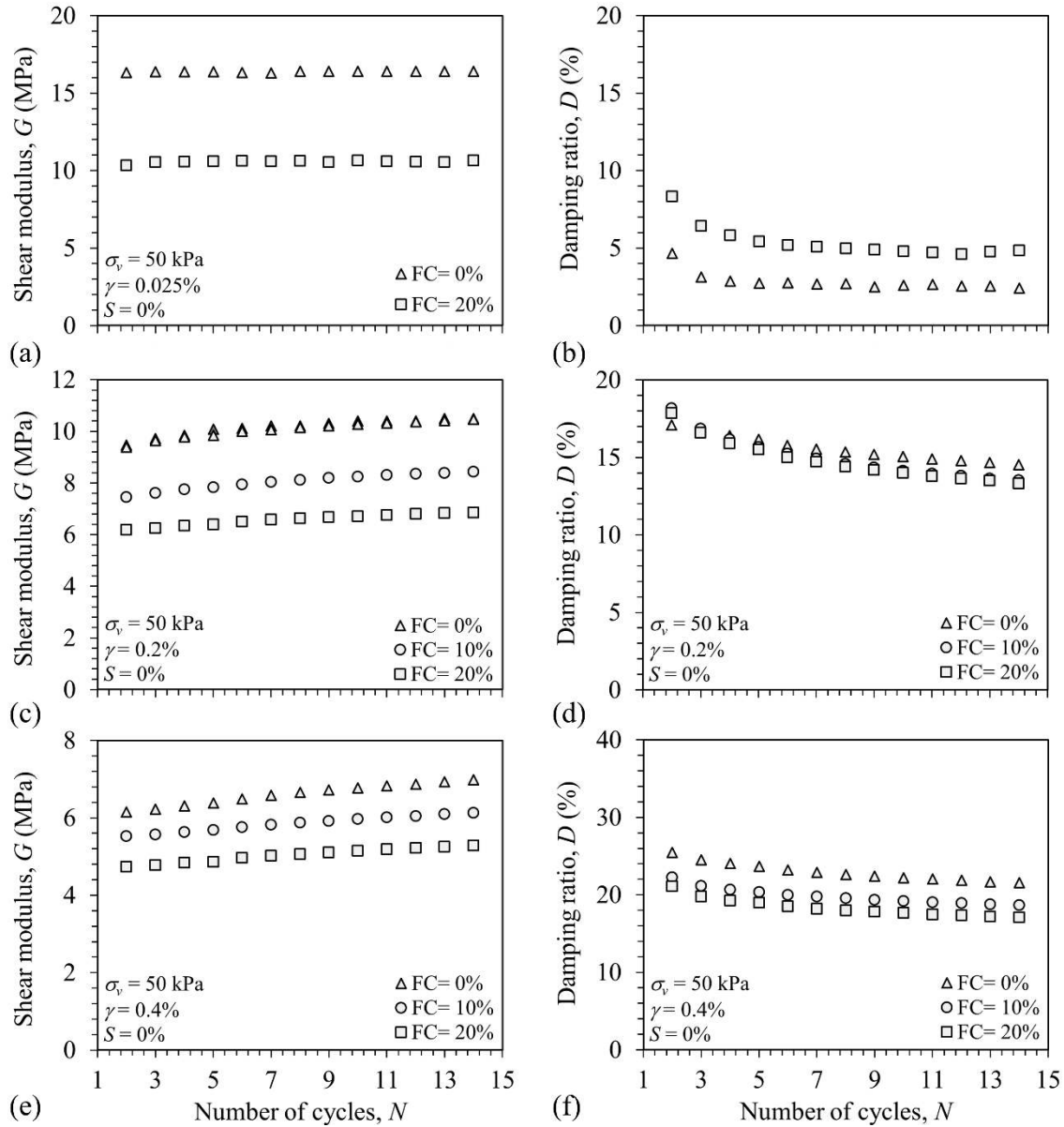
Figure 7-1. Variations of shear modulus and damping ratio of dry samples subjected to (a,b) 0.025%, (c,d) 0.2%, and (e,f) 0.4% shear strain amplitudes.

145
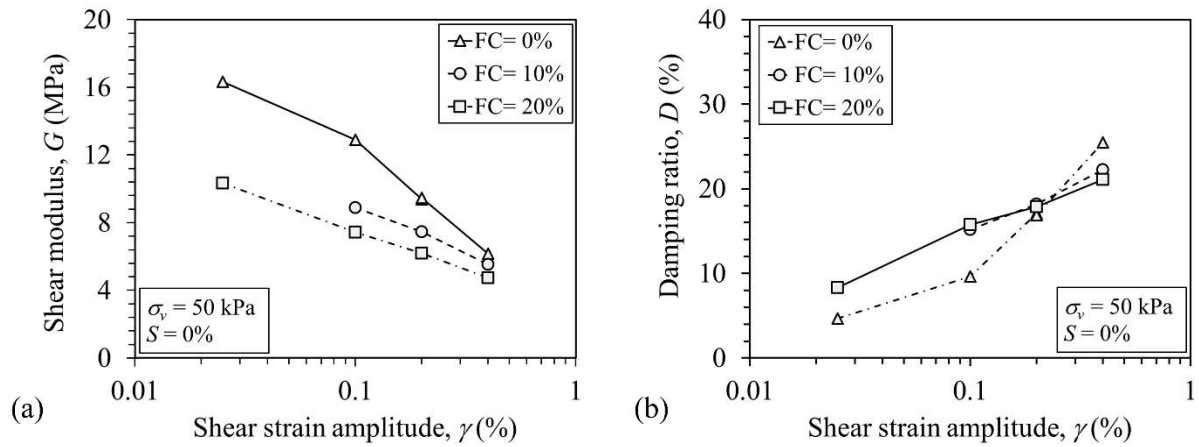
Figure 7-2. Shear modulus versus shear strain amplitude for dry sand and silty sand specimens at N= 2.

7.4.2. Dynamic properties of suction-controlled unsaturated samples

Shear modulus:

Figure 7-3 presents the variations of shear modulus with the degree of saturation and matric suction of specimens subjected to different amplitudes of shear strain that were prepared using the suction control method. Results are presented for the second cycle of loading. Regardless of the fines content, for $S \leq 0.8$, higher shear modulus values were observed in unsaturated specimens in comparison with those of saturated or dry specimens. This is in accordance with previous studies who reported higher shear modulus values in unsaturated soils (Khosravi and McCartney 2012; Hoyos et al. 2015; Dong and Lu 2016; Le and Ghayoomi 2017). The impact of degree of saturation was more pronounced in specimens with higher silt contents. For example, the shear moduli of the specimen with $S= 0.33$ were approximately 60 to 70% higher than those of the dry specimen for samples with FC= 20%, whereas only approximately 5 to 10% increase was observed in shear moduli of unsaturated clean sands compared to dry clean sands (Figure 7-3a-d). This confirms the impact of suction on the dynamic shear modulus of the soils. To better interpret the impact of

146

matric suction, the shear modulus magnitudes were also plotted against the matric suction (Figure 7-3e-h). According to these plots, generally, a nonlinear behavior was observed in G versus ψ curves, where an increase in matric suction from saturated condition, initially, results in an increase in the shear modulus value followed by a drop in shear modulus at matric suction corresponded to dry condition, ψ_{dry} (i.e., assumed ψ_{dry}= 1000 MPa here).

The experimental data indicates lower G values for fully saturated and nearly saturated samples (i.e., S> 0.8) compared to unsaturated and dry ones. The difference between the two was higher for specimens subjected to larger shear strain amplitudes; for example, G value of saturated silty sand with FC= 20% tested at γ= 0.4% was 40% lower than that of the dry one while the difference between their shear moduli was approximately 15% at γ= 0.025%. This can be attributed to reduction in effective stress during cyclic loading in undrained condition due to the pore pressure generation. Larger induced shear strain amplitudes lead to higher excess pore pressure during cyclic loading and more reduction in effective stress (Jafarzadeh and Sadeghi 2012; Mousavi and Ghayoomi 2020a).
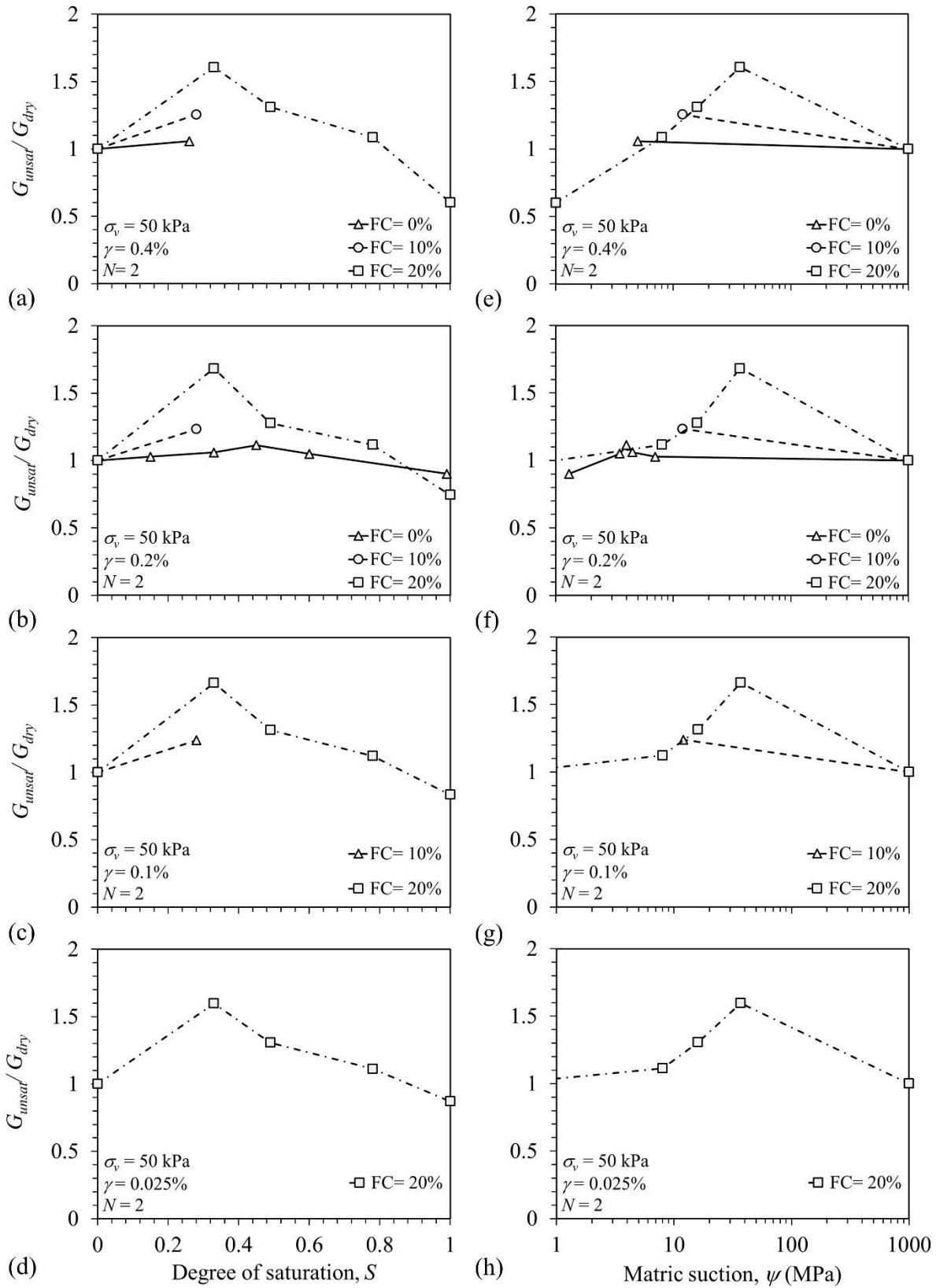
Figure 7-3. Shear modulus versus degree of saturation variations for specimens tested using suction control method.

148

In order to better visualize the impact of excess pore pressure generation on strain dependent shear modulus of specimens with S>0.8, time histories of G values (i.e., G versus N) were plotted along with the time histories of the excess pore pressure ratio, r_u, in Figure 7-4. The excess pore pressure ratio time histories were obtained by the measurement of excess pore pressure, Δu, during cyclic loading and dividing it to the initial vertical effective stress, σ'_v calculated using Equation (2-11) (i.e., $r_u = \Delta u / \sigma'_v$). Figure 7-4 presents G and r_u measurements for FC= 20% silty sand specimens subjected to γ= 0.4% at variable degrees of saturation. For the fully saturated specimen, a gradual drop was observed in G values with increasing N, a behavior which corresponds very well with the trends in r_u versus N. No meaningful reduction in shear modulus was observed in unsaturated specimens as minimal excess pore pressure was generated in these samples. This confirms the softer response of saturated soil to undrained cyclic loading as a result of excess pore pressure generation.
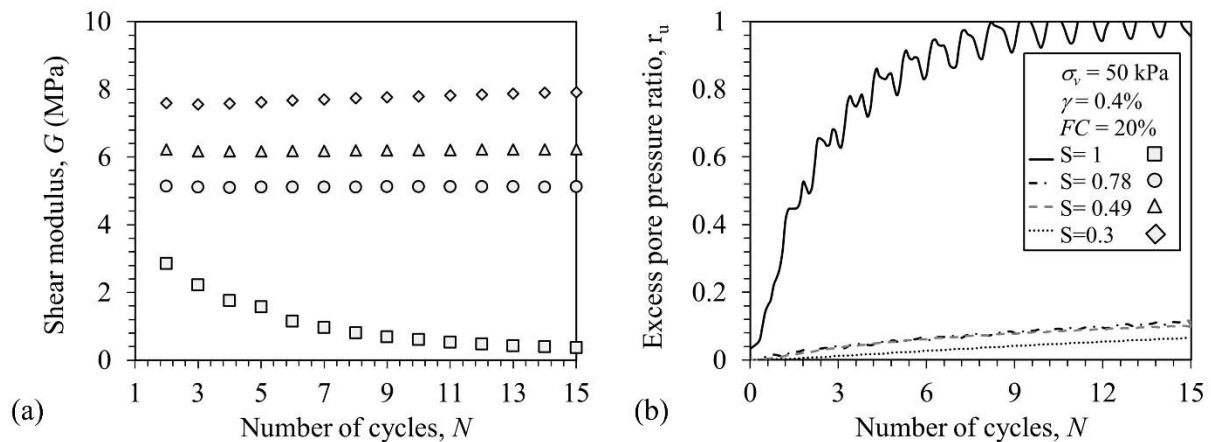
Figure 7-4. Shear modulus and excess pore pressure ratio time histories for FC= 20% silty sand specimens subjected to γ= 0.4%.

149

Damping ratio:

Variations of damping ratio values with the degree of saturation and matric suction in specimens subjected to different amplitudes of shear strain that are prepared using the suction control method are illustrated in Figure 7-5. Regardless of the fines content lower D values were observed in unsaturated specimens in comparison with those of saturated specimens. In general, the damping ratio decreased as the matric suction decreased from fully saturated condition down to intermediate suction levels tested in this study. Similar behavior is reported by previous studies who observed a decrease in D_{min} values with increasing matric suction for intermediate suction ranges in unsaturated soils (Hoyos et al. 2015). Similar to the shear modulus results, the impact of degree of saturation was more pronounced in specimens with higher silt contents. Damping ratio values in fully/nearly saturated samples were consistently higher than those in dry condition, which is consistent with previous results (e.g., Seed and Idriss 1970) In general, similar trends to shear modulus, but in reverse order, was observed in D versus ψ curves (Figure 7-5e-h). For specimens with high degree of saturation, softening of the soil as a result of pore pressure generation led to elevation of damping ratio (e.g., Figure 7-6).
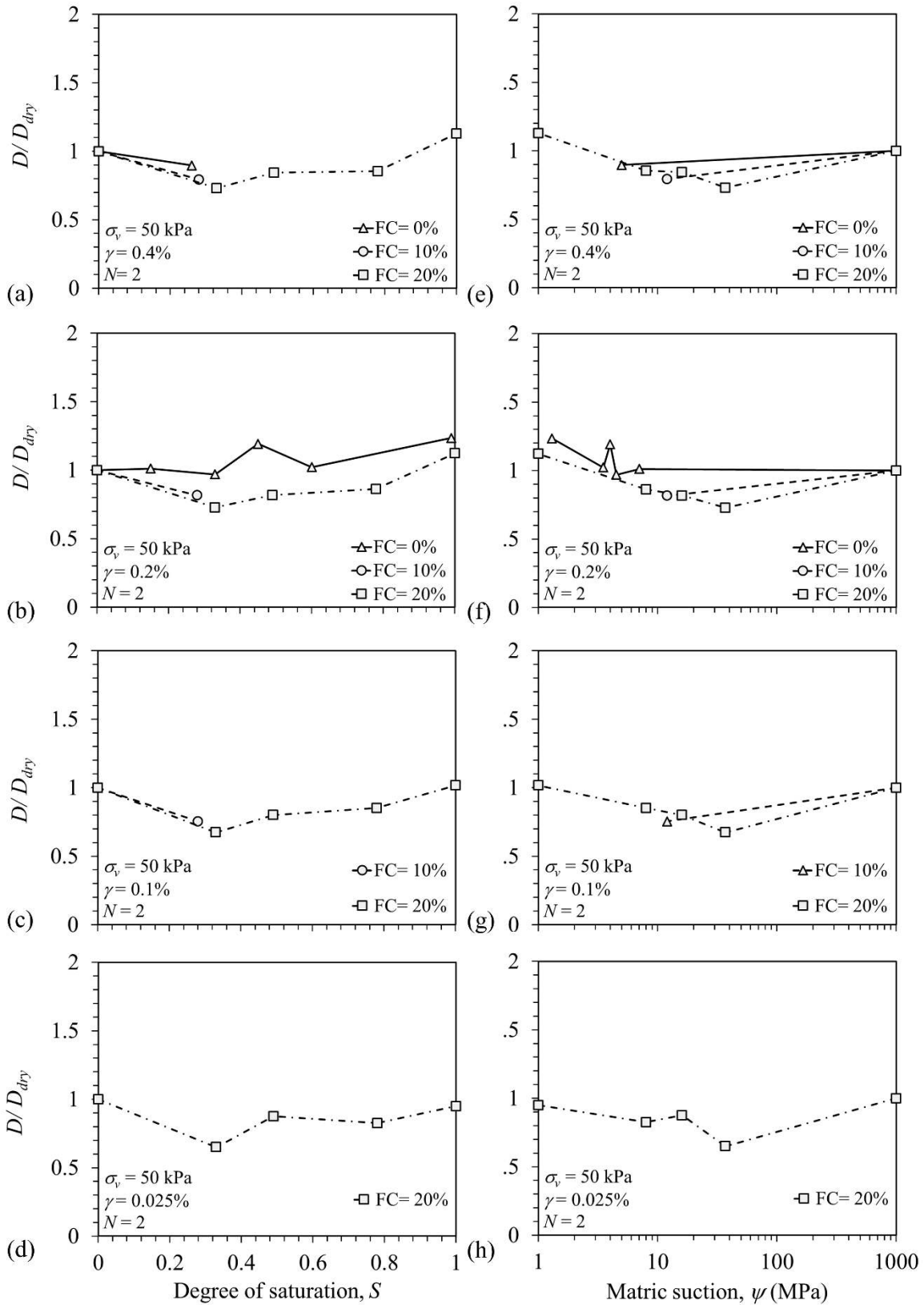
Figure 7-5. Damping ratio versus degree of saturation variations for specimens tested using suction control method.

151
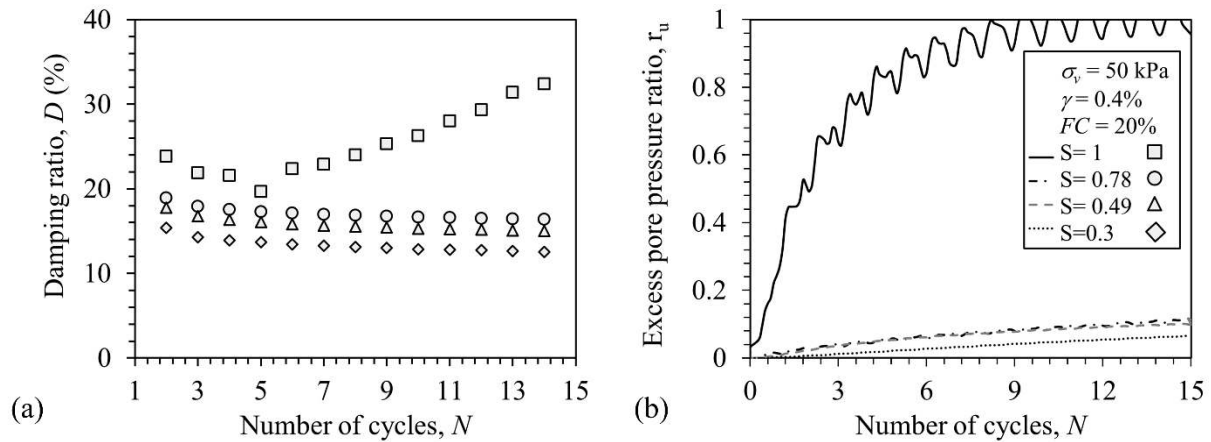
Figure 7-6. Damping ratio and excess pore pressure ratio time histories for FC= 20% silty sand specimens subjected to γ= 0.4%.

7.4.3. Impact of the state of saturation on dynamic properties of soils

Undrained cyclic DSS tests on samples with similar initial conditions but prepared with different desaturation techniques enabled independent evaluation of the effect of state of saturation and sample preparation technique on dynamic properties of soils. Figure 7-7 compares G values obtained from MIPS, wet-compaction, and suction control desaturated techniques for silty sand specimens tested at S≈ 0.8 and variable shear strain amplitudes. Regardless of shear strain amplitude, data presented in Figure 7-7 indicates higher G values obtained from suction-controlled tests than the other two methods. This validates the earlier theoretical discussion that, at the same level of saturation, entrapped gas bubbles in a partially saturated soil may affect soil dynamic properties through a different mechanism than unsaturated soils with negative pore water pressure. While in unsaturated soil (i.e., suction control method) suction-induced stiffness through negative pore pressure and elevated effective stress both impact the shear stiffness of the specimens, entrapped gas bubbles in partially saturated soils (i.e., MIPS method) with positive pore pressure is not likely to change effective stress, although it is likely that they induce suction stiffness.

152
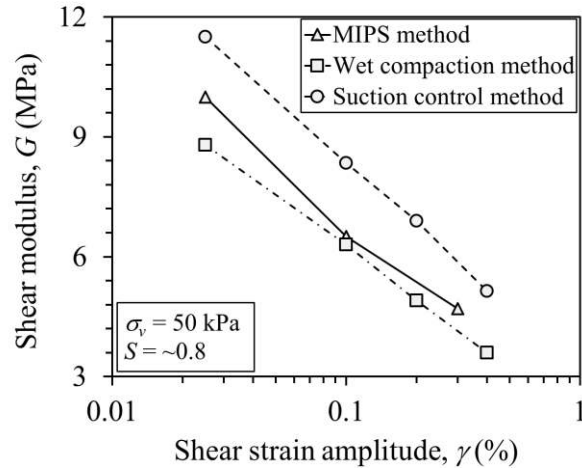
Figure 7-7. Comparison of shear modulus versus shear strain amplitude variations for specimens prepared through MIPS, wet-compaction, and suction control methods.

The comparison of shear moduli values obtained from MIPS and wet-compaction methods suggested that both methods may affect the soil dynamic stiffness through similar mechanisms. The reason for this observation is that the compaction of soil at high degree of saturation, similar to MIPS, may entrap air bubbles in soil leading to partially saturated. It is noteworthy that comparisons of the three methods at low degrees of saturation was not possible since desaturation plateau at relatively high degrees of saturation in induced partial saturation methods (O'Donnell et al. 2017a; Pham et al. 2017; Mousavi et al. 2019). This is due to connection of gas bubbles in soil pores which results in gas escape from the soil (Mahabadi et al. 2018; Mousavi et al. 2019). Thus, in order to evaluate the impact of the desaturation technique on dynamic properties of soil at full range of degree of saturation, experimental G and D measurements from suction control unsaturated tests were compared to those of wet-compaction tests (Figure 7-8). Data presented in Figure 7-8(a,b) indicate that shear modulus values obtained from unsaturated, suction-controlled tests fall above those obtained from wet-compaction method. A behavior which is similar to small

strain shear modulus measurement reported by (Kim et al. 2003). This can be attributed to impact of wet-compaction method on the state of stress and soil structure during compaction. Comparisons of damping ratio values obtained from the two methods suggests no significant impact of desaturation method on the damping ratio of soils (Figure 7-8 c,d); this may require further testing and analysis.
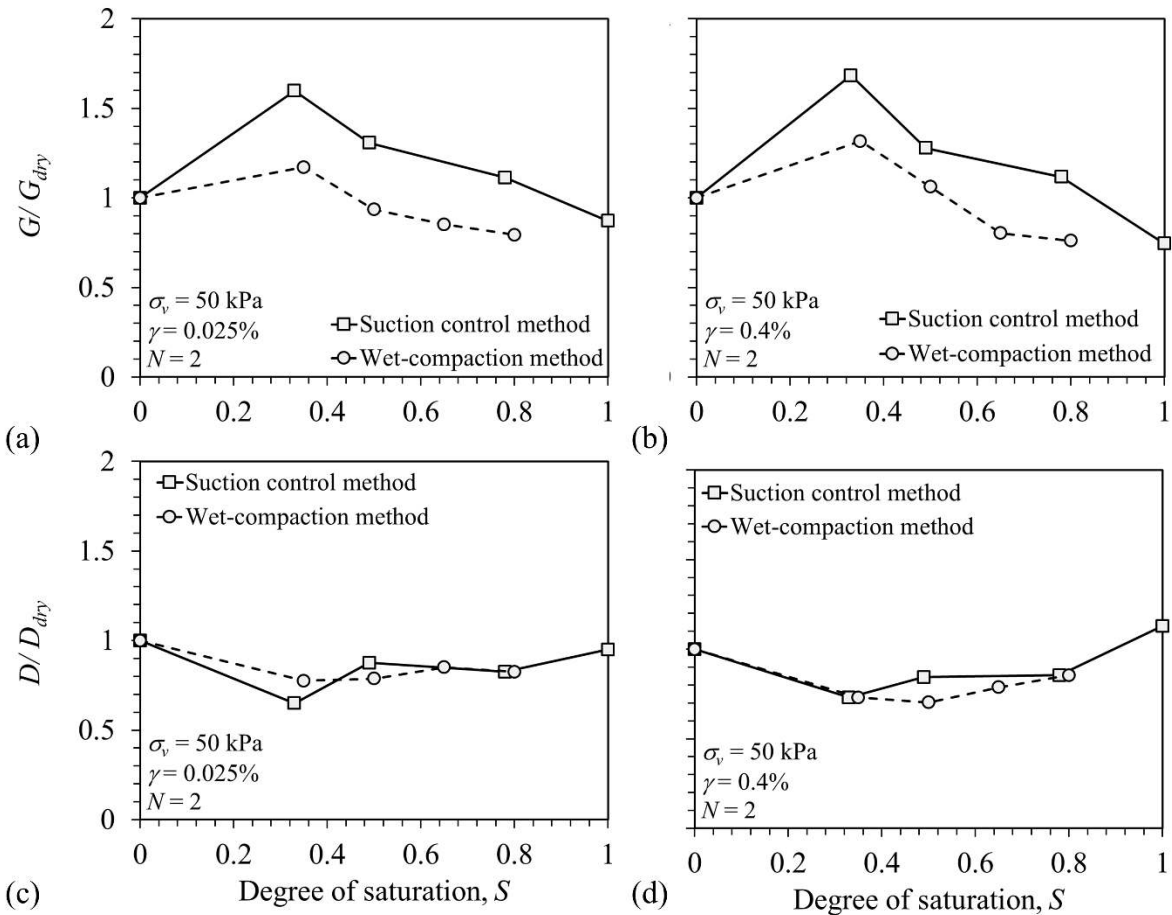
Figure 7-8. Comparison of shear modulus and damping ratio variations with degree of saturation for specimens prepared through MIPS, wet-compaction, and suction control methods.

7.5. ANALYSIS

7.5.1. Effects of fines content and shear strain amplitude on shear modulus

Ishibashi and Zhang (1993) suggested that the strain-dependent shear modulus of sands and clays can be expressed in the following general form:

$$G = K_{(\gamma,PI)}F(e)P'^{m_{(\gamma,PI)}}_0 \tag{7-1}$$

where PI= plastic index, $K_{(\gamma,PI)}$ =a reduction factor depending on shear strain amplitude and PI, and $m_{(\gamma,PI)}$ controls the contribution of mean effective stress. From Equation (7-1) it could be concluded that the ratio of shear modulus of silty sand to that of clean sand is correlated to:

$$\frac{G_{FC}}{G_{FC=0}} \propto \frac{F(e_{FC})}{F(e_{FC=0})} \tag{7-2}$$

This equation suggests that the ratio of moduli of the base clean sand and silty sand is correlated with the ratio of their void ratios. However, as discussed in section 2.6, the void ratio of sands containing fines does not reflect their mechanical behavior since fine particles in the soils with the fines content below FC_{th} are mainly positioned in the base sand pore space and are considered to be "non-active" in the load transfer. A number of researchers suggested that the small strain shear modulus of sand containing fines can be estimated using the equivalent void ratio concept described in chapter 2 and reviewed herein. Thevanayagam et al. (2002) defined the equivalent void ratio as the void ratio of soil particles that actively participate in load transfer. For FC< FC_{th}, e^* is estimated by the following equation (Thevanayagam et al. 2002):

$$e^* = \frac{e + (1-b)FC}{1 - (1-b)FC} \tag{7-3}$$

where (1-*b*) is the nonactive fraction of fines in the soil mixture and varies between 0 to 1. Parameter *b* can be estimated using the following semi-empirical relationship (Rahman et al. 2008):

$$b = [1 - \exp{(-\frac{0.3 \left(\frac{FC}{FC_{th}}\right)}{k})}] \times [r \left(\frac{FC}{FC_{th}}\right)] \qquad (7\text{-}4)$$

where $r = d_{50,fines}/D_{10,sand}$ and $k = 1 - r^{0.25}$. $d_{50,fines}$ is the median grain size of fines and $D_{10,sand}$ is the lower 10% fractile of the host sand.

From this line of logic, it is expected that:

$$\frac{G_{FC}}{G_{FC=0}} = \frac{F(e*_{FC})}{F(e_{FC=0})} \qquad (7\text{-}5)$$

In order to evaluate the Equation (7-5), $\frac{G_{FC}}{G_{FC=0}}$ data obtained from experiments were compared to those estimated using the equivalent void ratio concept and Equation 7-5 (as shown in Figure 7-9). *F(e)* is estimated using the functions proposed by Hardin and Black (1966):

$$F(e) = \frac{(2.17-e)^2}{1+e} \qquad (7\text{-}6)$$

According to Figure 7-9, the predicted $\frac{G_{FC}}{G_{FC=0}}$ values correspond relatively well to their measured values at smaller strain range (i.e., $\gamma = 0.1\%$, $\gamma = 0.2\%$). However, Equation (7-5) does not provide a reasonable prediction for $\frac{G_{FC}}{G_{FC=0}}$ values for the largest strain levels. This was expected since as discussed earlier, the equivalent void ratio concept may hold valid only at small strain levels when fine particles are not active in the load transfer mechanisms. At larger shear strains, it is likely that fine particles become active in shearing and increase the shearing contact area and

consequently soil modulus. Therefore, it can be concluded that $\frac{G_{FC}}{G_{FC=0}}$ are correlated with both

fines content and shear strain amplitude:

$$\frac{G_{FC}}{G_{FC=0}} \propto \frac{F(e_{FC})}{F(e_{FC=0})} \propto \gamma \tag{7-7}$$
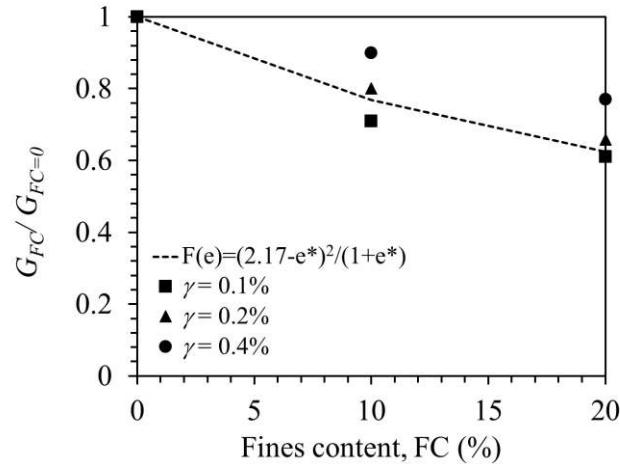
Figure 7-9. Variations of $\frac{G_{FC}}{G_{FC=0}}$ values with FC. Comparisons of estimated values using Equation (7-5) with measured data.

The strain dependent shear modulus can also be estimated using non-linear hyperbolic

reduction functions. For example, the model proposed by Menq (2003) uses soil coefficient of

uniformity to estimate modulus reduction factors for granular soils with different grain size

distribution:

$$\frac{G}{G_{max}} = \frac{1}{1 + (\frac{\gamma}{\gamma_r})^a} \tag{7-8}$$

where:

$$\gamma_r = 0.12 \times C_u^{-0.6} \left(\frac{P\prime}{P_a}\right)^{0.5 C_u^{-0.15}}$$
(7-9)

$$a = 0.86 + 0.1 \times \log\left(\frac{P\prime}{P_a}\right)$$
(7-10)

Further, Oztoprak and Bolton (2013) compiled a large number of data reported in literature for modulus reduction of different non-plastic soils and developed the following equation:

$$\frac{G}{G_{max}} = \frac{1}{1 + \left(\dfrac{\gamma - \gamma_e}{\gamma_r}\right)^a}$$
(7-11)

where:

$$\gamma_r \ (\%) = 0.01 C_u^{-0.3} \left(\frac{p\prime}{P_{atm}}\right) + 0.08 e D_r$$
(7-12)

$$a = C_u^{-0.075}$$
(7-13)

$$\gamma_e = 0.0002 + 0.012 \gamma_r$$
(7-14)

In addition to parameters considered by Menq (2003), Oztoprak and Bolton (2013) model uses soil void ratio and relative density for estimation of shear modulus reduction. Equations (7-8) and (7-15) were used to analyze the measured shear modulus values in dry condition. In this regard, G_{max} of the dry sand was first estimated using the semi-empirical equation proposed by Hardin and Black (1969) and introduced in section 2.9.1:

$$G_{max} = A \times F(e) P_a^{1-n} P\prime^n$$
(7-15)

The values for A are provided in Table 2-3. G_{max} values for silty sand specimens were obtained using the equivalent void ratio for the calculation of F(e). Table 7-4 presents the G_{max} values and parameters used for their calculation.

Table 7-4. G_{max} **values and parameters used for their calculation.**

Soil type	A	e	e^*	n	G_{max} (MPa)
Clean sand	7000	0.64	0.64	0.5	54
FC= 10%	7000	0.54	0.74	0.5	44
FC= 20%	7000	0.5	0.85	0.5	35

The strain-dependent shear modulus values obtained from the experiments were normalized by the estimated G_{max} values for each soil to obtain the shear modulus reduction plot (Figure 7-10). Further, the G/G_{max} predictive curves were also obtained using Menq (2003) and Oztaprak and Bolton (2013) models. Figure 7-10a presents the measured G/G_{max} data for clean sand along with the predicted ones using Menq (2003) and Oztaprak and Bolton (2013) models. For $\gamma > 0.1\%$, the G/G_{max} data fall between the predicted values using the two models. In general, the Oztaprak and Bolton (2013) model provides a better prediction of experimental data. For $\gamma = 0.025$, the measured G/G_{max} value is considerably lower than that predicted by both models. The same observation was made by Miller (1994) who performed cyclic DSS tests on sandy soils. Miller (1994) compiled their G/G_{max} data and those available in literature and showed that for intermediate to small shear strain amplitudes measured G/G_{max} values generally fall below the predictive models when DSS apparatus is used for testing.

Figure 7-10b presents the measured G/G_{max} versus γ data for sand with variable fines content along with the predicted ones using Oztaprak and Bolton (2013) model. This figure shows that Oztaprak and Bolton (2013) predictive model was able to capture the trends observed in the

experimental G/G_{max}-γ data. Specifically, the model predicts higher G/G_{max} for sand with FC= 20%

than that of clean sand at the largest shear strain amplitude where this is reverse for γ= 0.1%, a

behavior which corresponds relatively well with the experimental observations.

(a)

(b)
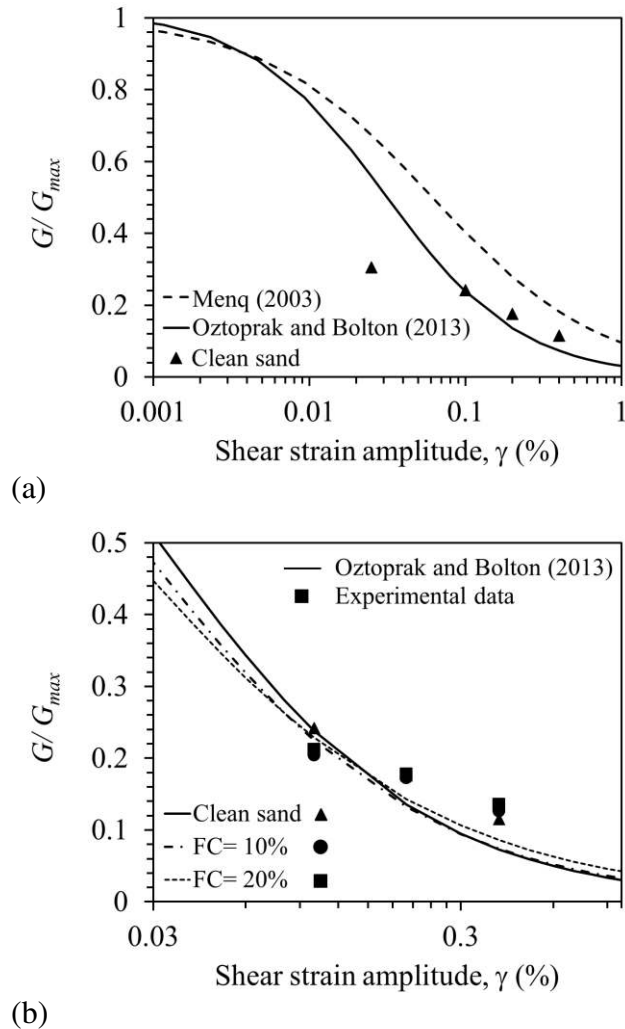
Figure 7-10. G/G_{max} **reduction data compared with** G/G_{max} **predictive curves obtained using Menq (2003) and Oztaprak and Bolton (2013) models (a) for clean sand and (b) for sand containing fines.**

7.5.2. Effects of fines content and shear strain amplitude on damping

The strain-dependent damping ratio model proposed by Menq (2003) is used to analyze

the experimental trends observed in D with fines content and shear strain amplitude. The model is

discussed in section 2.9.4 and is reviewed herein. The strain-dependent damping ratio model proposed by Menq (2003) has the following form:

$$D = b \left(\frac{G}{G_{max}}\right)^{0.1} \times D_{masing} + D_{min} \tag{7-16}$$

where D_{masing} is the damping ratio based on Masing rule (Masing1926) and b is a scaling coefficient which depends on the number of the cycle of loading. The minimum damping ratio, D_{min} is estimated from the following empirical relationship (Menq 2003):

$$D_{min} = 0.55 * C_u^{0.1} \times D_{50}^{-0.3} \times \left(\frac{P\prime}{P_a}\right)^{-0.08} \tag{7-17}$$

Parameter b is obtained from the following empirical relationship (Menq 2003):

$$b = 0.6329 - 0.0057 \times \ln(N) \tag{7-18}$$

D_{masing} is determined from theoretical material damping Masing behaviour (Menq 2003):

$$D_{Masing,a=1}(\%) = \frac{100}{\pi}\left[4\frac{\gamma - \gamma_r \ln\left(\frac{\gamma + \gamma_r}{\gamma_r}\right)}{\frac{\gamma^2}{\gamma + \gamma_r}} - 2\right] \tag{7-19}$$

$$D_{Masing}(\%) = c_1 D_{Masing,a=1}(\%) + c_2 D_{Masing,a=1}(\%)^2 + c_3 D_{Masing,a=1}(\%)^3 \tag{7-20}$$

where

$$c_1 = -1.1143a^2 + 1.8618a + 0.2523$$

$$c_2 = 0.0805a^2 - 0.071a - 0.0095$$

$$c_3 = -0.0005a^2 + 0.0002a + 0.0003.$$

The estimated G/G_{max} data, and parameters γ_r, and a obtained from Oztaprak and Bolton (2013)'s model were used to obtain D versus γ predictive curves for the tested specimens with variable fines content in the dry condition. Figure 7-11 compares the experimentally measured D data compared with D predictive curves obtained using Equation (7-16). For the shear strain amplitude ranges

161

tested in this study, Figure 7-11 indicates a good agreement between the experimental *D* measurements and predictive curves for variable fines content. Specifically, Equation (7-16) was able to capture the different trends in *D*-γ observed in the experimental data when the parameters obtained from Oztaprak and Bolton (2013)'s model is used in the equation.
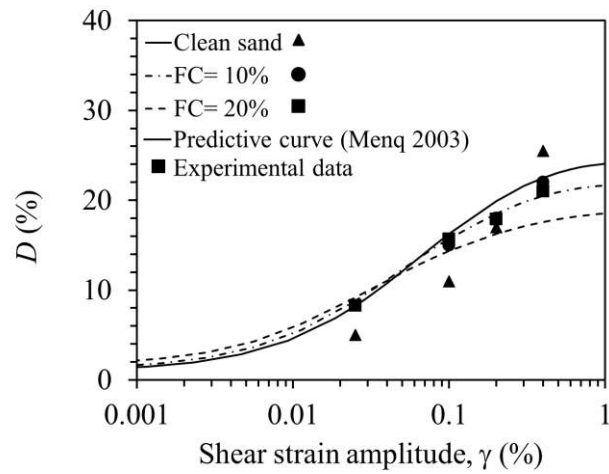
Figure 7-11. Experimentally measured *D* data compared with *D* predictive curves obtained using Menq (2003) model for specimens with variable fines content at dry condition.

7.5.3. Effects of degree of saturation on shear modulus

As discussed earlier in sections 2.9.2 and 2.9.3, previous studies on shear modulus of unsaturated soils mostly focused on small strain behavior and limited studies are available on strain-dependent shear modulus. The comparison of the experimental trends in *G* versus *S* observed in this study with those reported in the literature for small-strain modulus is valid only if the impact of degree of saturation on the shear modulus, for the range of shear strain amplitude tested in this study and the same effective stress magnitude, is independent of shear strain amplitude. This statement was examined by comparing the normalized shear modulus (G/G_{dry}) values at a given degree of

162

saturation but different shear strain amplitudes, as shown in Figure 7-12. A visual evaluation of

G/G$_{dry}$ versus γ data presented in Figure 7-12 indicates that the impact of degree of saturation on

shear modulus is relatively independent of the amplitude of shear strain. This was also statistically

evaluated by the analysis of variance (ANOVA) method using JMP Pro.14. Results confirm that

the impact of the degree of saturation on G values is not significantly dependent on the amplitude

of shear strain (P= 0.999). It is noteworthy that this conclusion may only be valid for the type of

soils tested in this research. For example, previous research on high plastic silt and clay showed

that the amplitude of shear strain does alter the impact of degree of saturation on shear modulus.

Oh and Vanapali (2014) suggested that the maximum shear modulus in unsaturated soils

can be related to that of saturated soils:

$$G_{max}^{unsat} = G_{max}^{sat}[1 + \zeta\psi S^{\xi}]$$ (7-21)

where ζ and ξ are fitting parameters. Oh and Vanapali (2014) compiled the available literature

G_{max} data for non-plastic sands and reported that ζ and ξ are correlated with soils' coefficient of

uniformity as presented in Table 7-5.

Table 7-5. Values of ζ and ξ reported by Oh and Vanapali (2014) for different sands.

USCS	PI	C$_u$	ζ	ξ
SP	NP	1.2	0.5	0.35
SP	NP	1.7	0.5	0.2
SP	NP	1.9	0.5	0.035
SW	NP	6.9	1	0.025
SW	NP	7.5	1	0.025
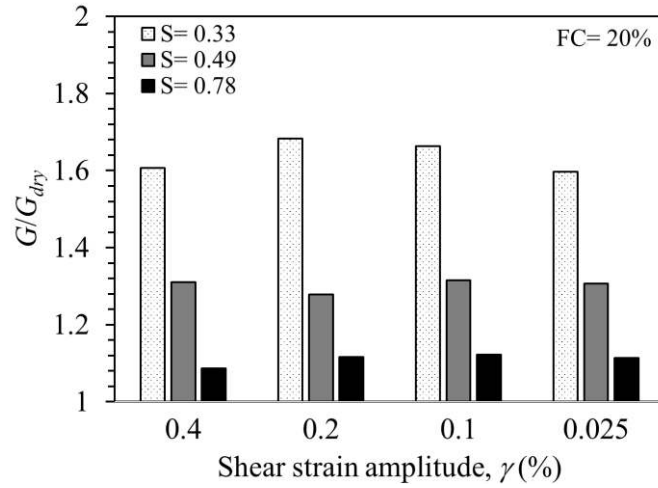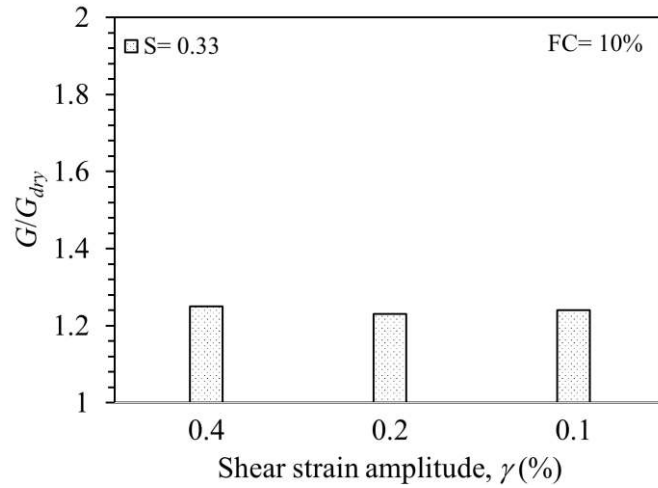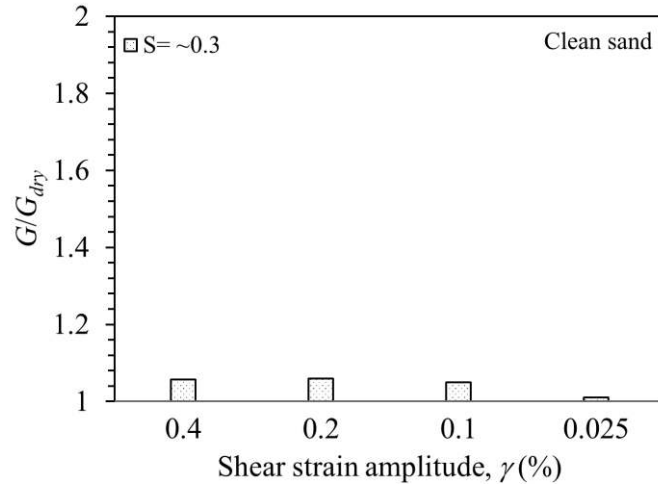
Figure 7-12. Comparison of measured G/G$_{dry}$ values at different γ and *S* and (a) FC= 20%, (b) FC= 10%, and (c) clean sand.

Equation (7-21) indicates that shear modulus in dry condition ($S= 0$) is equal to that of full saturated condition. Therefore Equation (7-21) can be rewritten in the following form:

$$\frac{G_{max}^{unsat}}{G_{max}^{dry}} = [1 + \zeta \psi S^{\xi}] \tag{7-22}$$

Equation (7-22) was used to analyze the G/G_{dry} data in this research. The fitting parameters ζ and ξ were obtained based on C_u of the tested specimens and the calibrated values presented in Table 7-5. Figure 7-13 compares the G/G_{dry} data along with those predicted using Oh and Vanapalli's (2014) model. For S< ~0.8, Figure 7-13 shows a very good agreement between the experimental G/G_{dry} data and those predicted using Equation (7-22) for both silty sand and clean sand specimens. However, for S> ~0.8, a considerable difference exists between the experimental data and the predicted ones. One reason for this observation can be the reduction in the effective stress due to the excess pore water pressure generation during large strain shearing of unsaturated samples. However, in small strain testing, elastic deformations do not result in excess pore pressure generation. It is expected that G/G_{dry} be equal to $\frac{G_{max}^{unsat}}{G_{max}^{dry}}$, if they are compared at the same level of initial effective stress. According to Hardin and Black's (1969) model (Equation (7-15)), for a soil with an initial effective stress, P'_0, and, and initial small strain shear modulus, $G_{max,0}$, the small strain shear modulus after excess pore pressure generation can be calculated using the following expression:

$$\frac{G_{max}}{G_{max,0}} = [\frac{(P'_0 - \Delta u)}{P'_0}]^n \tag{7-23}$$

or

$$G_{max} = G_{max,0}[1 - r_u]^n \tag{7-24}$$

where n is the fitting parameter in their model. Assuming that at the same initial effective stress

G/G_{dry} is equal to $\frac{G_{max}^{unsat}}{G_{max}^{dry}}$, the following model can be developed for prediction of G/G_{dry}:

$$\frac{G}{G_{dry}} = (1 - r_u)^n [1 + \zeta \psi S^\xi]$$

(7-25)

It should be noted that magnitude of excess pore pressure ratio can change in each cycle of loading

and shear modulus is to be calculated based on excess pore pressure magnitude at each cycle. r_u

for each cycle of loading can be estimated based on the model presented in Chapter 5.

Figure 7-14 compares the G/G_{dry} data along with those predicted using the developed

equation. According to this figure, the newly developed model was able to capture the observed

trends in the measured G/G_{dry} values for the full degree of saturation range. Specifically, the model

predicted lower G/G_{dry} value for fully saturated condition than that of dry condition, a behavior

which is due to excess pore pressure generation in soils with high degrees of saturation and

corresponds very well with the experimental data.
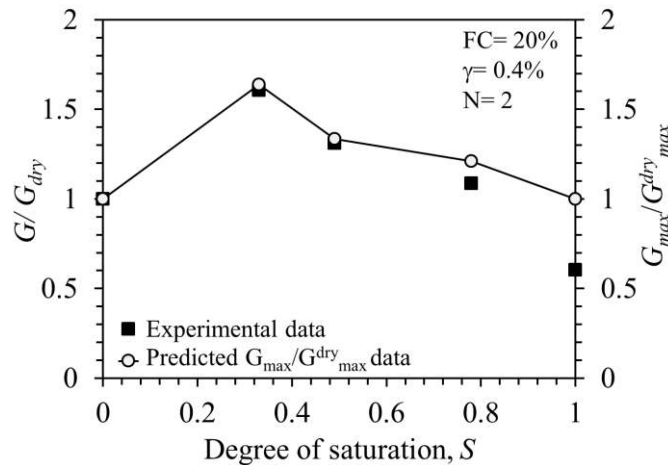
(a)
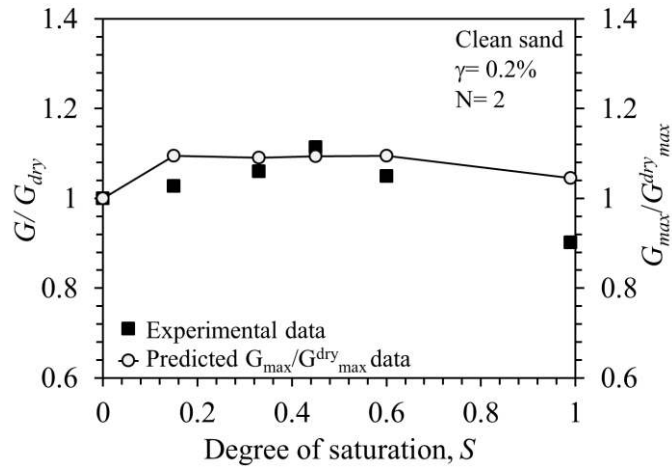
(b)

Figure 7-13. Experimental G/G$_{dry}$ data along with those predicted using Oh and Vanapali (2014) model.

(a)
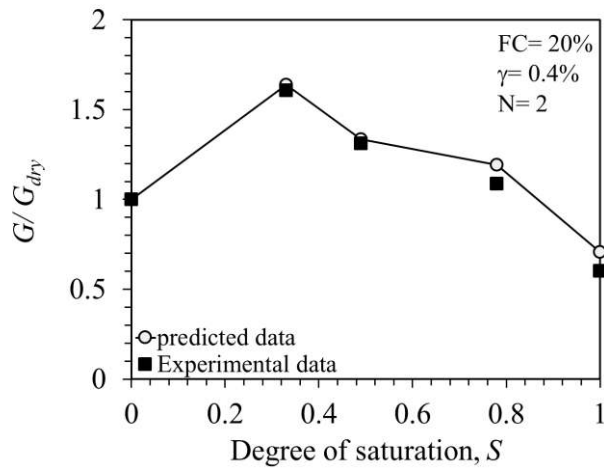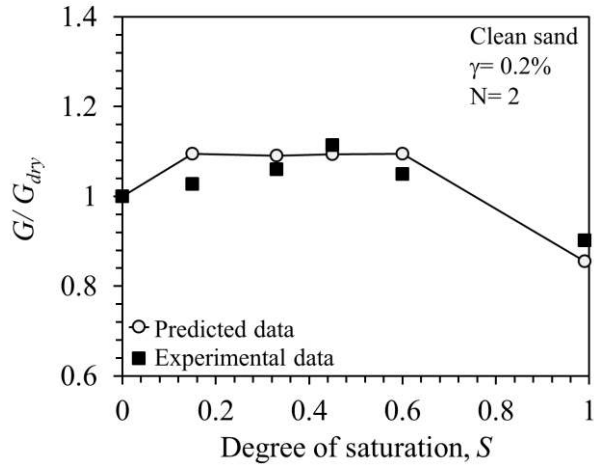
Figure 7-14. Experimental G/G_{dry} data along with the predicted values using the developed equation; (a) FC= 20% and (b) clean sand specimens.

7.6. CONCLUSIONS

The impacts of fines content, degree of saturation and the technique to achieve it on dynamic properties of sand and silty sands were evaluated and interpreted. This involved interpretation of the strain-controlled, cyclic DSS tests on suction control unsaturated, wet-compacted, and MIPS treated specimens in terms of dynamic shear modulus and damping ratio. The results indicated a nonlinear correlation between the soil's dynamic properties and its fines content. While an increase in fines content resulted in a significant reduction in shear modulus and elevation of damping ratio in smaller shear strains, different behavior was observed for larger shear strains. Fines content had lower impact on shear modulus at larger shear strains, while the damping ratio decreased with addition of fines at the larger shear strain amplitudes.

For suction control unsaturated samples, the degree of saturation considerably influenced the dynamic properties of soil. The impact of degree of saturation was more pronounced in sands with higher fines content. The comparisons between suction control, wet-compaction, and MIPS

methods revealed significant impact of state of saturation and saturation technique on shear modulus of the specimens. For the same degree of saturation, specimens prepared with MIPS and wet-compacted methods had lower shear modulus than those prepared using suction control technique. However, the state of saturation and method of desaturation had no meaningful influence on damping ratio of samples.

The results obtained from this study was further analyzed using available shear modulus and damping ratio predictive models reported in the literature. It was shown that available models can capture the trends in fines content with shear modulus at smaller shear strain amplitudes when interparticle void ratio is used for the analysis of the results. For larger strains, the trends in fines content with shear modulus may be captured by using Oztoprak and Bolton's shear modulus reduction model and considering the impact of fines on coefficient of uniformity.

For the ranges of degrees of saturation, shear strain amplitudes, and materials tested in this research, analysis of results suggested that, for the same effective stress condition, the impact of degree of saturation on shear modulus is independent of the amplitude of shear strain. However, excess pore pressure generation at high degrees of saturation can results in a change in initial effective stress and consequently the shear modulus of the soils. Based on these considerations, it was proposed that the existing models for estimation of small strain shear modulus in unsaturated soils can be used for strain-dependent shear modulus if the effect of excess pore pressure generation in each cycle of loading is justified in the model. This was validated by modifying an existing model originally developed for estimation of small strain shear modulus and comparing it with experimental measurements in this study. The comparisons of results showed that the proposed model estimates corresponded well with the experimental shear modulus data when the model accounts for the excess pore pressure generation.

CHAPTER 8

SUMMARY, CONCLUSIONS, AND FUTURE WORK

8.1.   ABSTRACT

This chapter presents a summary of the objectives of this study, the strategy to address them, conclusions of the results, recommendations for future work, and intellectual merit of the dissertation. This study experimentally and theoretically evaluated and characterized the response of soils including excess pore pressure generation, induced volumetric deformation, shear modulus, and damping to dynamic loading at different state of saturations and a wide range of degrees of saturation. Three different techniques, including MIPS, wet-compaction, and tensiometric suction control technique were employed to evaluate the impact of state of saturation, saturation level, and the path to reach that level on dynamic properties and performance of non-plastic soils. In addition, the dynamic response of sandy specimens with variable non-plastic fines were evaluated to understand the mechanisms by which fines can alter the dynamic behavior of sands. The following section discuss the summary, conclusions, and potential future research ideas generated after this dissertation.

8.2. SUMMARY AND CONCLUISON

The primary objectives, solution strategies, and the outcome and conclusions of the study are listed below:

8.2.1. Objective (1):

The first objective was to investigate the impact of compositional, mechanical, and environmental factors on the efficiency of biogenic gas production in saturated soils.

Solution Strategies:

In order to address Objective 1, batch and soil column bio-denitrification tests were conducted, and the efficiency of gas generation was investigated. The experimental program was set to explore the impact of initial nutrient concentrations including nitrate and ethanol, different compositional factors including grain size and soil density, environmental factors including pH and temperature, and geostatic effective stress on the effectiveness and success of MIPS.

Outcomes and Conclusions:

1. Results from batch experiments revealed that the volume of gas generation could be adjusted by changing the initial nitrate and ethanol concentrations. High initial nitrate concentration not only resulted in generation of substantial volume of gas, but also elevated pH levels providing a suitable condition for potential calcite precipitation.

2. Results from soil experiments indicated that substantial gas loss from the soil surface restricts further gas accumulations inside the pores at high initial nitrate concentrations. Gas loss could significantly lower the efficiency of the treatment system in desaturation of samples.

171

3. In general, an increase in soils density, overburden stress, or fines content led to increase in the efficiency of the treatment system.

4. Despite the significant effect of environmental factors, i.e. temperature and pH, on denitrification rate, they were found to have minimal effect on final desaturation level for the range of values in this study.

8.2.2. Objective (2):

The second objective was to investigate the performance and effectiveness of MIPS process for mitigation of seismically induced excess pore pressure in sands with variable non-plastic fines content. This involves evaluation of the impact of fines content, degree of saturation, and induced shear strain amplitude on excess pore pressure generation in fully saturated and induced partially saturated samples.

Solution Strategies:

The approach to address the second objective included a series of undrained, strain-controlled cyclic DSS tests on MIPS treated and untreated (i.e., fully saturated) clean sand and silty sand specimens subjected to different dynamic loadings. The results were evaluated in terms of excess pore pressure generation, volumetric deformation, and shear modulus.

Outcomes and Conclusions:

1. Experimental results suggested that the magnitude of excess pore pressure generation in saturated soils is strongly correlated with the amplitude of induced shear strain.

2. For shear strain amplitudes below a threshold value, minimal excess pore pressure was generated in tested specimens. However, an increase in shear strain amplitude above the

threshold resulted in significant increase in excess pore pressure generation in fully saturated samples.

3. In general, lower excess pore pressure was generated in silty sand specimens in comparison with clean sand tested under the same initial conditions (i.e., relative density, degree of saturation, and effective vertical stress).

4. For the range of shear strain amplitudes tested in this study, no liquefaction was observed in MIPS treated samples when degree of saturation was merely reduced to 95-96% from full saturation.

5. A semi-empirical model was adopted to capture the impact of partial saturation on r_u of sands and silty sands. The model has the capability of capturing the impacts of fluid bulk modulus reduction in desaturated soils on r_u. The capability of the model was evaluated by comparing the r_u values obtained from experiments in this study as well as data reported in literature and the values predicted by the model.

6. The model was found to satisfactorily capture the trends in the r_u measurements for different degrees of saturation in this study. Specifically, the model was capable of capturing the dramatic drop in r_u with the degree of saturation reduction as observed in the experimental results.

8.2.3. Objective (3):

The third objective was to evaluate the impact of the fines content, desaturation technique, and the degree of saturation on seismically-induced volumetric deformation of soils. Also, the goal was to formulate a degree of saturation-dependent seismic compression equation.

Solution Strategies:

To fulfil this objective, two sets of DSS tests were performed on unsaturated and partially saturated soil specimens prepared with (a) tensiometric control of suction and (b) wet-compaction technique at variable degrees of saturation. The results were interpreted in terms of induced volumetric deformation. Results of these tests along with MIPS treated tests were utilized to characterize and formulate the seismically induced volumetric deformation in sands and silty sands.

Outcomes and Conclusions:

1. A strong correlation between induced shear strain amplitude and the magnitude of volumetric deformation was observed in this study.

2. The results of the experiments revealed the significant impact of the degree of saturation and methods of desaturation on seismic volumetric deformation.

3. In general, suction-controlled unsaturated samples showed lower volumetric deformation than fully saturated and dry ones.

4. A meaningful difference was observed between volumetric deformations of samples prepared using suction control and those of partially saturated samples. In general, for the initial conditions and soils tested in this study, partial saturation had minimal impact on volumetric strain material characteristics.

5. Wet-compacted samples showed different volumetric behavior than unsaturated and MIPS treated ones when tested at high degrees of saturation. The change in behavior was attributed to the change in soil structure during compaction.

6. Based on the experimental results, it was concluded that the degree of saturation may impact volumetric deformation of soils through altering one or both (1) volumetric strain material characteristics through suction development (2) seismic demand (i.e., induced

174

shear strain amplitude) through suction development and reduction of excess pore pressure generation.

7. On the basis of theoretical considerations and experimental observations, a strain-based seismic compression model was adapted and modified to estimate the compression of sands and silty sands in unsaturated conditions by incorporating the seismic demand and volumetric strain material parameters. The comparison between the model predictions and experimental data indicated the suitability of the model in estimating the seismic compression of unsaturated soils, especially in low to intermediate degrees of saturation.

8.2.4. Objective (4):

The last objective in this research was to characterize the impact of fines content, state of saturation, degree of saturation, and desaturation method on strain-dependent soil dynamic properties including shear modulus and damping ratio.

Solution Strategies:

In order to fulfill the set objectives, the experimental data from the three sets of experiments (i.e., MIPS, suction control, and wet-compaction) were compiled and interpreted in terms of dynamic shear modulus and damping ratio. The experimental results and trends in dynamic properties with degree of saturation were compared with available experimental results and predictive equations.

Outcomes and Conclusions:

1. The results indicated a nonlinear correlation between sand dynamic properties and fines content. While an increase in fines content resulted in a significant reduction in shear modulus and elevation of damping ratio in smaller shear strains, different behavior was observed for larger shear strain. Fines content had lower impact on shear modulus at larger

shear strains, while damping ratio decreased with addition of fines at the larger shear strain amplitudes.

2. For suction control unsaturated samples, the degree of saturation considerably influenced the dynamic properties of soil. The impact of degree of saturation was more pronounced in sands with higher fines content. The comparisons between suction control, wet-compaction, and MIPS methods revealed significant impact of state of saturation and saturation technique on shear modulus of specimens. For the same degree of saturation, specimens prepared with MIPS and wet-compacted methods had lower shear modulus than those prepared using suction control technique. However, the state of saturation and method of desaturation had no meaningful influence on damping ratio of samples.

3. The results obtained from this study was further analyzed using available shear modulus and damping ratio predictive models reported in the literature. It was shown that available models can capture the trends in fines content with shear modulus at smaller shear strain amplitudes when interparticle void ratio is used for the analysis of the results. For larger strains, the trends in fines content with shear modulus may be captured by using Oztoprak and Bolton's shear modulus reduction model and considering the impact of fines on coefficient of uniformity.

4. For the ranges of degree of saturation, shear strain amplitudes, and material tested in this research, analysis of results suggested that, for the same effective stress condition, the impact of degree of saturation on shear modulus is independent of the amplitude of shear strain. However, excess pore pressure generation at high degrees of saturation can results in a change in initial effective stress and consequently the shear modulus of soils. Based on these considerations, it was proposed that the existing models for estimation of small

176

strain shear modulus in unmatured soils can be used for strain dependent shear modulus if the effect of excess pore pressure generation in each cycle of loading is justified in the model. This was validated by modifying an existing model originally developed for estimation of small strain shear modulus and comparing it with experimental measurements in this study. The comparisons of results showed that the proposed model estimations corresponded well with the experimental shear modulus data when the model accounts for the excess pore pressure generation.

8.3. RECOMMENDATIONS FOR FUTURE WORK

Although this research provided insights and formulations on some fundamental issues regarding the impact of degree of saturation and state of saturation on dynamic response of sand and silty sands; it had some inherent limitations, while several questions remain unanswered. The following recommendations are provided to improve the knowledge on dynamic performance of partially saturated and unsaturated soils.

- This study was limited to certain soil types and initial conditions such as effective stress, void ratio, and grain distribution. The generalization of observations and developed equations for other soils and initial conditions requires more testing.

- This study investigated the response of soil at intermediate shear strain amplitudes. Laboratory tests at small and large shear strain amplitudes could complement the results obtained in this study.

- Although element-scale strain-controlled testing method used in this study provides a fundamental basis for the study of excess pore pressure generation, volumetric strain characteristic, and dynamic properties of soils, large-scale testing of soil with boundary

177

conditions close to field condition would help to validate and extend the findings of this study in practice.

- The results of this study apply to free field condition. The possible impact of soil-structure-interaction on soil dynamic performance in unsaturated and partially saturated conditions is to be investigated.

CHAPTER 9

REFERENCES

Airey, D. W., and Wood, D. M. (1987). "An evaluation of direct simple shear tests on clay." *Géotechnique*, Thomas Telford Ltd , 37(1), 25–35.

Akunna, J. C., Bizeau, C., and Moletta, R. (1992). "Denitrification in anaerobic digesters: Possibilities and influence of wastewater COD/N-NOX ratio." *Environmental Technology (United Kingdom)*, Taylor & Francis Group , 13(9), 825–836.

De Alba, P., Seed, H., and Chan, C. (1976). "Sand liquefaction in large-scale simple shear tests." *Journal of Geotechnical and Geoenvironmental Engineering*, 102.

Bang, S. S., Lippert, J. J., Yerra, U., Mulukutla, S., and Ramakrishnan, V. (2010). "Microbial calcite, a bio-based smart nanomaterial in concrete remediation." *International Journal of Smart and Nano Materials*, Taylor and Francis Ltd., 1(1), 28–39.

Blackmer, A. M., and Bremner, J. M. (1978). "Inhibitory effect of nitrate on reduction of N2O to N2 by soil microorganisms." *Soil Biology and Biochemistry*, Pergamon, 10(3), 187–191.

Borghei, A., Ghayoomi, M., and Turner, M. (2020). "Effects of Groundwater Level on Seismic Response of Soil-Foundation Systems." *Journal of Geotechnical and Geo-Environmental*

Engineering, Under review.

Boudreau, B. P. (2012). "The physics of bubbles in surficial, soft, cohesive sediments." *Marine and Petroleum Geology*, Elsevier.

Boulanger, R. W., Meyers, M. W., Mejia, L. H., and Idriss, I. M. (1998). "Behavior of a fine-grained soil during the Loma Prieta earthquake." *Canadian Geotechnical Journal*, NRC Res Press, 35(1), 146–158.

Bray, J. D., Sancio, R. B., Durgunoglu, T., Onalp, A., Youd, T. L., Stewart, J. P., Seed, R. B., Cetin, O. K., Bol, E., Baturay, M. B., Christensen, C., and Karadayilar, T. (2004). "Subsurface Characterization at Ground Failure Sites in Adapazari, Turkey." *Journal of Geotechnical and Geoenvironmental Engineering*, American Society of Civil Engineers, 130(7), 673–685.

Budhu, M. (1984). "Nonuniformities imposed by simple shear apparatus." *Canadian Geotechnical Journal*, NRC Research Press Ottawa, Canada , 21(1), 125–137.

Burbank, M., Weaver, T., Lewis, R., Williams, T., Williams, B., and Crawford, R. (2013). "Geotechnical Tests of Sands Following Bioinduced Calcite Precipitation Catalyzed by Indigenous Bacteria." *Journal of Geotechnical and Geoenvironmental Engineering*, American Society of Civil Engineers, 139(6), 928–936.

Carlton, B. (2014). "An Improved Description of the Seismic Response of Sites with High Plasticity Soils, Organic Clays, and Deep Soft Soil Deposits." University of California, Berkeley.

Carraro, J. A. H., Prezzi, M., and Salgado, R. (2009). "Shear Strength and Stiffness of Sands Containing Plastic or Nonplastic Fines." *Journal of Geotechnical and Geoenvironmental*

Engineering, American Society of Civil Engineers (ASCE), 135(9), 1167–1178.

Cetin, K. O., and Bilge, H. T. (2012). "Cyclic large strain and induced pore pressure models for saturated clean sands." *Journal of Geotechnical and Geoenvironmental Engineering*, 138(3), 309–323.

Cetin, K. O., Bilge, H. T., Wu, J., Kammerer, A. M., and Seed, R. B. (2009). "Probabilistic Model for the Assessment of Cyclically Induced Reconsolidation (Volumetric) Settlements." *Journal of Geotechnical and Geoenvironmental Engineering*, ASCE - American Society of Civil Engineers, 135(3), 387–398.

Chaney, R., Stevens, E., and Sheth, N. (1979). "Suggested Test Method for Determination of Degree of Saturation of Soil Samples by B Value Measurement." *Geotechnical Testing Journal*, ASTM International, 2(3), 162.

Darendeli, M. B. (2001). "Development of a new family of normalized modulus reduction and material damping curves." Univ. of Texas at Austin, Austin, TX.

Dash, H. K., and Sitharam, T. G. (2009). "Undrained cyclic pore pressure response of sand-silt mixtures: Effect of nonplastic fines and other parameters." *Geotechnical and Geological Engineering*, 27(4), 501–517.

DeJong, J. T., Mortensen, B. M., Martinez, B. C., and Nelson, D. C. (2010). "Bio-mediated soil improvement." *Ecological Engineering*, 36(2), 197–210.

Dejong, J. T., Soga, K., Kavazanjian, E., Burns, S., Van Paassen, L. A., AL Qabany, A., Aydilek, A., Bang, S. S., Burbank, M., Caslake, L. F., Chen, C. Y., Cheng, X., Chu, J., Ciurli, S., Esnault-Filet, A., Fauriel, S., Hamdan, N., Hata, T., Inagaki, Y., Jefferis, S., Kuo, M., Laloui,

L., Larrahondo, J., Manning, D. A. C., Martinez, B., Montoya, B. M., Nelson, D. C., Palomino, A., Renforth, P., Santamarina, J. C., Seagren, E. A., Tanyu, B., Tsesarsky, M., and Weaver, T. (2013). "Biogeochemical processes and geotechnical applications: Progress, opportunities and challenges." *Geotechnique*, 63(4), 287–301.

Dobry, R. (1985). *Liquefaction of soils during earthquakes. National Research Council, Rep. No. CETS-EE-001, NRC, Committee on Earthquake Engineering*. Washington, D.C.

Dobry, R., Ladd, R. S., Yokel, F. Y., Chung, R. M., and Powell, D. (1982). *Prediction of pore water pressure buildup and liquefaction of sands during earthquakes by the cyclic strain method. National Bureau of Standards building science series 138, U.S. Dept. of Commerce/National Bureau of Standards (NBS)*. Washington, D.C.

Dong, Y., and Lu, N. (2016). "Dependencies of shear wave velocity and shear modulus of soil on saturation." *Journal of Engineering Mechanics*, 142(11), 1–8.

Dong, Y., Lu, N., and McCartney, J. S. (2016). "Unified model for small-strain shear modulus of variably saturated soil." *Journal of Geotechnical and Geoenvironmental Engineering*, 142(9), 1–10.

Dror, I., Berkowitz, B., and Gorelick, S. M. (2004). "Effects of air injection on flow through porous media: Observations and analyses of laboratory-scale processes." *Water Resources Research*, 40(9).

Duku, P. M., Stewart, J. P., Whang, D. H., and Yee, E. (2008). "Volumetric strains of clean sands subject to cyclic loads." *Journal of Geotechnical and Geoenvironmental Engineering*, 134(8), 1073–1085.

Eseller-Bayat, E., Yegian, M. K., Alshawabkeh, A., and Gokyer, S. (2013). "Liquefaction response of partially saturated sands. I: Experimental results." *Journal of Geotechnical and Geoenvironmental Engineering*, 139(6), 863–871.

Finn, W. D. L., Martin, G. R., and Byrne, P. M. (1976). "Seismic response and liquefaction of sands." *Journal of the Geotechnical Engineering Division*, 102(8), 841–856.

Finno, R. J., Zhang, Y., and Buscarnera, G. (2017). "Experimental validation of Terzaghi's effective stress principle for gassy sand." *Journal of Geotechnical and Geoenvironmental Engineering*, 143(12), 1–11.

Fredlund, D. G., and Anqing Xing. (1994). "Equations for the soil-water characteristic curve." *Canadian Geotechnical Journal*, NRC Research Press Ottawa, Canada , 31(4), 521–532.

Fredlund, D. G., and Rahardjo, H. (1993). *Soil Mechanics for Unsaturated Soils*. *Soil Mechanics for Unsaturated Soils*, John Wiley & Sons, Inc., Hoboken, NJ, USA.

Frost, J. D., and Park, J. Y. (2003). "A critical assessment of the moist tamping technique." *Geotechnical Testing Journal*, ASTM International, 26(1), 57–70.

Fry, V. a., Selker, J. S., and Gorelick, S. M. (1997). "Experimental investigations for trapping oxygen gas in saturated porous media for in situ bioremediation." *Water Resources Research*, 33(12), 2687–2696.

van Genuchten, M. T. (1980). "A Closed-form Equation for Predicting the Hydraulic Conductivity of Unsaturated Soils." *Soil Science Society of America Journal*, Wiley, 44(5), 892–898.

Ghayoomi, M., McCartney, J., and Ko, H. (2011). "Compression of Partially Saturated Sand Layers." *Geotechnical Testing Journal*, 34(4), 1–11.

Ghayoomi, M., McCartney, J. S., and Ko, H. Y. (2013). "Empirical methodology to estimate seismically induced settlement of partially saturated sand." *Journal of Geotechnical and Geoenvironmental Engineering*, 139(3), 367–376.

Ghayoomi, M., Suprunenko, G., and Mirshekari, M. (2017). "Cyclic triaxial test to measure strain-dependent shear modulus of unsaturated sand." *International Journal of Geomechanics*, 17(9), 1–11.

Goudarzy, M., König, D., and Schanz, T. (2018). "Small and intermediate strain properties of sands containing fines." *Soil Dynamics and Earthquake Engineering*, Elsevier Ltd, 110(April), 110–120.

Guarnaccia, J., Pinder, G., and Fishman, M. (1997). *NAPL: Simulator Documentation*.

Hamdan, N., Kavazanjian, E., Rittmann, B. E., and Karatas, I. (2017). "Carbonate Mineral Precipitation for Soil Improvement Through Microbial Denitrification." *Geomicrobiology Journal*, 34(2), 139–146.

Hardin, B. O., and Black, W. L. (1966). "SAND STIFFNESS UNDER VARIOUS TRIAXIAL STRESSES." *Journal of Soil Mechanics & Foundations Div*, 92(SM2).

Hardin, B. O., and Drnevich, V. P. (1972). "SHEAR MODULUS AND DAMPING IN SOILS: DESIGN EQUATIONS AND CURVES." *Journal of Soil Mechanics & Foundations Div*, 98(sm7).

Hardin, B. O., and Richart, F. E. (1963). "Elastic Wave Velocities in Granular Soils." *Journal of the Soil Mechanics and Foundations Division*, 89(1), 33–65.

Hashash, Y. M. A. (2009). "DEEPSOIL V3.5 1-D nonlinear and equivalent linear wave

propagation analysis program for geotechnical seismic site response analysis of soil deposits." Dept. of Civil and Environmental Engineering, Univ. of Illinois at Urbana-Champaign, Urbana, IL.

Hazirbaba, K., and Rathje, E. M. (2010). "Pore pressure generation of silty sands due to induced cyclic shear strains." *Journal of Geotechnical and Geoenvironmental Engineering*, 135(12), 1892–1905.

He, J., Chu, J., and Ivanov, V. (2013). "Mitigation of liquefaction of saturated sand using biogas." *Geotechnique*, 63(4), 267–275.

He, J., Chu, J., Liu, H. L., and Gao, Y. F. (2015). "Microbial soil desaturation for the mitigation of earthquake liquefaction." *15th Asian Regional Conference on Soil Mechanics and Geotechnical Engineering, ARC 2015: New Innovations and Sustainability*, 784–787.

Heitor, A., Indraratna, B., and Rujikiatkamjorn, C. (2013). "Laboratory study of small-strain behavior of a compacted silty sand." *Canadian Geotechnical Journal*, NRC Research Press, 50(2), 179–188.

Hoyos, L. R., Suescún-Florez, E. A., and Puppala, A. J. (2015). "Stiffness of intermediate unsaturated soil from simultaneous suction-controlled resonant column and bender element testing." *Engineering Geology*, Elsevier B.V., 188, 10–28.

Hsiao, D. H., Phan, V. T. A., Hsieh, Y. T., and Kuo, H. Y. (2015). "Engineering behavior and correlated parameters from obtained results of sand-silt mixtures." *Soil Dynamics and Earthquake Engineering*, Elsevier, 77, 137–151.

Hsu, C. C., and Vucetic, M. (2004). "Volumetric threshold shear strain for cyclic settlement."

Journal of Geotechnical and Geoenvironmental Engineering, 130(1), 58–70.

Huang, Y., and Wang, L. (2016). "Laboratory investigation of liquefaction mitigation in silty sand using nanoparticles." *Engineering Geology*, Elsevier B.V., 204, 23–32.

Idriss, I. M., and Boulanger, R. W. (2006). "Semi-empirical procedures for evaluating liquefaction potential during earthquakes." *Soil Dynamics and Earthquake Engineering*, Elsevier, 26(2-4 SPEC. ISS.), 115–130.

Ishibashi, I., and Zhang, X. (1993). "Unified Dynamic Shear Moduli and Damping Ratios of Sand and Clay." *Soils and Foundations*, The Japanese Geotechnical Society, 33(1), 182–191.

Ishihara, K., and Yoshimine, M. (1992). "Evaluation of Settlements in Sand Deposits Following Liquefaction During Earthquakes." *Soils and Foundations*, The Japanese Geotechnical Society, 32(1), 173–188.

Islam, M. T., Chittoori, B. C. S., and Burbank, M. (2020). "Evaluating the Applicability of Biostimulated Calcium Carbonate Precipitation to Stabilize Clayey Soils." *Journal of Materials in Civil Engineering*, American Society of Civil Engineers (ASCE), 32(3), 04019369.

Istok, J. D., Park, M. M., Peacock, A. D., Oostrom, M., and Wietsma, T. W. (2007). "An experimental investigation of nitrogen gas produced during denitrification." *Ground Water*, Ground Water, 45(4), 461–467.

Iwasaki, T., and Tatsuoka, F. (1977). "Effects of Grain Size and Grading on Dynamic Shear Moduli of Sands." *Soils and Foundations*, The Japanese Geotechnical Society, 17(3), 19–35.

Jafarzadeh, F., and Sadeghi, H. (2012). "Experimental study on dynamic properties of sand with

emphasis on the degree of saturation." *Soil Dynamics and Earthquake Engineering*, Elsevier, 32(1), 26–41.

Jain, A. K., and Juanes, R. (2009). "Preferential mode of gas invasion in sediments: Grain-scale mechanistic model of coupled multiphase fluid flow and sediment mechanics." *Journal of Geophysical Research: Solid Earth*, Blackwell Publishing Ltd, 114(8).

Karanasios, K. A., Vasiliadou, I. A., Pavlou, S., and Vayenas, D. V. (2010). "Hydrogenotrophic denitrification of potable water: A review." *Journal of Hazardous Materials*, Elsevier, 180(1–3), 20–37.

Khosravi, A., and McCartney, J. S. (2012). "Impact of hydraulic hysteresis on the small-strain shear modulus of low plasticity soils." *Journal of Geotechnical and Geoenvironmental Engineering*, 138(11), 1326–1333.

Khosravi, A., Mousavi, S., and Khosravi, M. (2017). "A semi-empirical shear strength model for infilled rock fractures with infills in an unsaturated state." *Geotechnical Special Publication*, American Society of Civil Engineers (ASCE), 529–538.

Khosravi, A., Mousavi, S., and Serej, A. D. (2016a). "Hydraulic Behavior of Infilled Fractured Rocks under Unsaturated Conditions." *Geotechnical and Structural Engineering Congress 2016*, American Society of Civil Engineers, Reston, VA, 1708–1718.

Khosravi, A., Rahimi, M., Gheibi, A., and Shahrabi, M. M. (2018). "Impact of plastic compression on the small strain shear modulus of unsaturated silts." *International Journal of Geomechanics*, 18(2), 1–12.

Khosravi, A., Serej, A. D., Mousavi, S. M., and Haeri, S. M. (2016b). "Effect of hydraulic

hysteresis and degree of saturation of infill materials on the behavior of an infilled rock fracture." *International Journal of Rock Mechanics and Mining Sciences*, Elsevier, 88, 105–114.

Kim, D. S., Seo, W. S., and Kim, M. J. (2003). "Deformation characteristics of soils with variations of capillary pressure and water content." *Soils and Foundations*, Japanese Geotechnical Society, 43(4), 71–79.

Kjellman, W. (1951). "Testing The Shear Strength of Clay in Sweden." *Géotechnique*, Thomas Telford Ltd , 2(3), 225–232.

Kokusho, T. (1980). "Cyclic Triaxial Test of Dynamic Soil Properties for Wide Strain Range." *Soils and Foundations*, The Japanese Geotechnical Society, 20(2), 45–60.

Kraft, B., Strous, M., and Tegetmeyer, H. E. (2011). "Microbial nitrate respiration - Genes, enzymes and environmental distribution." *Journal of Biotechnology*, Elsevier, 155(1), 104–117.

Kramer, S. L. S. (1996). *Geotechnical earthquake engineering*. *gee*, Prentice Hall, Englewood Cliffs, NJ.

Ladd, R. (1978). "Preparing Test Specimens Using Undercompaction." *Geotechnical Testing Journal*, ASTM International, 1(1), 16.

Lade, P. V., Liggio, C. D., and Yamamuro, J. A. (1998). "Effects of Non-Plastic Fines on Minimum and Maximum Void Ratios of Sand." *Geotechnical Testing Journal*, ASTM International, 21(4), 336–347.

Le, K. N. (2016). "A direct simple shear device for the dynamic characterization of partially

saturated soils." University of New Hampshire, Durham, NH.

Le, K. N., and Ghayoomi, M. (2017). "Cyclic Direct Simple Shear Test to Measure Strain-Dependent Dynamic Properties of Unsaturated Sand." *Geotechnical Testing Journal*, ASTM International, 40(3), 381–395.

Lee, K. L., and Albaisa, A. (1974). "Earthquake Induced Settlements in Saturated Sands." *Journal of the Geotechnical Engineering Division*, 100(4), 387–406.

Li, Y., Flores, G., Xu, J., Yue, W. zhong, Wang, Y. xin, Luan, T. gang, and Gu, Q. bao. (2013). "Residual air saturation changes during consecutive drainage-imbibition cycles in an air-water fine sandy medium." *Journal of Hydrology*, Elsevier, 503, 77–88.

Lu, N. (2016). "Generalized Soil Water Retention Equation for Adsorption and Capillarity." *Journal of Geotechnical and Geoenvironmental Engineering*, American Society of Civil Engineers (ASCE), 142(10), 04016051.

Lu, N., Godt, J. W., and Wu, D. T. (2010). "A closed-form equation for effective stress in unsaturated soil." *Water Resources Research*, American Geophysical Union (AGU), 46(5).

Lu, N., and Likos, W. (2004). *Unsaturated soil mechanics*.

Lu, N., and Likos, W. J. (2006). "Suction Stress Characteristic Curve for Unsaturated Soil." *Journal of Geotechnical and Geoenvironmental Engineering*, American Society of Civil Engineers, 132(2), 131–142.

Maag, M., and Vinther, F. P. (1996). "Nitrous oxide emission by nitrification and denitrification in different soil types and at different soil moisture contents and temperatures." *Applied Soil Ecology*, Elsevier, 4(1), 5–14.

189

Mahabadi, N., Zheng, X., Yun, T. S., van Paassen, L., and Jang, J. (2018). "Gas Bubble Migration and Trapping in Porous Media: Pore-Scale Simulation." *Journal of Geophysical Research: Solid Earth*, Blackwell Publishing Ltd, 123(2), 1060–1071.

Mancuso, C., Vassallo, R., and d'Onofrio, A. (2002). "Small strain behavior of a silty sand in controlled-suction resonant column - Torsional shear tests." *Canadian Geotechnical Journal*, NRC Research Press Ottawa, Canada , 39(1), 22–31.

Martin, G. R., Seed, H. B., and Finn, W. D. L. (1975). "Fundamentals of liquefaction under cyclic loading." *Journal of the Geotechnical Engineering Division*, 101(5), 423–438.

Masing, G. (1926). "Eigenspannungen und Verfestigung Bei Messing." Proceedings, Second International Congress of Applied Mechanics, 332–335.

Matasovic, N. (2006). *D-MOD_2—a computer program for seismic response analysis of horizontally layered soil deposits, earthfill dams, and solid waste landfills*.

Matasovic, N., and Vucetic, M. (1993). *Seismic response of horizontally layered soil deposits*.

Mele, L., and Flora, A. (2019). "On the prediction of liquefaction resistance of unsaturated sands." *Soil Dynamics and Earthquake Engineering*, Elsevier Ltd, 125(November 2018), 105689.

Mele, L., Tian, J. T., Lirer, S., Flora, A., and Koseki, J. (2019). "Liquefaction resistance of unsaturated sands: Experimental evidence and theoretical interpretation." *Geotechnique*, ICE Publishing, 69(6), 541–553.

Menq, F.-Y. (2003). "Dynamic properties of sandy and gravelly soils."

Miller, H. J. (1994). "Development of Instrumentation to Study the Effects of Aging on the Small Strain Behavior of Sands." University of New Hampshire, Durham, NH.

Mirshekari, M., and Ghayoomi, M. (2017). "Centrifuge tests to assess seismic site response of partially saturated sand layers." *Soil Dynamics and Earthquake Engineering*, Elsevier Ltd, 94, 254–265.

Montoya, B. M., DeJong, J. T., and Boulanger, R. W. (2013). "Dynamic response of liquefiable sand improved by microbial-induced calcite precipitation." *Geotechnique*, 63(4), 302–312.

Mousavi, S., and Ghayoomi, M. (2018). "Dynamic shear modulus of microbial induced partially saturated sand Dynamic Performance of Microbial Induced Partially Saturated Soils." *Proceedings of International Symposium on Bio-mediated and Bio-inspired Geotechnics*, Atlanta, GA, 1–6.

Mousavi, S., and Ghayoomi, M. (2019). "Liquefaction Mitigation of Silty Sands via Microbial Induced Partial Saturation." *Geotechnical Special Publication*, American Society of Civil Engineers (ASCE), 304–312.

Mousavi, S., and Ghayoomi, M. (2020a). "Liquefaction Mitigation of Sands with Non-Plastic Fines via Microbial Induced Partial Saturation." *Journal of Geotechnical and Geoenvironmental Engineering*, Under review.

Mousavi, S., and Ghayoomi, M. (2020b). "A semi-empirical model to predict excess pore pressure generation in partially saturated sand." *4th European conference on unsaturated soils*, Lisboa, Portugal, 1-6 (In press).

Mousavi, S., and Ghayoomi, M. (2020c). "Seismic Compression of Unsaturated Silty Sands: A Strain-Based Approach." *Journal of Geotechnical & Geoenvironmental Engineering*, (Under review).

Mousavi, S., Ghayoomi, M., and Jones, S. H. (2019). "Compositional and geoenvironmental factors in microbially induced partial saturation." *Environmental Geotechnics*, 1–13.

Mousavi, S., Ghayoomi, M., and McCartney, J. S. (2020). "Discussion of 'Simplified Procedure for Prediction of Earthquake-Induced Settlements in Partially Saturated Soils' by Abdülhakim Zeybek and Santana Phani Gopal Madabhushi." *Journal of Geotechnical and Geoenvironmental Engineering*, In press.

Ng, C. W. W., Kaewsong, R., Zhou, C., and Alonso, E. E. (2017). "Small strain shear moduli of unsaturated natural and compacted loess." *Geotechnique*, 67(7), 646–651.

O'Donnell, S. T., Kavazanjian, E., and Rittmann, B. E. (2017a). "MIDP: Liquefaction mitigation via microbial denitrification as a two-stage process. II: MICP." *Journal of Geotechnical and Geoenvironmental Engineering*, 143(12), 1–12.

O'Donnell, S. T., Rittmann, B. E., and Kavazanjian, E. (2017b). "MIDP: Liquefaction mitigation via microbial denitrification as a two-stage process. I: Desaturation." *Journal of Geotechnical and Geoenvironmental Engineering*, 143(12), 1–11.

Oh, W. T., and Vanapalli, S. K. (2014). "Semi-empirical Model for Estimating the Small-Strain Shear Modulus of Unsaturated Non-plastic Sandy Soils." *Geotechnical and Geological Engineering*, 32(2), 259–271.

Okamura, M., and Noguchi, K. (2009). "Liquefaction resistances of unsaturated non-plastic silt." *Soils and Foundations*, Japanese Geotechnical Society, 49(2), 221–229.

Okamura, M., and Soga, Y. (2006). "Effects of Pore Fluid Compressibility on Liquefaction Resistance of Partially Saturated Sand." *Soils and Foundations*, Japanese Geotechnical

Society, 46(5), 695–700.

Okamura, M., Takebayashi, M., Nishida, K., Fujii, N., Jinguji, M., Imasato, T., Yasuhara, H., and Nakagawa, E. (2011). "In-situ desaturation test by air injection and its evaluation through field monitoring and multiphase flow simulation." *Journal of Geotechnical and Geoenvironmental Engineering*, 137(7), 643–652.

Orense, R. P., Kiyota, T., Yamada, S., Cubrinovski, M., Hosono, Y., Okamura, M., and Yasuda, S. (2011). "Comparison of liquefaction features observed during the 2010 and 2011 Canterbury earthquakes." *Seismological Research Letters*, GeoScienceWorld, 82(6), 905–918.

Oztoprak, S., and Bolton, M. D. (2013). "Stiffness of sands through a laboratory test database." *Géotechnique*, Thomas Telford Ltd, 63(1), 54–70.

van Paassen, L. A. (2011). "Bio-Mediated Ground Improvement: From Laboratory Experiment to Pilot Applications." *Geo-Frontiers 2011*, American Society of Civil Engineers, Reston, VA, 4099–4108.

van Paassen, L. A., Daza, C. M., Staal, M., Sorokin, D. Y., van der Zon, W., and van Loosdrecht, M. C. M. (2010). "Potential soil reinforcement by biological denitrification." *Ecological Engineering*, Elsevier, 36(2), 168–175.

Park, J. Y., and Yoo, Y. J. (2009). "Biological nitrate removal in industrial wastewater treatment: Which electron donor we can choose." *Applied Microbiology and Biotechnology*, Springer, 82(3), 415–429.

Parkin, T. B., Sexstone, A. J., and Tiedje, J. M. (1985). "Adaptation of Denitrifying Populations

to Low Soil pH †." *Applied and Environmental Microbiology*, American Society for Microbiology, 49(5), 1053–1056.

Pham, V. P., Nakano, A., Van Der Star, W. R. L., Heimovaara, T. J., and Van Paassen, L. A. (2017). "Applying MICP by denitrification in soils: A process analysis." *Environmental Geotechnics*, 5(2), 79–93.

Pham, V. P., van Paassen, L. A., van der Star, W. R. L., and Heimovaara, T. J. (2018). "Evaluating strategies to improve process efficiency of denitrification-based MICP." *Journal of Geotechnical and Geoenvironmental Engineering*, 144(8).

Polito, C. P., and Martin II, J. R. (2001). "Effects of Nonplastic Fines on the Liquefaction Resistance of Sands." *Journal of Geotechnical and Geoenvironmental Engineering*, American Society of Civil Engineers, 127(5), 408–415.

Porcino, D. D., and Diano, V. (2017). "The influence of non-plastic fines on pore water pressure generation and undrained shear strength of sand-silt mixtures." *Soil Dynamics and Earthquake Engineering*, Elsevier Ltd, 101(June), 311–321.

Pradel, D. (1998). "Procedure to Evaluate Earthquake-Induced Settlements in Dry Sandy Soils." *Journal of Geotechnical and Geoenvironmental Engineering*, American Society of Civil Engineers (ASCE), 124(4), 364–368.

Puzrin, A. M., Tront, J., Schmid, A., and Hughes, J. B. (2011). "Engineered use of microbial gas production to decrease primary consolidation settlement in clayey soils." *Geotechnique*, 61(9), 785–794.

Qian, X., Gray, D. H., and Woods, R. D. (1991). "Resonant column tests on partially saturated

sands." *Geotechnical Testing Journal*, 14(3), 266–275.

Rahman, M. M., Lo, S. R., and Gnanendran, C. T. (2008). "On equivalent granular void ratio and steady state behaviour of loose sand with fines." *Canadian Geotechnical Journal*, 45(10), 1439–1456.

Rebata-Landa, V., and Santamarina, J. C. (2006). "Mechanical limits to microbial activity in deep sediments." *Geochemistry, Geophysics, Geosystems*, John Wiley & Sons, Ltd, 7(11), n/a-n/a.

Rebata-Landa, V., and Santamarina, J. C. (2011). "Mechanical effects of biogenic nitrogen gas bubbles in soils." *Journal of Geotechnical and Geoenvironmental Engineering*, 138(2), 128–137.

Rong, W., and McCartney, J. S. (2020). "Drained Seismic Compression of Unsaturated Sand." *Journal of Geotechnical and Geoenvironmental Engineering*, American Society of Civil Engineers (ASCE), 146(5), 1–14.

Rouf, M. A., Singh, R. M., Bouazza, A., Rowe, R. K., and Gates, W. P. (2016). "Gas permeability of partially hydrated geosynthetic clay liner under two stress conditions." *Environmental Geotechnics*, ICE Publishing, 3(5), 325–333.

Sadrekarimi, A. (2013). "Influence of fines content on liquefied strength of silty sands." *Soil Dynamics and Earthquake Engineering*, Elsevier, 55, 108–119.

Saggar, S., Jha, N., Deslippe, J., Bolan, N. S., Luo, J., Giltrap, D. L., Kim, D. G., Zaman, M., and Tillman, R. W. (2013). "Denitrification and N2O: N2 production in temperate grasslands: Processes, measurements, modelling and mitigating negative impacts." *Science of the Total Environment*, Elsevier, 465, 173–195.

Saleh-Lakha, S., Shannon, K. E., Henderson, S. L., Goyer, C., Trevors, J. T., Zebarth, B. J., and Burton, D. L. (2009). "Effect of pH and temperature on denitrification gene expression and activity in Pseudomonas mandelii." *Applied and Environmental Microbiology*, American Society for Microbiology, 75(12), 3903–3911.

Salgado, R., Bandini, P., and Karim, A. (2000). "Shear Strength and Stiffness of Silty Sand." *Journal of Geotechnical and Geoenvironmental Engineering*, American Society of Civil Engineers, 126(5), 451–462.

Sawangsuriya, A., Edil, T. B., and Bosscher, P. J. (2009). "Modulus-suction-moisture relationship for compacted soils in postcompaction state." *Journal of Geotechnical and Geoenvironmental Engineering*, 135(10), 1390–1403.

Seed, H. B., and Idriss, I. M. (1970). *Soil Moduli and Damping Factors for Dynamic Response Analyses, Report No. EERC70-10*.

Seed, H. B., Seed, R. B., Harder, L. F., and Jong, H. L. (1989). *Re-Evaluation of the Lower San Fernando Dam. Report 2. Examination of the Post-Earthquake Slide of February 9, 1971*. ORINDA CA.

Seed, H. B., Wong, R. T., Idriss, I. M., and Tokimatsu, K. (1986). "Moduli and Damping Factors for Dynamic Analyses of Cohesionless Soils." *Journal of Geotechnical Engineering*, American Society of Civil Engineers, 112(11), 1016–1032.

Sierra-Alvarez, R., Beristain-Cardoso, R., Salazar, M., Gómez, J., Razo-Flores, E., and Field, J. A. (2007). "Chemolithotrophic denitrification with elemental sulfur for groundwater treatment." *Water Research*, Elsevier Ltd, 41(6), 1253–1262.

Silver, M. L., and Seed, H. B. (1971). "VOLUME CHANGES IN SANDS DURING CYCLIC LOADING." *Journal of Soil Mechanics & Foundations Div*.

Šimek, M., and Cooper, J. E. (2002). "The influence of soil pH on denitrification: Progress towards the understanding of this interaction over the last 50 years." *European Journal of Soil Science*, John Wiley & Sons, Ltd, 53(3), 345–354.

Smith, M. S., and Tiedje, J. M. (1979). "Phases of denitrification following oxygen depletion in soil." *Soil Biology and Biochemistry*, Pergamon, 11(3), 261–267.

Stewart, J. P., Bray, J. D., McMahon, D. J., Smith, P. M., and Kropp, A. L. (2001). "Seismic performance of hillside fills." *Journal of Geotechnical & Geoenvironmental Engineering*, 127(11), 905–919.

Stewart, J. P., Smith, P. M., Whang, D. H., and Bray, J. D. (2004). "Seismic Compression of Two Compacted Earth Fills Shaken by the 1994 Northridge Earthquake." *Journal of Geotechnical and Geoenvironmental Engineering*, American Society of Civil Engineers, 130(5), 461–476.

Terzaghi, K. (1943). *Theoretical Soil Mechanics*. *Theoretical Soil Mechanics*, John Wiley & Sons, Inc., Hoboken, NJ, USA.

Thevanayagam, S., and Mohan, S. (2000). "Intergranular state variables and stress-strain behaviour of silty sands." *Geotechnique*, Thomas Telford Services Ltd, 50(1), 1–23.

Thevanayagam, S., Shenthan, T., Mohan, S., and Liang, J. (2002). "Undrained Fragility of Clean Sands, Silty Sands, and Sandy Silts." *Journal of Geotechnical and Geoenvironmental Engineering*, American Society of Civil Engineers (ASCE), 128(10), 849–859.

Tokimatsu, K., and Seed, H. B. (1987). "Evaluation of Settlements in Sands Due to Earthquake

Shaking." *Journal of Geotechnical Engineering*, American Society of Civil Engineers, 113(8), 861–878.

Tsukamoto, Y. (2019). "Degree of saturation affecting liquefaction resistance and undrained shear strength of silty sands." *Soil Dynamics and Earthquake Engineering*, Elsevier Ltd, 124(April), 365–373.

Tsukamoto, Y., Kawabe, S., Matsumoto, J., and Hagiwara, S. (2014). "Cyclic resistance of two unsaturated silty sands against soil liquefaction." *Soils and Foundations*, Elsevier, 54(6), 1094–1103.

Unno, T., Kazama, M., Uzuoka, R., Sento, N., and Sentos, N. (2008). "Liquefaction of unsaturated sand considering the pore air pressure and volume compressibility of the soil particle skeleton." *Soils and Foundations*, Japanese Geotechnical Society, 48(1), 87–99.

Weier, K. L., and Gilliam, J. W. (1986). "Effect of Acidity on Denitrifcation and Nitrous Oxide Evolution from Atlantic Coastal Plain Soils." *Soil Science Society of America Journal*, Wiley, 50(5), 1202–1205.

Weier, K. L., MacRae, I. C., and Myers, R. J. K. (1993). "Denitrification in a clay soil under pasture and annual crop: Losses from 15N-labelled nitrate in the subsoil in the field using C2H2 inhibition." *Soil Biology and Biochemistry*, Pergamon, 25(8), 999–1004.

Whang, D. H., Moyneur, M. S., Duku, P., and Stewart, J. P. (2005). "Seismic compression behavior of non-plastic silty sands." *Int. Symp. on Advanced Experimental Unsaturated Soil Mechanics*, Balkema, Lisse, Netherlands, 257–263.

Whang, D. H., Stewart, J. P., and Bray, J. D. (2004). "Effect of compaction conditions on the

seismic compression of compacted fill soils." *Geotechnical Testing Journal*, 27(4), 371–379.

Wheeler, S. J. (1988). "A conceptual model for soils containing large gas bubbles." *Geotechnique*, Thomas Telford Ltd , 38(3), 389–397.

Whitman, W. B., Coleman, D. C., and Wiebe, W. J. (1998). "Prokaryotes: The unseen majority." *Proceedings of the National Academy of Sciences of the United States of America*, National Academy of Sciences, 95(12), 6578–6583.

Wilt, P. M. (1986). "Nucleation rates and bubble stability in water-carbon dioxide solutions." *Journal of Colloid And Interface Science*, Academic Press, 112(2), 530–538.

Wood, D. M., and Maeda, K. (2008). "Changing grading of soil: Effect on critical states." *Acta Geotechnica*, Springer, 3(1), 3–14.

Yamamuro, J. A., and Lade, P. V. (1998). "Steady-State Concepts and Static Liquefaction of Silty Sands." *Journal of Geotechnical and Geoenvironmental Engineering*, ASCE, 124(9), 868–877.

Yang, J., and Liu, X. (2016). "Shear wave velocity and stiffness of sand: the role of non-plastic fines." *Géotechnique*, ICE Publishing, 66(6), 500–514.

Yang, J., Liu, X., Rahman, M. M., Lo, R., Goudarzy, M., and Schanz, T. (2018). "Shear wave velocity and stiffness of sand: The role of non-plastic fines." *Geotechnique*, 68(10), 931–934.

YANG, J., and WEI, L. M. (2012). "Collapse of loose sand with the addition of fines: the role of particle shape." *Géotechnique*, Thomas Telford Ltd , 62(12), 1111–1125.

Yang, X., Wang, S., and Zhou, L. (2012). "Effect of carbon source, C/N ratio, nitrate and dissolved oxygen concentration on nitrite and ammonium production from denitrification process by

Pseudomonas stutzeri D6." *Bioresource Technology*, Elsevier, 104, 65–72.

Yee, E., Duku, P. M., and Stewart, J. P. (2014). "Cyclic volumetric strain behavior of sands with fines of low plasticity." *Journal of Geotechnical and Geoenvironmental Engineering*, 140(4), 2–11.

Yegian, M. K., Eseller-Bayat, E., Alshawabkeh, A., and Ali, S. (2007). "Induced-Partial Saturation for Liquefaction Mitigation: Experimental Investigation." *Journal of Geotechnical and Geoenvironmental Engineering*, American Society of Civil Engineers, 133(4), 372–380.

Yoshimi, Y., Tanaka, K., and Tokimatsu, K. (1989). "Liquefaction Resistance of A Partially Saturated Sand." *Soils and Foundations*, The Japanese Geotechnical Society, 29(3), 157–162.

Youd, T. L., and Bennett, M. J. (1983). "Liquefaction Sites, Imperial Valley, California." *Journal of Geotechnical Engineering*, American Society of Civil Engineers, 109(3), 440–457.

Yu, P., and Richart, F. E. (1984). "Stress Ratio Effects on Shear Modulus of Dry Sands." *Journal of Geotechnical Engineering*, American Society of Civil Engineers, 110(3), 331–345.

Zamani, A., and Montoya, B. M. (2019). "Undrained cyclic response of silty sands improved by microbial induced calcium carbonate precipitation." *Soil Dynamics and Earthquake Engineering*, Elsevier Ltd, 120, 436–448.

Zeybek, A., and Madabhushi, S. P. G. (2017). "Influence of air injection on the liquefaction-induced deformation mechanisms beneath shallow foundations." *Soil Dynamics and Earthquake Engineering*, Elsevier Ltd, 97(February), 266–276.

Zeybek, A., and Madabhushi, S. P. G. (2019). "Simplified Procedure for Prediction of Earthquake-Induced Settlements in Partially Saturated Soils." *Journal of Geotechnical and*

Geoenvironmental Engineering, American Society of Civil Engineers (ASCE), 145(11), 1–9.

Zhang, B., and Muraleetharan, K. K. (2018). "Liquefaction of level ground unsaturated sand deposits using a validated fully coupled analysis procedure." *International Journal of Geomechanics*, 18(10), 1–14.

Zhang, C., and Lu, N. (2020). "Unified Effective Stress Equation for Soil." *Journal of Engineering Mechanics*, American Society of Civil Engineers (ASCE), 146(2), 04019135.